CRANFIELD UNIVERSITY

AYAT ADNAN ATWAH

THE INFLUENCE OF MICROSCOPIC FEATURES ON THE SELF-CLEANING ABILITY OF 3D PRINTED FABRIC-LIKE STRUCTURES

THE SCHOOL OF AEROSPACE, TRANSPORT AND MANUFACTURING

PhD in Manufacturing

PhD

Academic Year: 2019-2022

Supervisor: Dr Muhammad Khan

Associate Supervisor: Dr Indrat Aria

September 2022

CRANFIELD UNIVERSITY

THE SCHOOL OF AEROSPACE, TRANSPORT AND MANUFACTURING

PhD

Academic Year: 2019-2022

AYAT ADNAN ATWAH

The Influence of Microscopic Features on the Self-cleaning Ability of 3D Printed Fabric-like Structures

Supervisor: Dr Muhammad Khan
Associate Supervisor: Dr Indrat Aria
September 2022

This thesis is submitted in partial fulfilment of the requirements for the degree of PhD

© Cranfield University year 2022. All rights reserved. No part of this publication may be reproduced without the written permission of the copyright owner.

ABSTRACT

Self-cleaning surfaces are getting significant attention within multiple scientific and industrial fields. Especially for textile fabrics, it is observed that self-cleaning textile fabric surfaces are created by manipulating the surface features with the help of coatings and nanoparticles, which are considered costly and far more complicated. However, the exploration of the potential for self-cleaning by controlling the fabrication parameters of textile fabrics at the microscopic level has not been addressed. The purpose of this study was to establish the context of self-cleaning textile fabrics by controlling the fabrication parameters of the fabric at the microscopic level. The control of the fabrication parameters is not easy in conventional fabric manufacturing techniques. Due to this reason, most textile fabrics use surface coating methods for self-cleaning features.

The current evolution in 3D printed technology provides an opportunity to control the fabrication parameters during fabric manufacturing and generate self-cleaning features at the woven structural level. This study focuses on the possibility of developing a 3D-printed self-cleaning textile fabric using different printing parameters. It also identifies the significance of the fabric's microscopic features, such as porosity, surface roughness, and wettability, along with the aesthetic look after optimizing these features. Further, the influence of these features on mechanical strength at the fabric woven structure level was tested. The optimization of printing parameters was modelled to identify the optimum self-cleaning properties for the 3D-printed specimens and the validation model was accomplished under a set of experimental methods.

The study includes the combination of three printing parameters: layer height (LH) (0.15, 0.13, 0.10 mm) and extruder width (EW) (0.5, 0.4, 0.3 mm), along with two different angular printing orientations (O) (45 ° and 90 °). The other parameters, such as nozzle temperature (℃), print speed (mm/s), and infill density (%), remained constant for all the samples. Three different thermoplastic flexible filaments printing materials are used: thermoplastic polyurethane (TPU 98A), thermoplastic elastomers (TPE felaflex), and thermoplastic co-polyester (TPC

flex45). The 162 prepared samples are tested based on an experimental scheme to evaluate the self-cleaning ability. The microscopic features (porosity, roughness, and wettability) which are mainly responsible for this ability, are measured and recorded to evaluate and compare the best values for self-cleaning between the three chosen materials. The data are analysed to define the optimal self-cleaning number. Lastly, the experimental outputs are used in analytical calculations to find the relationship between changes in printing parameters and microscopic features.

The study revealed that the printing parameters significantly affect the self-cleaning properties when optimizing the selection of the process parameter combination of layer height, extruder width, and printing orientation. The study successfully created a linear regression model to demonstrate the relationship between 3D printing parameters (layer height, extruder width, and orientation) and the self-cleaning microscopic features of the 3D-printed polymeric textile fabrics. It also identified that the (TPE) has a better self-cleaning ability than the other two materials.

Keywords:

3D printing, Self-cleaning polymeric fabrics, Microscopic features, Printing parameters, Thermoplastic polyurethane (TPU 98A), Thermoplastic elastomers (TPE felaflex), and Thermoplastic co-polyester (TPC flex45).

ACKNOWLEDGEMENTS

I am extremely grateful to Allah Almighty for providing me with energy and strength throughout the process of this research and far beyond.

I would like to express my deepest appreciation to my supervisor, Dr. Muhammad Khan, for his invaluable and continuous support, encouragement, and mentorship throughout the duration of this study. His levels of patience, knowledge, and ingenuity is something I will always keep aspiring to. This research work would not be possible without his inspiration and cooperation.

I also would like to thank Mr. Alan Heaume, the technician who has helped me with the experiments.

I would also like to thank the research student, Mr. Mohammed Dukhi S Almutairi, for his effort and support during the experiments. His help was greatly appreciated.

I also would like to thank everyone who has been so kind as to help me out in all manner of ways. I truly appreciate all their support.

Lastly, I would also to express my special thanks, love, and gratitude to my family; my husband Dr. Saleh Baqader who has always supported, encouraged, and believed in me, there are no words could express my thanks and gratitude for his patience and confidence in me. Thanks for what you have sacrificed to make this journey possible. My beloved children: Mohammed, Mysarah, and Hind for their patience, understanding, support and endless love, without which this work could not have been accomplished.

I would like to dedicate this thesis and all my academic achievement to my family; my dearest husband, and our beautiful children: Mohammed, Mysarah, and Hind

LIST OF PUBLICATION

1. Atwah, A.A., Almutairi, M.D., He, F., and Khan, M.A. (2022) ‘Influence of Printing Parameters on Self-cleaning Ability of 3D Printed Polymeric Fabrics’, Polymers, 14(15), p3128.
2. Atwah AA, Khan MA. Influence of Microscopic Features on The Self-Cleaning Ability of Textile Fabrics. Textile Research Journal. 2022;0(0).
3. Chan, K. P., He, F., Atwah, A. A., & Khan, M. (2023). Experimental Investigation of Self-Cleaning Behaviour of 3D-Printed Textile Fabrics with Various Printing Parameters. Polymer Testing, 119, 107941.

Table of Contents

ABSTRACT i
ACKNOWLEDGEMENTS iii
LIST OF PUBLICATION iv
LIST OF FIGURES viii
LIST OF TABLES xiii
LIST OF EQUATIONS xiv
LIST OF ABBREVIATIONS xv
1 IDENTIFICATION AND SIGNIFICANCE OF THE RESEARCH 1
1.1 Research Background 1
1.2 Research Problem 2
1.3 Research Objectives 3
1.4 Research Methodology 3
1.5 Thesis Structure 4
2 LITERATURE REVIEW 6
2.1 Introduction 6
2.2 Conventional Methods of Self-Cleaning 7
2.2.1 Dip-Coating (Sol-Gel) Method 8
2.2.2 Spin Coating Method 12
2.2.3 Spray Coating and Electro-Spraying Method 13
2.2.4 Electrospinning Method 16
2.2.5 Chemical Etching and Chemical Vapour Deposition (CVD) Methods 16
2.2.6 Hydrothermal Treatment (HTT) Method 17
2.2.7 Layer-by-Layer Self-Assembly (LBL) Method 18
2.2.8 Wet Chemical Synthesis Method 19
2.3 The Development of Self-Cleaning Textiles with Additional Properties 20
2.3.1 Antimicrobial Properties. 20
2.3.2 UV-Protection Properties. 21
2.3.3 Water/Oil Separation Properties. 22
2.3.4 Laundering and Rubbing Durability. 22
2.4 The Influence of Microscopic Features on Textile Fabrics Self-Cleaning Ability 23
2.4.1 Microscopic Features at Self-Cleaning Coating Level 23
2.4.2 Microscopic Features at Woven Structural Level 26
2.5 The Challenges in the Existing Processes for Making Self-Cleaning Textile Fabric and their Effectiveness 29
2.6 IDENTIFICATION OF MICROSCOPIC GEOMETRICAL AND STRUCTURAL SELF-CLEANING FEATURES 31
2.6.1 Microscopic Geometrical and Structural Features of Self-Cleaning Surfaces 31

2.6.2 Identifying the Key Microscopic Geometrical and Structural Features that Provide Self-Cleaning Ability in Fabric Textile Surfaces..... 35
2.7 Analysing the Possibility to Create a Self-Cleaning Surface Using a 3D Printer 38
2.7.1 The 3D printing technology 38
2.7.2 The 3D-printed of textiles 43
2.7.3 The advances in self-cleaning 3D-printed structures..... 45
2.8 Conclusion 48
3 METHODOLOGY 50
3.1 Introduction 50
3.2 Self-Cleaning Textile Fabrics and Associated Challenges..... 52
3.3 Design of Experiments..... 52
3.4 Mathematical and Statistical Tools for Modelling 54
3.5 Critical Discussion on the Obtained Model 55
3.6 Validation of The Model 55
4 DESIGN OF EXPERIMENTS, METHODS FOR MEASUREMENT AND MODELLING 58
4.1 Introduction 58
4.2 Design of Experiment..... 59
4.3 The 3D Printing Parameters 60
4.4 FFF Materials..... 64
4.5 Sample Preparation 65
4.5.1 The Measurement Method for Porosity: 70
4.5.2 The Measurement Method of Surface Roughness 70
4.5.3 The Measurement Method of Wettability..... 72
4.5.4 The Unit Cell Measure..... 73
4.5.5 Data Process..... 74
5 RESULT AND DISCUSSION 77
5.1 Introduction 77
5.1.1 The Influence of Printing Parameters on Porosity 77
5.1.2 The Parameters Influence on Surface Roughness..... 81
5.1.3 The Parameters Influence on Wettability Contact Angle 85
5.2 The Relationship Between the Printing Parameters and the Microscopic Features..... 92
5.3 The Self-Cleaning Number 95
5.4 Mechanical Strength Test 96
5.5 Conclusion 99
6 THE OPTIMIZATION OF PRINTING PARAMETERS 101
7 VALIDATION 108
7.1 The self-cleaning number for the validation 114

7.2 Discussion on Experimental Error in Predictions of Porosity, Surface Roughness and Wettability for the Three Materials 115
8 CONCLUSIONS 119
8.1 Achievement of Objectives 121
8.2 Contribution to Knowledge 125
8.2.1 Influence of Microscopic Features on Self-Cleaning Ability 125
8.2.2 Influence of the Printing Parameter on Microscopic Features 125
8.2.3 Relationship Between Printing Parameters and Microscopic Features 126
8.3 Future Work 126
REFERENCES 128
APPENDICES Appendix A: MATLAB code 152

LIST OF FIGURES

Figure 2-1 (a) a typical example of a superhydrophobic surface in nature Lotus leaf with self-cleaning properties and SEM image of the surface structures of the lotus leaf. Schematic illustration of the “self-cleaning” concept. A water droplet rolling off on (b) a lotus leaf rough surface and (c) a water droplet on a hydrophilic solid surface [15][16]. 7

Figure 2-2. Illustration of the industrialized version of the dip-pad-dry-cure method used to apply the photo responsive materials on the textile substrate [26].. 9

Figure 2-3. Wash fastness of ZnONPs coated cotton fabrics, showing different wash times [22]..... 10

Figure 2-4 A. The degradation of methylene blue spot in cotton textile by dipping in acrylic acid for 24 $\boldsymbol{h}$ on (a) non-coated cotton; (b) cotton coatedwithTiO_2;(c) cotton coated with SiO_2; (d) cotton coated with TiO_2-SiO_2(1:1); (e) cotton coated with TiO_2-SiO_2(2:1) and (f) cotton coated with TiO_2-SiO_2(1:2). B. The degradation pattern of methylene blue on cotton fibres coated with different Ti:Si molar ratio under UV irradiation at ʎmax= 661 $\boldsymbol{nm}$ [39]..... 13

Figure 2-5. Sessile water droplets on the (a and b) un-sprayed, and (c and d) electro-sprayed polyester fabrics with the aerogel/fluorocarbon mixture for 16 $\boldsymbol{h}$. (f) a schematic design for the basic setup of the electro-spraying device used in this study [24]. 14

Figure 2-6. The abrasion and mechanical durability of PCL-PTFOA(4h) microsphere-coated cotton fabric. A to C, sandpaper abrasion tests and D, tape adhesion tests [43]..... 15

Figure 2-7. Schematic of the basic set-up for electrospinning [46]. 16

Figure 2-8. (a) Schematic diagram of the textile coating setup, (b) Schematic and dimensions of the CVD reaction chamber, (c) picture of CVD reaction chamber, (d) heating element, and (e) temperature controller [47]..... 17

Figure 2-9. Schematic illustration of the fabrication of multifunctional superhydrophobic fabric.40 b PEI: sequential assembly of poly(ethylenimine); APP: ammonium polyphosphate; CNT_s: carbon nanotubes; PDMS: post-treatment with poly(dimethylsiloxane) [55]. 19

Figure 2-10. Optical photographs of water droplets dyed with methyl blue on superhydrophobic TiO_2@Cotton fabric surfaces with different adhesion a–c) and the surface traces after the water droplet left the cotton fabrics d–f). Schematic illustration of three types of solid/liquid/air three-phase contact models with adhesive forces ranging from high to low: g) “area” contact model with high adhesion; h) “line” contact model with medium adhesion; i) “point” contact model with low adhesion [51]. 23

Figure 2-11. Wetting characteristic with models applied[82]..... 25

Figure 2-12. (a) Schematic of woven types prepared at OM Textile Industries. (b) Three types (two plain and one weft rib) of sisal woven pattern [93]. 27

Figure 2-13. Patterns of plain, twill and honeycomb weave simulated with TexGen [95]..... 27

Figure 2-14. 3D images of three woven fabrics and geometries of unit structure with liquid depositions (from left to right): a) plain, b) 2/1 twill, and c) 2/2 basket [89]. 29

Figure 2-15. Two models proposed for the potential mechanism of distinct adhesion [111]. 32

Figure 2-16. Front (left) and side (right) views of a sessile drop on a rough surface with parallel groove geometry. It is evident from the front view that the drop is sitting on top of the pillars [112]. 32

Figure 2-17. (A and B) Critical role of re-entrant curvature. The geometric parameters R, D, H, and W characterizing these surfaces are also shown. The blue surface is wetted while the red surface remains nonwetted when in contact with a liquid. (C and D) SEM micrographs for two micro-hoodoo surfaces having square and circular flat caps, respectively [113]. 33

Figure 2-18. SEM image of a polyurethane mushroom-shaped microfiber array [113]..... 33

Figure 2-19. Schematic and wetting of the four different surfaces. The largest contact area between the droplet and the surface is given in flat and microstructure surfaces but is reduced in nanostructured surfaces and is minimized in hierarchical structured surface [114]. 34

Figure 2-20. The nanostructures selected for the fabrication of the hierarchical structures and their static water contact angles. (a) Honeycomb pillars, (b) honeycomb lines, (c) nanopillars, (d) nano spikes [116] 34

Figure 2-21. Partial re-entrant geometry at the head of the nano-pillars: (a) SEM image of film etched using oxygen plasma (b) illustration of the partial re-entrant structure of the produced nano-pillar [57]. 35

Figure 2-22. The porosity of textile fabrics [119]. 36

Figure 2-23. Terminology illustration of (a) surface texture (b) surface roughness (Ra) [123]..... 37

Figure 2-24. The image and measurement of contact angle of a water droplet on fabric surface [129]. 38

Figure 2-25. A schematic of the fused filament fabrication (FFF) process [136] 40

Figure 2-26. The printing processes. 42

Figure 2-27. 3D printed fabric. Our technique can fabricate a textile that is woven using the movements of the nozzle of an FDM 3D printer [134]. 44

Figure 2-28. The full corset printed with flexible materials [149]. 45

Figure 3-1 Methodology diagram..... 51

Figure 3-2. The making of 3D printed self-cleaning textile polymeric fabrics.... 53

Figure 4-1. The design of the experiments. 61

Figure 4-2 Layer height and extruder width definition..... 62

Figure 4-3. Scheme showing two samples printed flat and loaded in the x/y direction 45° - 135°,0º - 90°. a) XY (90°) and, b) XY (45°). 63

Figure 4-4. a) The CAD model of the specimen b) The printed samples preview in IdeaMaker..... 66

Figure 4-5. The self-cleaning 3D printed textile-like structures with both orientation angle 45 ° - 90 ° for each material. 69

Figure 4-6. a) Fabric under the dino-lite microscope with led and upload picture to the application b) Image from the application c) Binary image converted by MATLAB d) The MATLAB code to calculate the porous. 70

Figure 4-7. a) the sample measured with the white-light Interfor-meter b) The surface roughness Ra-Rq measurement in $\boldsymbol{\mu m}$ from the filtered profiles. . 71

Figure 4-8. a) The measurement direction of roughness testing b) the peak height profile..... 71

Figure 4-9. a) Ossila Contact Angle Goniometer setup b) Image of water droplet on the fabric taken from the Ossila Contact Angle application (c) Image of (CA) analysis by the Ossila Contact Angle application. 72

Figure 4-10. The unit cell measurement for the porosity and the water droplet for TPU, TPE, and TPC. 73

Figure 5-1. Layer height influences on porosity for the three materials. 79

Figure 5-2. Extruder width influences on porosity numbers for the three materials 80

Figure 5-3. Orientation influences on porosity numbers for the three materials. 80

Figure 5-4. Layer height influences on surface roughness for the three materials. 82

Figure 5-5. Extruder width influences on surface roughness for the three materials. 83

Figure 5-6. Orientation influences on surface roughness for the three materials. 84

Figure 5-7. Layer height influences on wettability for the three materials 86

Figure 5-8. Extruder width influences on wettability for the three materials 87

Figure 5-9. Orientation influences on wettability for the three materials 88

Figure 5-10. (a) The contact angle on the TPU (b) The contact angle after 5 minutes and (c) The contact angle on after 10 minutes. 90

Figure 5-11 (a) The contact angle on the TPE (b) The contact angle after 5 minutes and (c) The contact angle after 10 minutes. 91

Figure 5-12. (a) The contact angle on the TPC. (b) The contact angle after 5 minutes and (c) The contact angle on after 10 minutes. 92

Figure 5-13. An Instron machine for the mechanical strength. 96

Figure 5-14. Procedure for (TPU 98A) tensile strength test. 97

Figure 5-15. Procedure for (TPE filaflex) tensile strength test. 97

Figure 5-16. Procedure for (TPC) tensile strength test. 98

Figure 5-17. The mechanical strength results. 99

Figure 6-1. The possible combination of the printing parameters range for (O), (LH), (EW) to achieve the best self-cleaning performance for porosity. ... 102

Figure 6-2. The possible combination of the printing parameters range for (O), (LH), (EW) to achieve the best self-cleaning performance for roughness. 102

Figure 6-3. The possible combination of the printing parameters range for (O), (LH), (EW) to achieve the best self-cleaning performance for wettability. 103

Figure 6-4. The possible combination of the printing parameters range for (O), (LH), (EW) to achieve the best self-cleaning performance for porosity. ... 104

Figure 6-5. The possible combination of the printing parameters range for (O), (LH), (EW) to achieve the best self-cleaning performance for roughness. 104

Figure 6-6. The possible combination of the printing parameters range for (O), (LH), (EW) to achieve the best self-cleaning performance for wettability. 105

Figure 6-7. The possible combination of the printing parameters range for (O), (LH), (EW) to achieve the best self-cleaning performance for porosity. ... 106

Figure 6-8. The possible combination of the printing parameters range for (O), (LH), (EW) to achieve the best self-cleaning performance for roughness. 106

Figure 6-9. The possible combination of the printing parameters range for (O), (LH), (EW) to achieve the best self-cleaning performance for wettability. 107

Figure 7-1. 3DP for validation samples..... 109

Figure 7-2. The 3D printed polymeric textile fabrics. 109

Figure 7-3. The contact angle measurement. 109

Figure 7-4. The porosity measurement..... 111

Figure 7-5. The surface roughness measurement. 112

Figure 7-6. Surface Roughness profile for the three materials. 112

Figure 7-7. Error ranges for porosity for TPU, TPE and TPC. 115

Figure 7-8 Error ranges for surface roughness for TPU, TPE and TPC. 116

Figure 7-9 Error ranges for wettability for TPU, TPE and TPC. 117

LIST OF TABLES

Table 4-1 Printing parameters 61

Table 4-2. The flexible filaments specifications and properties of the (FFF)-based 65

Table 4-3. The 3D parameters were used to produce the samples. 66

Table 4-4. The unit cell measurements. 73

Table 4-5. Standardized value for different parameters. 74

Table 7-1. The 3D parameters used to produce the samples. 108

Table 7-2. (TPU flex 98) - (O) 70 ° (first layer) - 210 ° (second layer). 109

Table 7-3. The wettability measurement for the samples. 110

Table 7-4. The porosity measurement for the samples. 111

Table 7-5. The surface roughness measurement for the samples. 113

Table 7-6. The self-cleaning number for the samples. 114

LIST OF EQUATIONS

(5-1)..... 74
(5-2)..... 76
(6-1)..... 92
(6-2)..... 92
(6-3)..... 92
(6-4)..... 93
(6-5)..... 93
(6-6)..... 93
(6-7)..... 94
(6-8)..... 94
(6-9)..... 94

LIST OF ABBREVIATIONS

3D	Three-Dimensional Printing
CAD	Computer Aided Design
EW	Extruder width
FFF	Fused filament fabrication
LH	Layer height
O	Orientations
P	Porosity
PETG	Polyethylene terephthalate Glycol-Modified
Ra	Surface roughness
STL	Stereolithography
TPC	Thermoplastic co-polyester
TPE	Thermoplastic Elastomers
TPU	Thermoplastic Polyurethane
WCA	Wettability contact angle

1 IDENTIFICATION AND SIGNIFICANCE OF THE RESEARCH

1.1 Research Background

Textiles are considered one of the most widely used materials in our daily life. They are known for their breathability, softness, and low cost. They are mainly used in the clothing, furnishing, and industrial fabrics industries [1]. The textile industry is one of the fastest growing and has been subjected to innovative improvements. Functional characteristics of textile surfaces, such as self-cleaning, antimicrobial, anti-sticking, and waterproofing features are of increasing interest in both scientific and industrial sectors [2]. Self-cleaning provides many benefits in various industries [3]. This property was inspired by natural phenomena that can be observed on leaves of lotus plants, rice plants, or animals, such as butterfly wings and fish scales [4]. A self-cleaning surface is potentially beneficial for many commercial products for economic, aesthetic, and environmental reasons [5]. Overall, it can maintain a clean and pollution-free surface either by decomposing the adsorbed stains and chemicals or by preventing dust and other pollutants from setting on the surface [6].

In recent years, an effort has been made to introduce innovations in the fabrication of textile materials and the growth of conventional textiles. Developing self-cleaning textile fabrics using finishing methods is one of textile technology's most promising research areas [7]. It has enormous potential for product improvement in the clothing and health industries. This technology supports maintaining a pollution-free environment and effectively decreases cleaning efforts by saving time and laundry costs and conserving considerable water and energy [3][8].

Self-cleaning fabric surfaces have previously been produced by creating micro-nano rough structures on surfaces with low surface energy or altering low-surface-energy materials to obtain rough surfaces [9]. Several chemical solutions have been used along with nanotechnology to enhance coatings for desirable

surface roughness or lower surface energy. A nano-layer of anatase TiO_2 and other nanoparticles has been successfully applied to the textile fabric's surface or incorporated into the fibre itself [10].

Identifying the key structural features in textile fabric self-cleaning surfaces is essential for improving the fabric's liquid-resistant/repellent surface properties. Critical microscopic features such as surface roughness, porosity, and wettability of a textile fabric are the primary influences on self-cleaning properties on the surface.

1.2 Research Problem

Many methods have been developed for the preparation of hydrophobic and photolytic coatings. However, preparation using these methods requires different chemicals and processes. Some are affordable and easy to handle, while others are complicated, expensive, and suitable for a laboratory scale. Previous studies examined the self-cleaning ability of textile fabric surface roughness and low surface energy by employing surface coatings using different chemical solutions. These coatings create a different surface on the fabric, and hence the changes in the microscopic features of this surface control the self-cleaning ability. Using these organic solvents and chemicals can cause environmental health hazards. Therefore, the development of user-friendly and cost-effective methods to structure self-cleaning surfaces can be an inspiration for excellent ideas.

As an alternative to using an additional coating, the microscopic features of the fabric itself can also influence the surface roughness and low surface energy and provide self-cleaning ability at the woven structural level. However, the influence of the microscopic features at the fabric's woven structural level has not been attributed in the past; a comprehensive effort is still required to evaluate the actual quantitative influence on the self-cleaning fabric phenomenon. The current evolution in 3D printed technology provides an opportunity to control the fabrication parameters during fabric manufacturing and generate self-cleaning features at the woven structural level. Still, no research has been conducted to

explore the potential of self-cleaning by controlling the fabrication parameters of the fabric at the microscopic level. The control of the fabrication parameters is not easy in conventional fabric manufacturing techniques.

Therefore, the main aim of this study is to establish the context of self-cleaning ability by controlling the fabrication parameters of the fabric at the microscopic level.

1.3 Research Objectives

The present study seeks to achieve four main objectives:

- To identify the microscopic features and their influence on the self-cleaning surface.
- To examine the possibility of making 3D printed self-cleaning textile fabric by changing the structural woven pattern with the help of the microscopic features.
- To model the self-cleaning ability and fabric printing parameters.
- To evaluate the optimum printing parameters for self-cleaning printed textile fabric.

1.4 Research Methodology

The study will be based on a critical review of existing research and empirical methods, as given in the following:

- Extensive literature review to identify the existing research on self-cleaning textile fabrics in general and discuss the research gap and its significance. This study will also highlight the surface features responsible for self-cleaning in a textile fabric.

- Design of experiments to examine the possibility of making 3D printed self-cleaning textile polymeric fabrics with the help of microscopic features as identified in the critical review of the existing literature.

- Use of mathematical and statistical tools to model the empirical results and develop a relationship between self-cleaning ability, microscopic features, and printing parameters.
- Critical discussion on the obtained model with the help of constraints and rules (as required to express self-cleaning of a printed fabric while keeping its aesthetic look) to establish the values of printing parameters where an optimum self-cleaning can be observed.
- Validation of the model by testing printed fabrics on arbitrary values of printing parameters.

1.5 Thesis Structure

This thesis is structured in nine chapters. **Chapter 1** presents the research background and problem, along with research objectives. An overview of the methodologies used to achieve each research objective is also presented. **Chapter 2** provides an extensive literature review to identify the existing research on self-cleaning textile fabrics in general and discuss the research gap and its significance. It describes the conventional methods of self-cleaning, the development of self-cleaning textiles with additional properties, the influence of microscopic features on textile fabrics' self-cleaning ability, and the challenges in the existing processes for self-cleaning textile fabric and their effectiveness. **Chapter 3** provides the research methodological approach that aims to achieve the research objectives. **Chapter 4** provides a further literature review to explain the identification of microscopic geometrical and structural self-cleaning features. It discusses the microscopic geometrical and structural features of self-cleaning surfaces, identifying the key microscopic geometrical and structural features that provide self-cleaning ability in fabric textile surfaces, and analysing the possibility to create a self-cleaning surface using 3D printing. **Chapter 5** provides the design of experiments and the methods for measurement and modelling. It describes the materials, sample preparation, experimental setup, measurement procedure, and data processing. **Chapter 6** discusses the results of the experiments. **Chapter 7**

provides self-cleaning features and optimization of printing parameters. **Chapter 8** sets out the validation of the results. **Chapter 9** provides a summary of the research findings and discusses the contributions. It also identifies the possibilities for future work.

2 LITERATURE REVIEW

2.1 Introduction

The self-cleaning concept is one of the fastest-growing research areas in industries around the world [11],[12]. Due to significant changes, several self-cleaning materials have been developed in many industries, such as fabrics, furnishing materials, windows, glass, outdoor construction materials, and solar cells [3]. Many scholars have published their findings on these materials in the academic field. According to publications, the self-cleaning concept can be defined as “the ability to clean the surface without any external source” [3], [12]. Furthermore, It is considered as an environmental advantage that reduces cleaning effort and saves a considerable amount of resources (i.e. time and cost) [13].

There are two main approaches used in developing self-cleaning ability. The first is based on the hydrophobic surface approach. It is also known as the lotus effect, as shown in Figure 2-1(a) [14]. In this approach, the water droplets roll off the surface and remove the dirt particles, as shown in Figure 2-1(b) [15]. The second is based on the hydrophilic surface approach, where the water drops spread over the surface and form a layer of water without removing any dirt; as in Figure 2-1 (c) both of the surfaces clean themselves with the use of water [16]. These approaches have been significantly used in various industries, such as textiles and medical textiles, athletic wear, military uniforms, and outdoor fabrics [17].

Self-cleaning abilities in textile fabrics have been comprehensively investigated over the last decade. Most of these investigations have used surface roughness and low surface energy features to establish a self-cleaning mechanism. Extensive research articles and reviews have been published to describe these processes, along with their microscopic features. However, when these were reviewed with a critical eye, it was found that a comprehensive effort is still required to compile all of these previous research studies, emphasizing how the microscopic features of textile fabrics can influence their self-cleaning ability. In

the presented review, the past investigations have been complied and critically analyzed to highlight the influence of microscopic features on self-cleaning ability.

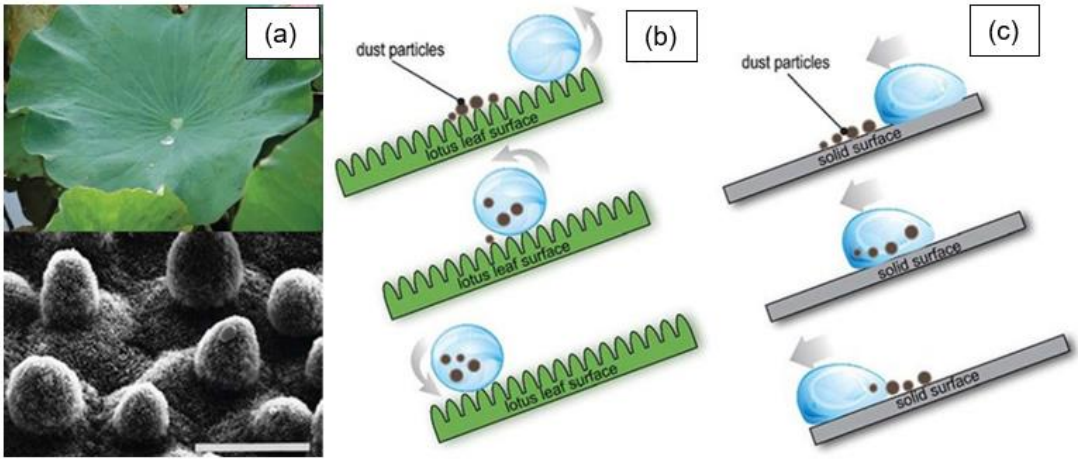

Figure 2-1 (a) a typical example of a superhydrophobic surface in nature Lotus leaf with self-cleaning properties and SEM image of the surface structures of the lotus leaf. Schematic illustration of the "self-cleaning" concept. A water droplet rolling off on (b) a lotus leaf rough surface and (c) a water droplet on a hydrophilic solid surface [15][16]**.**

In addition, challenges and research gaps that currently exist are also discussed. This review concludes that the current methods and processes for obtaining self-cleaning ability use the surface features of textile fabrics manipulated with the help of coatings and nanoparticles (NPs). However, as yet no research has been conducted to explore the self-cleaning potential of the microscopic geometrical features at the fibre surface morphology level.

2.2 Conventional Methods of Self-Cleaning

Previous studies examined the self-cleaning ability on textile fabric surface roughness and low surface energy by employing surface coatings with the use of different chemical solutions. These chemical solutions conventionally use nanotechnology to enhance the coatings for desirable surface roughness or low surface energy. Textile materials, such as cotton cellulose, silk, and wool, are useful for clothing properties due to their abundance, excellent moisture, and absorption [18]. These materials are technically called "hydrophilic" in nature. For

hydrophilic coatings, the dirt and other contaminants chemically break down when exposed to sunlight, and this process is called “photocatalysis” [19]. The hydrophilic nature can be further modified to superhydrophobic by increasing their surface roughness with the use of NPs such as titanium dioxide (TiO_2) and zinc oxide (ZnO). Those materials have been used to functionalize and oxidize the colouring ingredients in solutions and stains to have self-cleaning and other properties. Deposition (TiO_2) can change the surface energy, the absorption of liquids, and the adhesion of contaminants, permitting their photolytic degradation. As surface morphology is essential, the surface energy and sorption characteristics also play a part. So, an optimized surface microstructure and surface chemistry can create super-hydrophobicity [20], [21]. The potential of nanotechnology innovation in the textile industry is promising. The use of nanotechnology in the textile industry has increased rapidly [22],[23]. Nanocoating is a relatively new technique in the textile industry and is in the research and development phase. Therefore, nanotechnology has opened up enormous possibilities in textile finishing techniques by making chemical finishing more controllable, durable, and significantly enhanced. To generate superhydrophobic surfaces on textiles, which replicate the nanostructure of the lotus leaf and show signs of self-cleaning properties [23], different methods and materials were used to change the surface roughness and create self-cleaning ability in textile fabrics. This change can be obtained by creating hierarchical micro or nanostructures on the surface or by decreasing the surface energy with the help of low surface energy chemicals [24].

2.2.1 Dip-Coating (Sol-Gel) Method

The dip-coating method has a significant impact on the chemical finishing of textile materials. Researchers have paid much attention to the fabrication of superhydrophobic surfaces using this method. Simple dip-coating, self-cleaning, antibacterial, ultraviolet (UV) protection, and other finishes can be applied on textile surfaces [25]. In this method, the textile goes through two processes. Firstly, it is immersed in a solution that includes the needed chemicals (1. Dip),

then padded through a pressure of 2 bar (2. Pad); this process is called immerse and distribute. Secondly, the treated textile enters the “drying” (3. Dry) and “curing” (4. Cure) stages at a fixed temperature; this process is called heat treatment, as shown in Figure 2-2 [26]. Lee et al. developed self-cleaning textiles (cotton and nylon) with carbon nanotube (CNT)-TiO_2 and methyl methacrylate butyl acrylate (MMA/BA) suspension polymerization using the dip-coating process [8]. Lin et al. prepared a durable superhydrophobic and super-oleophobic cotton fabric with a dual-size hierarchical structure containing modified SiO_2 NPs and fluoropolymer. The coated textile fabrics showed excellent self-cleaning performance [27]. Yang et al. modified cotton textile surfaces with anatase TiO_2 sol and polydimethylsiloxane (PDMS) using a simple dip-coating method. As a result, a robust fluorine-free self-cleaning cotton textile was prepared with excellent durability, super hydrophobicity, and photocatalytic ability [28].

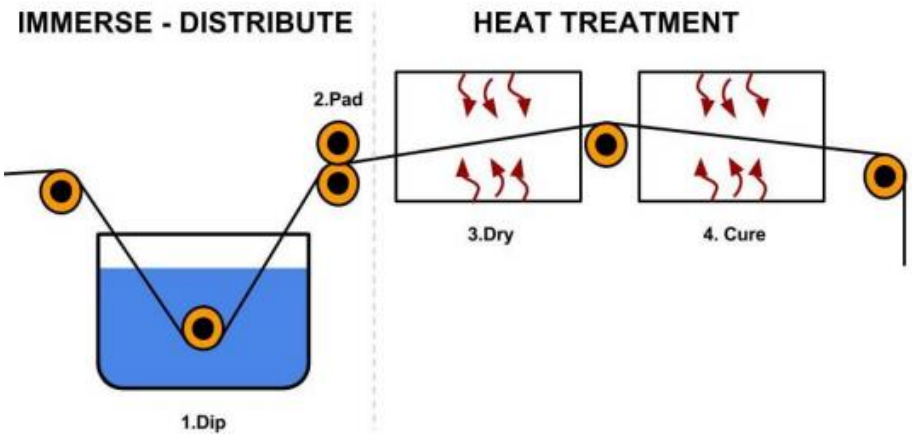

Figure 2-2. Illustration of the industrialized version of the dip-pad-dry-cure method used to apply the photo responsive materials on the textile substrate [26]**.**

Yang et al. prepared a superhydrophobic and photocatalytic self-cleaning cotton fabric by a sol–gel method. In this method, the glacial acetic acid was catalysed and then modified by heptadecafluoro-1,1,2,2-tetrahydrodecyl triethoxysilane (F-17) solution, which could provide superhydrophobicity owing to its low-energy hydrophobic groups (–CF_2, –CF_3). The achieved self-cleaning property was

excellent toward solid pollutants, daily liquids, oil, and organic chemicals [29]. Ahmad et al. presented a visible-light-driven self-cleaning cotton fabric coated with dye-sensitized TiO_2 nano-sol by the dip-coating (dip–pad–dry–cure) method. A phthalocyanine (PC) reactive dye (RB-25) was used for the photosensitization of the TiO_2. The coated textiles demonstrated good photocatalytic and self-cleaning results under visible light [7]. Qi et al. produced nanocrystalline anatase coatings on a cotton fabric surface under ambient pressure. They used hydrolysis of TiO_2 in an acidic aqueous solution and coated the fabric by the sol–gel (dip-pad–dry-cure) process. The TiO_2-coated cotton textile showed significant photocatalytic self-cleaning properties. [30]. Zhu et al. fabricated self-cleaning cotton fabrics by coating photocatalytic ZnO NPs on cotton surfaces, using a traditional dip-coating (dip–pad–dry–cure) process. The self-cleaning tests showed that the coated fabrics demonstrated good photocatalytic activity against methylene blue (MB) solution, good durability, and excellent UV blocking properties. As for wash fastness, it showed colour removal after 10 washing cycles under light irradiation, as shown in Figure 2-3. These findings provide a potential model for the practical application of self-cleaning textiles [22]. The sol–

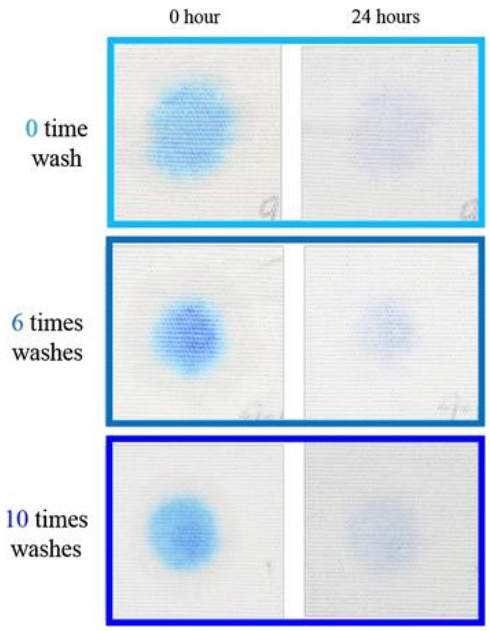

Figure 2-3. Wash fastness of ZnONPs coated cotton fabrics, showing different wash times [22]**.**

gel method is considered to be a high-quality, cost-efficient, low-thermal energy, and low-pressure procedure that can develop rough surfaces and fabricate superhydrophobic surfaces. It is often used to create the bond between NPs and a fabric [11]. Peter et al. decorated a cotton fabric surface with synthesized TiO_2 using the sol–gel approach. The TiO_2 fabrics became hydrophobic and exhibited a self-cleaning character successfully[31]. Montazer and Pakdel treated raw wool fabric and oxidized it by nano TiO_2 powder in an ultrasonic bath. They used butane tetracarboxylic acid and sodium hypophosphite as a catalyst to link this article to the wool surface. The self-cleaning property was achieved, and the increase in the concentration of nano TiO_2 in the bath can help to improve the property [32]. Galkina et al. produced modified cotton fibers with good self-cleaning properties. A nanocrystalline sol TiO_2 was obtained, and the aspects of cross- linking of TiO_2NP_s and 1,2,3,4 butane tetracarboxylic acid as a spacer were used. Photoactive nanoparticles were formed using a low-temperature sol-gel synthesis, which led to the formation of titanium dioxide of anatase-brookite modification [33]. Afzal et al. presented a new class of self-cleaning textiles with meso-tetra(4-carboxyphenyl) porphyrin (TCPP) followed by hydrophilization with trimethoxy octadecyl silane (OTMS). They used a simple post adsorption method that contained a stepwise deposition of anatase TiO_2. The prepared cotton fabrics showed successful superhydrophobic and visible-light photocatalytic activities along with self-cleaning ability [18]. Similarly, they coated another cotton fabric surface with thin films of TCPP with different metal centers (MTCPP, M ¼ Fe, Co, and ZnO) in combination with anatase TiO_2. The MTCPP/TiO_2-coated cotton fabrics developed a significant photocatalytic activity[34]. Zhu et al. combined photoactive TiO_2 and superhydrophobic SiO_2 to make TiO_2–SiO_2 composite particles with fluorine-free superhydrophobic cotton fabrics. The fabric showed superhydrophobic and photocatalytic properties along with excellent self-cleaning performance[22]. Pakdel et al. applied TiO_2 and TiO_2–SiO_2 nanocomposites on wool fabrics through a low-temperature sol–gel method. Titanium tetraisopropoxide (TTIP) and tetraethylorthosilicate (TEOS) were employed as precursors. The self-cleaning function and hydrophilicity of wool fabrics were

successfully prepared [35]. Tian et al. fabricated self-cleaning cotton fabric with superhydrophobicity and high amphiphilicity by building micro–nano structures with low surface energy. The TiO_2 and SiO_2NP_s blended by hydrolytic (heptadecafluoro-1,1,2,2-tetrahydrodecyl triethoxysilane) trimethoxysilane (F-17) were modified and co-deposited onto the cotton fabric. They used two different coating methods: (1) suction filtration for immobilizing the modified TiO_2/SiO_2 onto cotton fabric based on swollen cellulose action by N-methyl morpholine-N-oxide (NMMO) solution; (2) adhesion by spraying waterborne polyurethane (WPU) before coating. The accomplished self-cleaning fabric achieved excellent water and oil-repellency. It is considered a beneficial tool to improve the performance of textile production and provide new or enhanced properties [36]. In contrast, the cost of NP_s in mass production is expensive. It impacts the environment and human health due to the uncontrolled release of NP_s and the whole ecosystem is widely covered under the state of “nanotoxicology”[37].

2.2.2 Spin Coating Method

The process contains three steps: deposition, spinning, and curing. The substrate is deposited on the turntable then spun up and off, while the evaporation stage occurs at the end [38]. Teknologi et al. prepared a self-cleaning cotton textile by interacting an acrylic acid binder as a cross-linking agent followed by TiO_2–SiO_2 clusters using a spin-dip-coating machine. The qualitative measurement of the self-cleaning agent was carried out by observing the ability of the modified cotton textile ($3 \times 3\ \mathrm{cm}^2$) to degrade $75\ \mu\mathrm{L}$ of MB spot ($15\ \mathrm{ppm}$) under UV light. The quantitative measurement was carried out by checking the ability of the cotton textile to reduce $20\ \mathrm{mL}$ of 15 ppm MB spot in a $1 \times 1\ \mathrm{cm}^2$ cotton textile. The coated samples with Ti:Si molar ratios of (1:1), (1:2) and (2:1) at different dipping durations showed different results, as in Figure 2-4. From the results of the MB degradation under UV irradiation, the best self-cleaning effect was shown by the cotton textile coated with TiO_2–SiO_2 with a Ti:Si molar ratio of (1:2) [39]. Spin coating is generally used in the microelectronics industry, whereas it is less

popular in the textile coating industry [40]. It is considered a low-cost method used to deposit thin films on flat substrates [38].

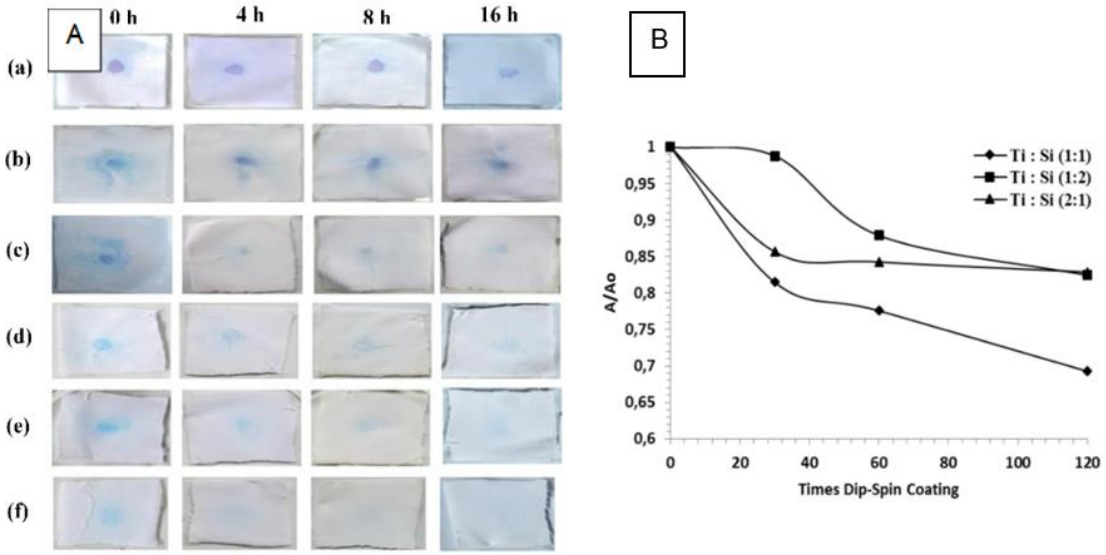

Figure 2-4 A. The degradation of methylene blue spot in cotton textile by dipping in acrylic acid for 24 h on (a) non-coated cotton; (b) cotton coatedwithTiO_2;(c) cotton coated with SiO_2; (d) cotton coated with TiO_2-SiO_2(1:1); (e) cotton coated with TiO_2-SiO_2(2:1) and (f) cotton coated with TiO_2-SiO_2(1:2). B. The degradation pattern of methylene blue on cotton fibres coated with different Ti:Si molar ratio under UV irradiation at ʎmax= 661 nm [39]**.**

2.2.3 Spray Coating and Electro-Spraying Method

Yao et al. modified a textile surface by fabricating a two-dimensional (2D) graphitic carbon nitride nanosheet (CNNS). The colloidal suspension of the CNNS was directly sprayed on the surface of the textile. These textiles obtained an excellent photocatalytic self-cleaning property [41]. Roy et al. developed a simple method with a sustainable superhydrophobic coating to produce self-cleaning–healing fabrics. The coating was created using cellulose nanofibers (CNF_s) as the raw material and spraying it on polyester and cotton fabrics. They became superhydrophobic with outstanding self-cleaning–healing ability [42]. An alternative method was used by Shams-Ghahfarokhi et al., who successfully coated polyester fabrics with silica aerogel particles using a fluorocarbon finishing

method via the electro-spraying process. They showed high insulation properties and high hydrophobicity with low dust-releasing behaviour. The results implied that the aerogel particles improved the hydrophobic properties of the electro-sprayed samples. Images of the un-sprayed and electro-sprayed polyester fabrics with the aerogel/fluorocarbon mixture for 16 h together and the sessile water droplets on their surfaces are present in Figure 2-5 [24].

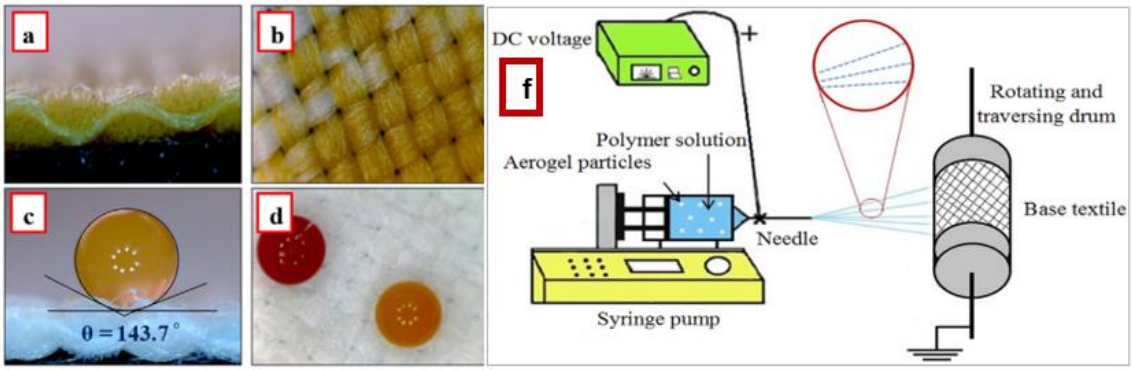

Figure 2-5. Sessile water droplets on the (a and b) un-sprayed, and (c and d) electro-sprayed polyester fabrics with the aerogel/fluorocarbon mixture for 16 *h*. (f) a schematic design for the basic setup of the electro-spraying device used in this study [24]**.**

Li et al. prepared a superhydrophobic and a robust superhydrophobic coated cotton woven fabric. A one-step single-solvent electro-sprayed polycaprolactone (PCL), which is considered to have excellent biocompatibility and degradation and low immunogenicity, along with honeycomb-like hierarchical structure microspheres (PCL-*b*-PTFOA) and abundant nano-meter pores of (PCL-*b*-PEG400) microspheres were used. They were fabricated by solvent evaporation and copolymer diffusion-induced separation during the electro-spraying. The coated fabric surface exhibited excellent self-cleaning and laundering durability properties, and good washing fastness against mechanical abrasion without significantly reducing the water contact angle (WCA). The bonding stability of PCL-*b*-PTFOA(4h) microsphere-coated cotton fabric was measured by liner abrasion [43]. As shown in Figure 2-6, the superhydrophobic property of coated fabric was decreased with the loss of microspheres. Figure 2-6 (A) shows the

coated fabric, and the result in Figure 2-6 (B) shows minor wear and tear in the scanning electron microscopy (SEM) morphology of the coated fabric, but the film was still able to repel water with a WCA of 150.6° after 10 abrasion cycles. However, once rubbed for 20 cycles, many microspheres were removed, part of the fibres were worn down, and the WCA decreased to 143.5°, as shown in Figure 2-6 (C). It was found that dyed water droplets maintained a spherical shape on the coated fabric surface with a WCA of 151.3 ± 0.5° after five tape adhesion cycles as shown in Figure 2-6 (D) [43]. The spray coating and electro-spraying coating of block copolymers can provide a simple, facile, and promising technique for producing multifunctional textiles. It can be easily applied to a large surface area and does not involve complicated and costly processes [41], [43].

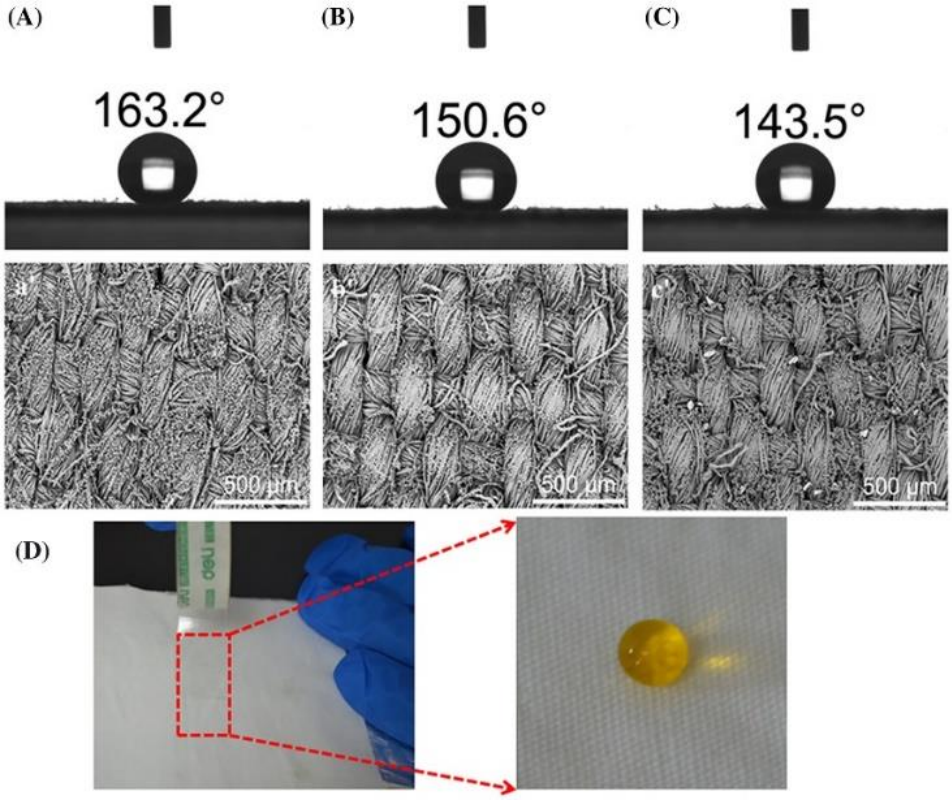

Figure 2-6. The abrasion and mechanical durability of PCL-PTFOA(4h) microsphere-coated cotton fabric. A to C, sandpaper abrasion tests and D, tape adhesion tests [43]**.**

2.2.4 Electrospinning Method

Electrospinning is a method that produces a nano-scale fibre both in laboratories and industrially. The basic principles of the electrospinning process consist of three main components: a feeding system, a high-voltage power supply, and a grounded collector [44]. Bedford et al. created photocatalytic self-cleaning textile fibres by using coaxial electrospinning. They used cellulose acetate for the core phase and dispersion of nanocrystalline TiO_2, as shown in Figure 2-7 [45]. Electrospinning is a promising technique to create superhydrophobic self-cleaning surfaces, which obtains the basic surface morphology due to a comprehensive set of parameters that effectively control the resulting web roughness. On the other hand, a manufacturing process that includes various steps is usually more expensive than a single-step process. The primary issue is the low production rate of single nozzle electrospinning. Therefore, needleless electrospinning was studied in several research studies with a higher production rate and was used for mass-scale production of electro-spun webs [46].

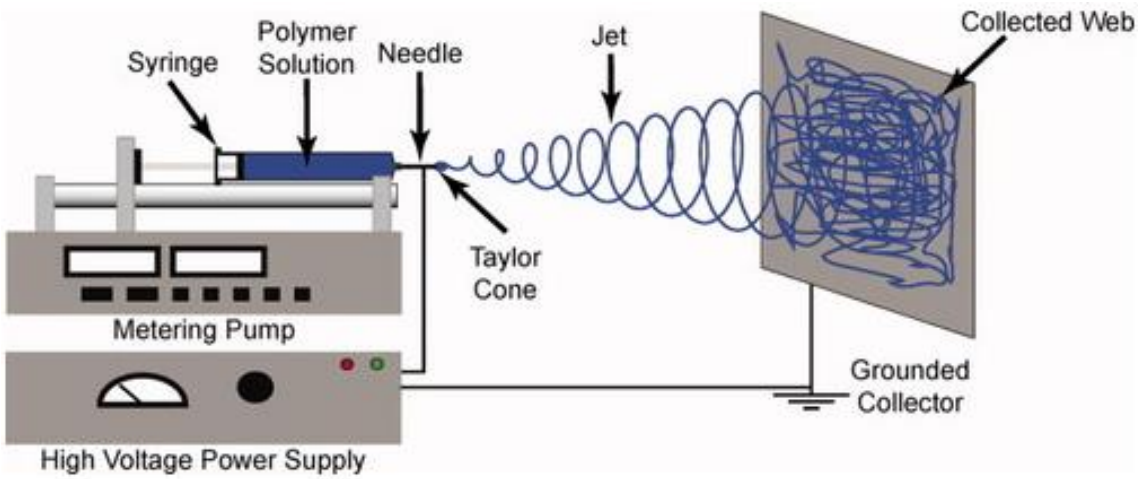

Figure 2-7. Schematic of the basic set-up for electrospinning [46]**.**

2.2.5 Chemical Etching and Chemical Vapour Deposition (CVD) Methods

Chemical etching and chemical vapour deposition (CVD) methods are used with polymers to fabricate functional surfaces with different geometries. They make

the surface exhibit hydrophilic and hydrophobic properties [47],[48]. Zheng et al. successfully created washable and wear-resistant superhydrophobic polyester resistant polyethylene terephthalate (PET) and developed a superhydrophobic and self-cleaning polyester fabric from a mixture of methyl trichlorosilane (MTS) and dimethyl dichlorvos silane (DDS) solution at the micro- and nanoscale. It was grown and fabricated with a layer of polydimethylsiloxane (PDMS) nanofilaments onto textile fibres [49]. Zareei Pour et al. coated a self-cleaning superhydrophobic and super-oleophilic commercial textile with an effective oil–water separation. The micro–nano meter scale roughness was achieved by a single fabrication step using a handmade CVD device, as presented in Figure 2-8 [47].

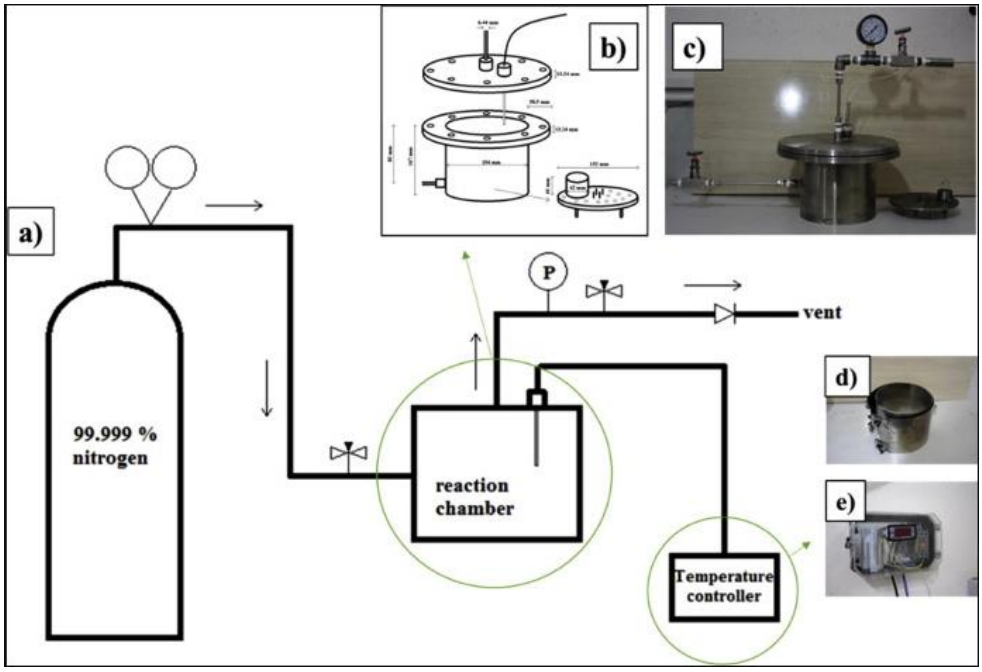

Figure 2-8. (a) Schematic diagram of the textile coating setup, (b) Schematic and dimensions of the CVD reaction chamber, (c) picture of CVD reaction chamber, (d) heating element, and (e) temperature controller [47]**.**

2.2.6 Hydrothermal Treatment (HTT) Method

Hydrothermal treatment (HTT) is considered an environmentally friendly technology. It is a basic technique that can effectively control the geomorphology of NPs, nanowires, and mesoporous inorganics [50]. Li et al. developed a facile

one-pot hydrothermal reaction method to create micro/nanostructure flower-like TiO_2 particles modified with fluoroalkyl silanes on the cotton fabric surface. The as-prepared TiO_2 cotton exhibited super-hydrophobicity, self-cleaning properties, laundering durability, and oil/water separation [51]. Huang et al. prepared a composite TiO_2 cotton fabric by a simple self-assembling coating process by soaking in a mixed methanolic solution of hydrolyzed puorodecyltriethoxysilane (PTES) and F-17 solution. They created marigold flower-like hierarchical TiO_2 particles through a one-pot hydrothermal reaction on the surface. The superhydrophobic F-17/TiO_2-coated fabrics showed excellent mechanical and environmental stability, good anti-UV ability, effective self-cleaning, and oil–water separation [52]. Tan et al. formed two kinds of self-cleaning cotton fabrics coated with TiO_2 NP_s by dipping the fabrics in the TiO_2 sols by peptizing and hydrothermal methods. The two methods were successful and showed high photocatalytic activity and good self-cleaning performance [53].

2.2.7 Layer-by-Layer Self-Assembly (LBL) Method

The layer-by-layer (LBL) assembly method is an efficient, facile, and multipurpose strategy for coating substrates with multilayers of different structures, properties, and functions for many applications, such as dipping, immobilization, spinning, spraying, and electrodeposition [54]. Uğur et al. coated a denim fabric with TiO2 NPs using the LBL deposition process as a continuous method. The coated denim fabrics showed self-cleaning properties, especially with the increase of NP concentration [55]. Hua et al. fabricated superhydrophobic, flame-retardant, and conductive cotton fabrics. They applied LBL assembly of polyethyleneimine, ammonium polyphosphate, CNTs, and post-treatment with PDMS at the end. The developed fabrics showed excellent superhydrophobic stability toward acid, alkali, organic solvent, UV irradiation, scratching, and long-time laundering. It provided an efficient layer on the cotton fabric surface to prevent the fiber from damage when it is burned, as shown in Figure 2-9 [1]. The LBL self-assembly methods provide the simplicity of process and equipment and the availability of materials and solutions, along with the flexibility of application to substances of

different shapes and sizes. They are suitable for most surfaces, and the control over the required thickness is stabilized [23].

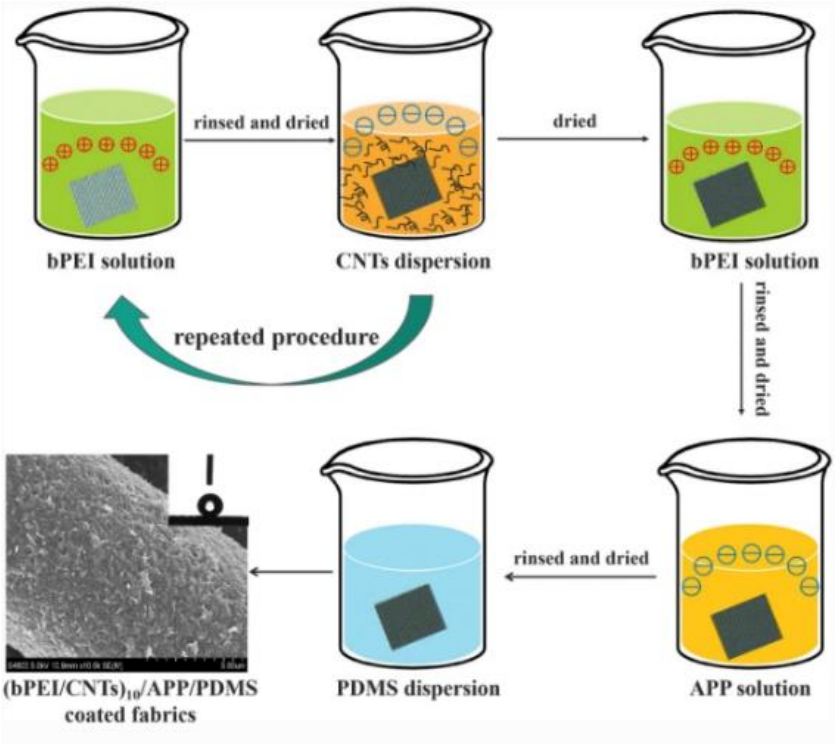

Figure 2-9. Schematic illustration of the fabrication of multifunctional superhydrophobic fabric.40 b PEI: sequential assembly of poly(ethylenimine); APP: ammonium polyphosphate; CNT_s: carbon nanotubes; PDMS: post-treatment with poly(dimethylsiloxane) [55]**.**

2.2.8 Wet Chemical Synthesis Method

The wet chemical synthesis method controls the structure of the produced nanostructures, NPs, nanowires, and mesoporous inorganics. This method has been commonly used to fabricate superhydrophobic surfaces [56],[57]. Komeily-Nia et al. coated multifunctional nylon fabric to form finely dispersed CuO/MnO_2 core/shell nanostructures on the surface via a wet chemical (in situ) [58]. Moridi-Mahdieh et al. coated a polyester/cellulose fabric by a facile single-step (in situ) synthesis method for $Ag–TiO_2$ NPs without adding any chemical agents. The fabric was immersed in a suspension containing TiO_2 NPs/$AgNO_3$ and then squeezed. The coated fabric showed good self-

cleaning [59]. Panda et al. coated cotton fabric by using two silane trichloro octadecyl silane (OTS) and pentafluorophenyl triethoxysilane (FAS) with a wet chemical immersion technique. The coated cotton fabric showed excellent self-cleaning and oil–water separation properties, making it suitable for industrial applications [60]. Jiang et al. treated cotton fabric with two kinds of nano TiO_2–polyacrylate hybrid dispersions. They were synthesized by in-situ suspension and solution immersion, respectively, to fix the nano TiO_2 on fabrics [61]. It is an efficient way for immobilizing nano TiO_2 on self-cleaning cotton fabrics successfully and a facile, cost-effective single-step method for superhydrophobic coating fabrication [62].

2.3 The Development of Self-Cleaning Textiles with Additional Properties

Superhydrophobic surfaces can be modified by improving specific properties through surface functionalization and combining new materials and technologies [36]. Currently, the development of textile finishes makes it possible to produce self-cleaning textiles with many properties, such as antimicrobial, UV protection, laundering durability, and water/oil repellence.

2.3.1 Antimicrobial Properties.

Karimi et al. coated cotton fabric with graphene oxide and the composite of TiO_2 with a simple dipping coating method. The treated cotton showed excellent self-cleaning and antimicrobial activity [63]. Scacchetti et al. prepared self-cleaning, antimicrobial cotton fabrics by a finishing process that combines microcapsules of phase change materials (MPCMs) and TiO_2 NPs [64]. Liu et al. dyed cotton fabrics with TiO_2 by adding cross-linking agents using the dip-coating process. The prepared fabrics showed excellent self-cleaning properties and UV light fastness, and improved antimicrobial activity [65]. Pakdel et al. coated wool fabrics by the functionality of TiO_2 NP sol, TiO_2/SiO_2, TiO_2/metal, and TiO_2/metal/SiO_2. They were modified by incorporating three types of noble metals (Ag, Au, and Pt) and silica under visible light through a low-temperature sol–gel

method. The coated wool fabrics showed an enhanced visible-light-induced self-cleaning property and, photocatalytic and antimicrobial activities [66]. Hebeish et al. coated antimicrobial and self-cleaning cotton textiles with TiO_2 nanowires and TiO_2 nanowire doped (Ag-PVP) nanocomposites. An alkaline solid medium by the hydrothermal method was used with TiO_2 NPs as a precursor. Based on the above results, coated cotton fabrics could be promising for possible medical and industrial applications [67]. Sundaresan et al. successfully treated cotton fabrics with nano TiO_2 combined with an acrylic binder. The layer was added on the cotton fabric surface by using the dip-coating method. It provided antimicrobial activity, UV protection, and self-cleaning ability[68].

2.3.2 UV-Protection Properties.

Abidi et al. modified cotton fabric by titania nano-sols prepared through the sol–gel process with tetrabutylorthotitanate [Ti $(OC4H9)_4$] as the active ingredient. The photocatalytic properties of titania nano solid treatment on the fabric surface imparted self-cleaning properties to the cotton fabric and showed excellent UV protection [69]. Wang al. coated a cotton textile with ZnO–SiO_2 nanorods to maintain superhydrophobic and UV blocking properties. The treated cotton textile showed an excellent UV blocking property with UV protection and durable superhydrophobicity under UV irradiation. This multifunctional cotton textile will have potential applications in various areas, such as medical, military, and biological industrial fields [70]. Qi et al. treated polyester fibres with low-temperature plasma coated with anatase TiO_2 prepared by an aqueous sol–gel process. The coated polyester showed significant improvement in self-cleaning performance, adhesion, and excellent UV protection [71]. Ahmed et al. coated pristine cotton fabric with Reactive Blue 21 (RB-21)/(TiO2) sol by the sol–gel method. It showed an excellent UV protection and photocatalytic self-cleaning performance [72]. Mishra et al. coated cotton fabric with TiO2 by using the sol–gel technique and a precursor through three different process routes (pad–dry–cure, pad–dry–hydrothermal, and pad–dry–solvothermal) to provide a stable

coating and improved wash durability, UV protection, and self-cleaning property successfully [73].

2.3.3 Water/Oil Separation Properties.

Jin et al. coated a superhydrophobic cotton textile by a cost-effective and straightforward dip-coating route using ZnO sol and mercapto silanes. Hydrophobic treated 3-mercaptopyl trimethoxysilane (MTS) and dodecafluoroheptyl methacrylate (DFMA) with thiol–ene click chemistry reaction was included. The prepared cotton superhydrophobic showed excellent self-cleaning and oil–water separation properties along with acid resistance [74]. Yang et al. fabricated robust superhydrophobic fabric by modifying the surface with anatase TiO_2 sol and mercapto silanes followed by hydrophilization with perfluorooctyl methacrylate (PFOMA) and the thiol–ene click reaction. The fabric showed great self-cleaning, along with photocatalytic degradation and resistance to intense acidic or alkaline environments. It also demonstrated excellent wettability behaviour and promising application in oil–water separation [75].

2.3.4 Laundering and Rubbing Durability.

Liu et al. presented self-cleaning cotton by immobilizing TiO_2 NPs onto the surface with co-graft polymerization of 2-hydroxyethyl acrylate (HEA). It showed improved hydrophilicity and photocatalyzed self-cleaning ability, well-retained after 30 accelerated laundering cycles [76] . Ashraf et al. grew ZnO seed into ZnO nanorods, then placed it on a polyester fabric surface and finalized it using the hydrothermal method. The functionalized fabric showed self-cleaning under UV light, excellent washing fastness, and good rubbing durability [77].

Previous studies examined the influence of microscopic features on textile fabrics at two different levels: the surface coating level with nanotechnology and the microscopic features at the fabric woven structural level. This research review seeks to identify the microscopic features and their influence on the self-cleaning ability of textile fabrics. The features mainly focused on are roughness, porosity,

and wettability. A detailed discussion of their influence from the existing literature is provided in the following sections.

2.4 The Influence of Microscopic Features on Textile Fabrics Self-Cleaning Ability

2.4.1 Microscopic Features at Self-Cleaning Coating Level

The surface of the textile fabrics is not flat, and its geometrical roughness is considerable and plays a significant role in the use of the fabric. The surface roughness amplifies the water-repellence of hydrophobic materials. In addition, the surface roughness and surface energy are two significant factors affecting the wettability, as shown in Figure 2-10 [51].

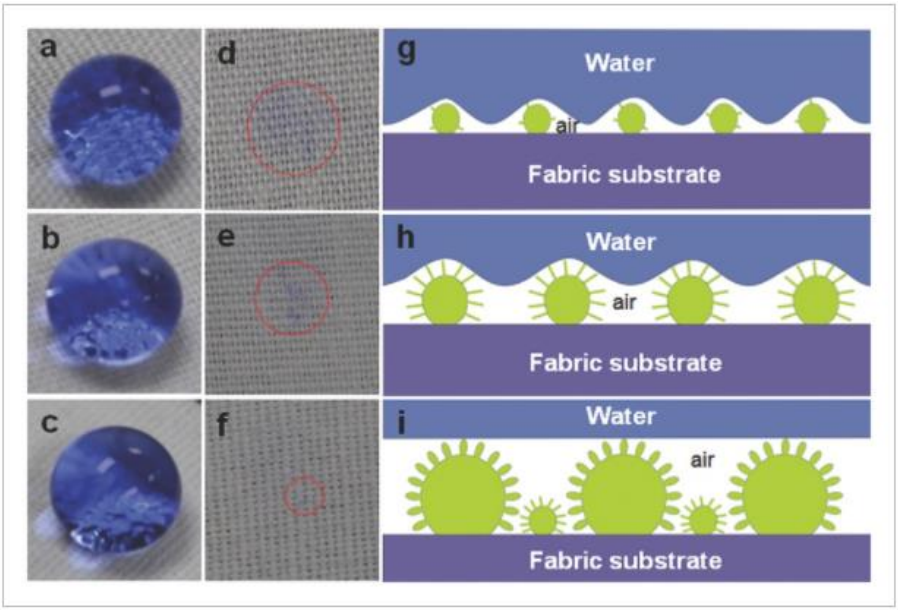

Figure 2-10. Optical photographs of water droplets dyed with methyl blue on superhydrophobic TiO_2@Cotton fabric surfaces with different adhesion a–c) and the surface traces after the water droplet left the cotton fabrics d–f). Schematic illustration of three types of solid/liquid/air three-phase contact models with adhesive forces ranging from high to low: g) "area" contact model with high adhesion; h) "line" contact model with medium adhesion; i) "point" contact model with low adhesion [51]**.**

The porosity which is the ratio of air volume to the total volume of a surface, is an important parameter. Therefore, the total porosity of woven fabrics usually comprises two types of porosity: the microporosity caused by the void spaces between fibres in yarns and the microporosity resulting from the void spaces between yarns [78]. The chemical properties and surface microstructure control the wettability of a solid surface with a liquid. It is determent by the interfacial energy between the solid, liquid, and vapour phases. Wetting is the term used to describe the study of how a drop of liquid spreads out on a solid surface and is divided into two different systems: total wetting and partial wetting [79],[80]. The contact angles (CAs) between a liquid with known surface tension and a solid are measured to evaluate the surface energy. Superhydrophobic surfaces should exhibit CAs with water greater than 150 ° and lower surface tensions than water. The principles of this fabrication were founded by Chen et al., who described CAs and different mechanisms of wetting on rough surfaces. According to Wenzel's model, the roughness factor plays an essential role in influencing the wettability of the surface where the roughness effects enhance both the hydrophobicity and WCA [81]. Ganesh et al. classified the production of hydrophobic and superhydrophobic surfaces into two kinds of approaches: (a) making a rough surface from a low surface energy material; (b) modifying the rough surface with low surface energy materials to produce superhydrophobic layers using chemicals such as silicones, PDMS, which is an organosilicon compound, inorganic materials, such as ZnO and TiO_2, and organic materials, such as low-density polyethylene (LDPE) [19]. Shim et al. designed a polyester woven fabric treated for surface energy with low surface tension materials such as silicone or fluoropolymer. Using the Cassie-Baxter equation, the contacts angles of the woven fabrics coated with silicone and fluoropolymer were determined. Both the silicone-treated and the fluoropolymer-treated fabrics showed high CAs from 131° to 156°. The woven fabrics were modelled for their structural definition and roughness estimation, and the models were fitted based on the wetting behaviour of the various fabric types. as shown in Figure 2-11[82]. Yang et al. coated cotton textile with the TiO_2 NPs nanoparticles and (heptadecafluoro-1,1,2,2-

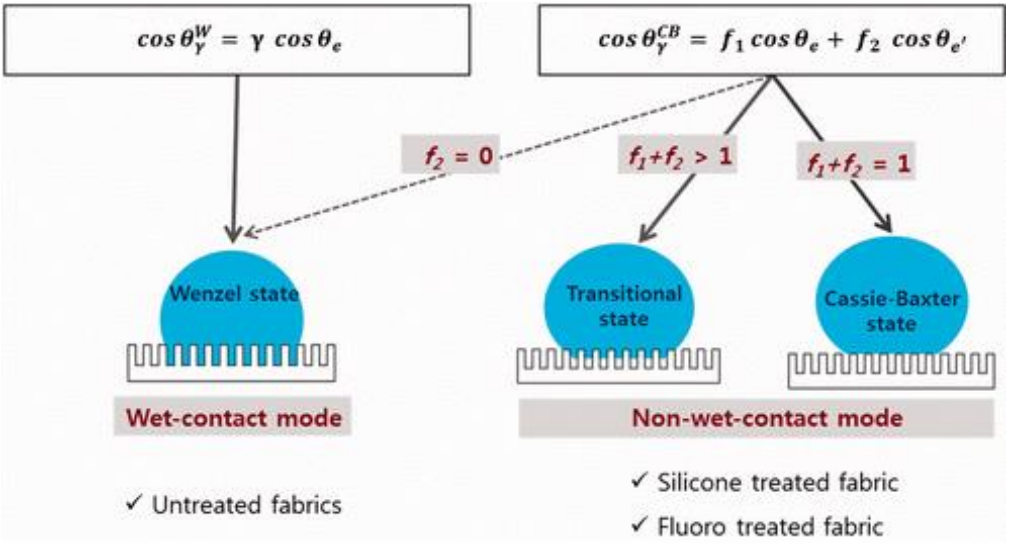

Figure 2-11. Wetting characteristic with models applied[82]**.**

tetrahydrodecyl) triethoxysilane (F-17) chemical to obtain the appropriate hierarchical roughness for superhydrophobic textile. The textile exhibited super-hydrophobicity with a wettability (CAs) of 160°, owing to the co-operative effect of the micro-/nano-binary surface and the low surface energy materials [75]. A thin transparent layer of nanocrystalline titania (TiO_2) particles can make the fabric surface rougher, therefore creating superhydrophobic textiles. For TiO_2/TCPP- coated fabrics, the super-hydrophobic character was achieved by combining the effect of surface roughness and the TiO_2 particles with low surface energy chemicals such as trimethoxy(octadecyl)silane (OTMS) [83]. Gao et al. created a super-hydrophobic coating composed of hybrid PVDF/SiO_2 microspheres in which SiO_2 was mainly trapped inside the PVDF microsphere with a low nanoparticle absorption. SiO_2 NP_s were uniformly distributed on the microsphere surface with increased concentration, exhibiting a hierarchical microstructure. An SiO_2 membrane was fabricated with a low CA of less than 140° and a high sliding angle (SA) of large than 90° [84]. Zhu et al. constructed the surface roughness of self-cleaning cotton fabric with "air cushion" (static air in it) by modifying (TiO_2/SiO_2) NPs of different sizes. A nanoarchitecture with low surface energy was successfully fabricated on the fabric surface and excellent water-repellence and oil-repellence were obtained, based on the contact angles

of 151.9° for water and 133.1° for diesel oil, respectively [85]. Chemical treatments on fabric surfaces were used to achieve low surface tension and rougher surfaces, which can also affect the visual wettability and WCA for determining the hydrophobicity of the surfaces [86],[87] ,[88].

Moreover, as woven fabrics essentially possess multiscale void spaces (porosity) and roughness due to the yarn and fabric structure, it is essential to consider them in order to create the liquid–vapour interface so that the area of the liquid contacting the solid can be reduced [89]. For this, surface roughening is required to reduce the spreading of a liquid on a solid surface, while the wetting behaviour controls the surface energy and the geometric structure of the surface [90].

2.4.2 Microscopic Features at Woven Structural Level

Weaving is the process of joining two upright sets of yarns, called the warp and the weft, to form a fabric. During the weaving process, warp yarns are fixed to the loom while weft yarns are inserted crossways. Depending on the pattern in which warps are raised, fabrics with very different forms and mechanical properties were produced [91]. The geometrical structures of fibres, yarns, and fabrics are considered important to magnify the energy of a surface. Thus, many researchers have focused on the morphology of fibre surfaces [92]. Nagamadhu et al. studied the dynamic mechanical properties of the three different woven structures of sisal fabric, as shown in Figure 2-12, Weft Rib (WR), (Plain1-Plain 2) P1-P2. The difference between Plain 1 and Plain 2 is grams per square meter (GSM); Plain 1 is heavier than Plain 2. The influence of textile physical properties such as grams per unit area, yarn diameter, yarn spacing/fabric density, and woven pattern on thermo-mechanical properties of reinforced epoxy composites was investigated. Thermo-mechanical properties improved 3 to 4 times by changing the woven pattern as observed in the case of Weft Rib (WR) composite woven pattern which was better than (Plain1-Plain 2) P1-P2 [93]. Li et al. used three kinds of fabrics woven with familiar textures: plain, twill and honeycomb weave with identical warp and weft density, as shown in Figure 2-13. They investigated the effect of structural factors of woven fabrics on acoustic absorption property.

The results showed that there is no significant connection between fabric sound absorption performance and surface density, although porosity, pore size, and pore shape were essential factors affecting the acoustic properties [94]. Liu et al. formed woven, knitted, or nonwoven through weaving technology, affecting the electrical and electrochemical properties. Therefore, the effects of textile structures, including porosity and pore configuration, were also studied. The porosity and pore configuration of the fabrics had an essential effect on the

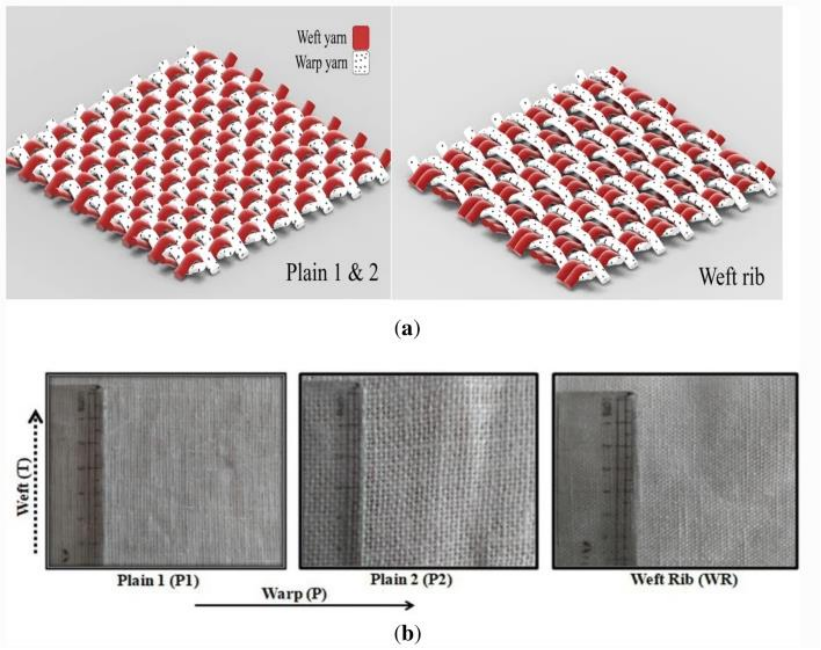

Figure 2-12. (a) Schematic of woven types prepared at OM Textile Industries. (b) Three types (two plain and one weft rib) of sisal woven pattern [93]**.**

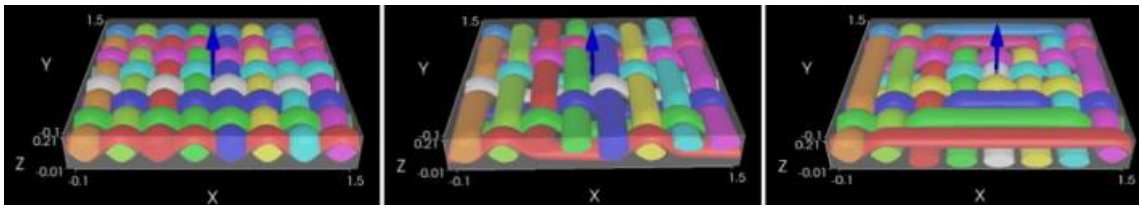

Figure 2-13. Patterns of plain, twill and honeycomb weave simulated with TexGen [95]**.**

Electrochemical properties. The woven one exhibited the best electrochemical performance compared with the other two fabrics, as the porosity and pore configuration can affect the self-cleaning ability [96]. Jaouani et al. measured

woven fabric structural and material parameters that affect dielectric properties and fabric surface roughness. The results were obtained by using 12 fabrics with different structures to measure their roughness. Moreover, it was noticed that the highest roughness values were on the plain weave and the lowest ones were on the sateen weave sample [97]. Huan et al. studied the influence of woven fabric structural and material parameters on dielectric properties. The yarn counts, fabric weaves, and fibre contents were the critical factors for different dielectric properties. The dielectric constants were associated with fabric yarn density, fabrics with high density, and fibres with high permittivity [98]. Asayesh et al. produced five different weave patterns (plain, hopsack 2/2, twill 2/2, twill 3/1, warp rib 2/2) with three different nominal weft densities and examined the effect of fabric structural parameters on the compressional properties. The results indicate that the compressibility parameters were affected by the fabric weft density and weave pattern. The increasing weft density decreases the dissipated compression energy and the fabric's compressibility [99]. Lim et al. developed a fabric with different weave structures (plain-woven fabric, 2/2 basket, and 2/1 twill) and studied the wetting behaviour of fabrics based on the geometry of woven fabrics: they obtained an improvement of the liquid-resistant/repellent surface. The results indicated that the CAs of the fabrics were the highest for plain-woven fabric, lower in 2/2 basket, and the lowest in 2/1 twill, (see Figure 2-14). These results are in line with experiments on synthetic woven fabrics [89]. Similarly, they created void spaces at multiple scales (i.e. macro, micro, and nano) to increase the energy surface that the liquid-vapour interface requires. They used different void spaces in the weft direction to obtain an oil-resistant or repellent surface. The created models implied that the oil resistance of the fabric increases as the void space increases [100].

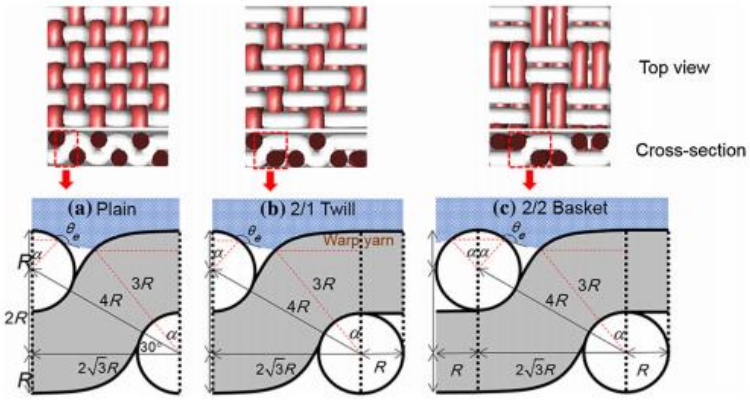

Figure 2-14. 3D images of three woven fabrics and geometries of unit structure with liquid depositions (from left to right): a) plain, b) 2/1 twill, and c) 2/2 basket [89]**.**

Researchers have examined the woven level by focusing on the strength and durability along with other properties. They used microscopic features to increase the mechanical strength of the fabric. However, they did not apply it to change the microscopic features at the woven level to make a self-cleaning ability. Changing the shape of the surface to obtain self-cleaning properties has been done in other areas, such as polymers. Researchers changed the geometry of the microscopic features of the top specimen surface to create a self-cleaning ability [101].

The previous efforts on self-cleaning processes were critically analysed as a particular focus is given to those efforts, which describe the influence of fabrics' inherent microscopic features on their self-cleaning ability. The associated challenges to obtaining a self-cleaning surface, in general, are provided below.

2.5 The Challenges in the Existing Processes for Making Self-Cleaning Textile Fabric and their Effectiveness

Despite the significant accomplishments that have been achieved for creating self-cleaning textile fabric, there are complexities and challenges. From Li et al. the connections between the textile and chemical reagents' primary mechanism during the fabrication process are difficult to handle. Most fabrication methods

hold only for laboratory use and are not suitable for large-scale industrial production. The mechanical durability of water-repellent fabric suffers from poor mechanical stability and durability during laundering [102]. Although many research experiments have worked successfully in the laboratory, they failed when used in real-time products. “Peeling off” of the coatings from the surface is a significant concern that must be addressed while developing self-cleaning. The coating should be deposited onto the surface to avoid any air gaps. The behaviour of the water droplets on the coated surface is an area that should be focused on as well. The produced coating should not allow the water droplets to assemble on the surface, but to just roll off. [103]. Dalawai et al. claim that the drawbacks of having a self-cleaning property were poor mechanical strength and lack of ability to withhold the surface property under severe environmental changes. Also, the use of hazardous chemicals and high-cost treatment that takes a longer time could affect the usage of the self-cleaning surface property in many applications [11]. Li et al. state that the major challenge of having flexible self-cleaning was the loss of the property due to the number of usages or after several washing cycles [104]. Padmanabhan and John. addressed some critical challenges and concerns in developing self-cleaning surfaces and coatings; the primary issue is based on the surface's mechanical durability and chemical stability after the coating. The exposure to detergents and outdoor temperature changes leads to the separation of the material from the surface or distortion to the used material, which increasingly reduced the coatings' performance. Taking a long time to decompose stains on the cloth, the mechanism of high decomposition power affects the fibres and the durability of the cloth due to repeated laundering cycles [105]. For Roy et al. for superhydrophobic self-cleaning textiles surface the low robustness of the coating limits applications; when mechanically or chemically damaged, they lose their hydrophobic property, and the performances will eventually decline. The main problem with the previous research studies is that they achieved the superhydrophobic surfaces on fabrics with the help of fluorinated compounds and various organic/inorganic NPs, which are harmful to the environment and human skin. Moreover, with the increase of

environmental pollution and climate changes, the demand for efficient and sustainable material sources has grown enormously. As a result, sustainability in superhydrophobic surfaces has become a priority and a significant challenge to researchers [106].

On the other hand, the effectiveness of having the self-cleaning ability has many benefits in various industries. They are reducing cleaning efforts which can improve environmental protection, making the textiles last longer by improving aging behaviour and extending surface purity. Heavy laundry bills can be reduced by lowering the number of washing cycles, as the new “easy-washable” textile is very economical and satisfies the market demand [20], [105]. Self-cleaning fabrics have environmentally friendly properties as they successfully reduce cleaning efforts, preserve a considerable amount of water and energy, and save time and money laundering [12],[107],[108]. Considering the limitations associated with surface coatings, such as surface peel off, chemical affinity with washing material, and so on, it is worth evaluating whether we can obtain the self-cleaning ability by using the geometrical microscopic features at the woven structural level, as ultimately this ability can be obtained by changing the surface roughness and surface energy level [109], [110].

2.6 IDENTIFICATION OF MICROSCOPIC GEOMETRICAL AND STRUCTURAL SELF-CLEANING FEATURES

2.6.1 Microscopic Geometrical and Structural Features of Self-Cleaning Surfaces

Many studies on the natural and bioinspired artificial surfaces reveal that special designs of microstructures bring special adhesion properties. For instance, the geometry and size of micro-and nanostructures have a great influence on the value of liquid-solid adhesion, such as low and high adhesion and directional adhesion on the superhydrophobic surface when the water droplet can easily roll off the surface in a specific direction (downward or upward) depending on the geometry of the surface and the direction of an airflow across the surface. It is shown that this unique ability called the direction-dependent arrangement of

flexible nanotips on the top of ridging nanostrips and microscales overlapped on the super-hydrophobic surface at the one-dimensional level as shown in Figure 2-15 [111]. Surface roughness improves the water-repellent property of the

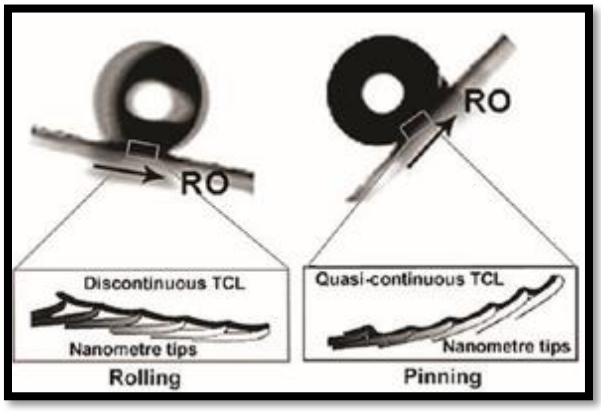

Figure 2-15. Two models proposed for the potential mechanism of distinct adhesion [111]**.**

hydrophobic materials. If the surface roughness geometry has parallel grooves, it can exhibit superhydrophilicity and self-cleaning property as shown in Figure 2-16 [112] In other cases, the re-entrant textures allow the possibility of creating

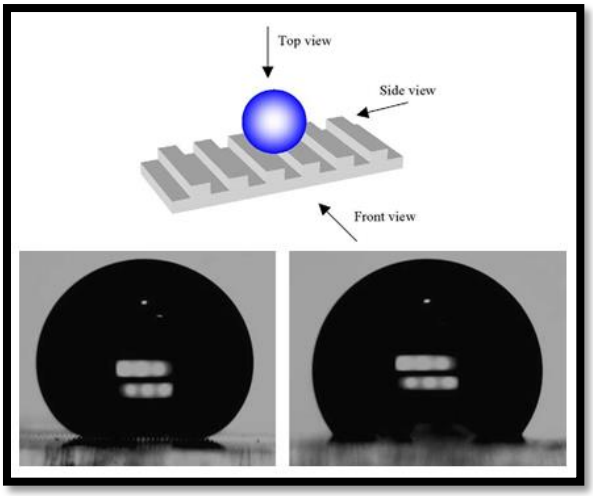

Figure 2-16. Front (left) and side (right) views of a sessile drop on a rough surface with parallel groove geometry. It is evident from the front view that the drop is sitting on top of the pillars [112]**.**

non-wetting surfaces that can support the Cassie state with water and various organic liquids. There is also a hydrophilic polyurethane mushroom-shaped tip ending the geometry of the micro-fibre arrays which can possess self-cleaning ability using the lotus effect; it is one of the significant design parameters for developing contamination-resistant polymer fibrillar adhesives. The fibre array can be a re-entrant textured surface, as in Figure 2-17 [113].

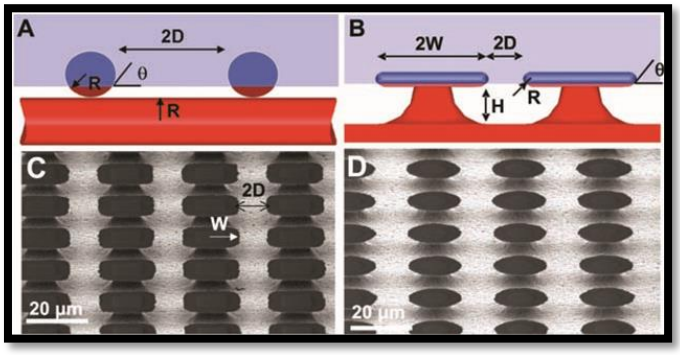

Figure 2-17. (A and B) Critical role of re-entrant curvature. The geometric parameters R, D, H, and W characterizing these surfaces are also shown. The blue surface is wetted while the red surface remains nonwetted when in contact with a liquid. (C and D) SEM micrographs for two micro-hoodoo surfaces having square and circular flat caps, respectively [113]**.**

It has been reported in many kinds of research that all super-hydrophobic and self-cleaning leaves consist of a fundamental hierarchical structure that can provide air pocket formation, leading to the least interaction area of a water droplet as in Figure 2-18[113]. Nano or microscale structures and low surface

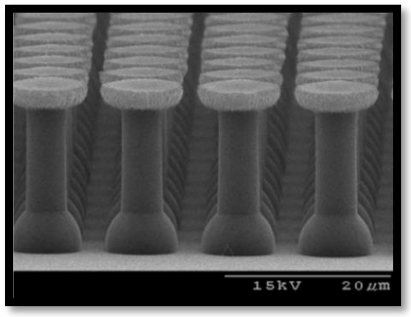

Figure 2-18. SEM image of a polyurethane mushroom-shaped microfiber array [113]**.**

energy is generally necessary to make superhydrophobic surfaces. Micro-, nano and hierarchical patterned structures have been made by using coating techniques which include the copying of micro patterns, self-assembly of hydrophobic alkanes, and a spray coating of carbon nanotubes as in Figure 2-19 [114]. In recent years, several groups have demonstrated the fabrication of

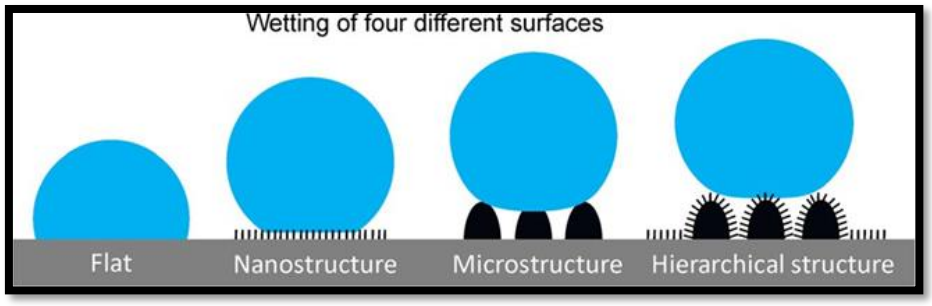

Figure 2-19. Schematic and wetting of the four different surfaces. The largest contact area between the droplet and the surface is given in flat and microstructure surfaces but is reduced in nanostructured surfaces and is minimized in hierarchical structured surface [114]**.**

photocatalytic TiO_2 materials anchored on cotton, wool, and cotton-polyester fabrics showing self-cleaning activity [115]. Another different combination of hierarchical, micro- nanostructures has been analysed for their application to self-cleaning surfaces, along with a static contact angle value of 170° with a hysteresis of 4° which was achieved with the fabrication of a multiscale structure with various geometrical parameters in a controlled manner as shown in Figure 2-20 [116]

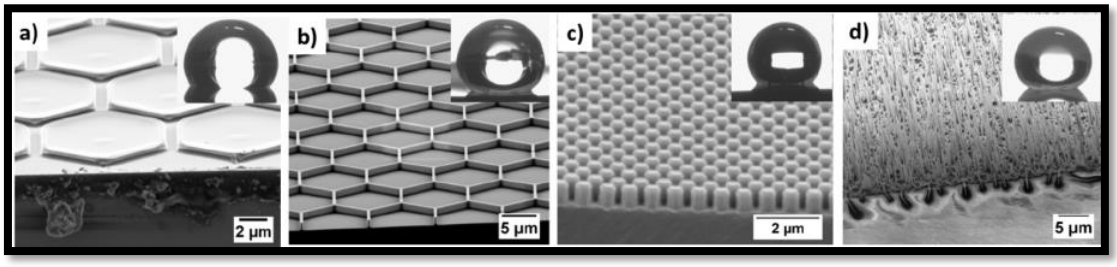

Figure 2-20. The nanostructures selected for the fabrication of the hierarchical structures and their static water contact angles. (a) Honeycomb pillars, (b) honeycomb lines, (c) nanopillars, (d) nano spikes [116]

Some studies explained how to obtain non-wetting surfaces by forming the 're-entrant' structures at the surface. The geometric parameters of the roughening structures such as the height, width, and thickness of the re-entrant structures are needed to have a self-cleaning effect on the fabric surface as in Figure 2-21 [57]

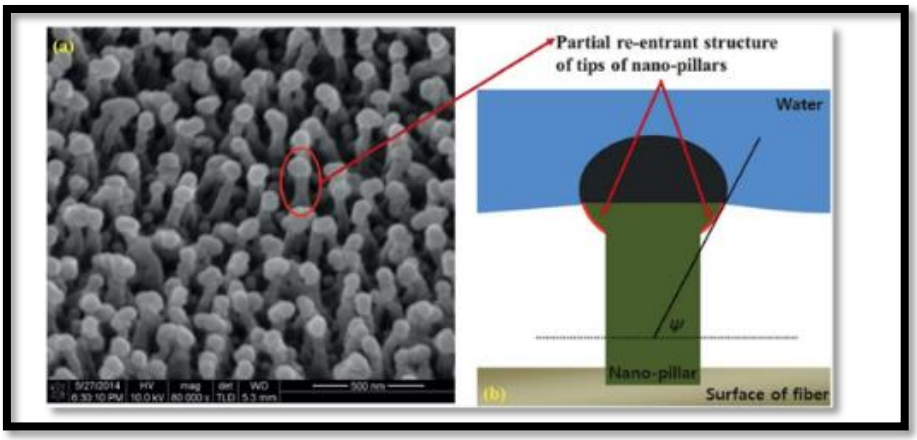

Figure 2-21. Partial re-entrant geometry at the head of the nano-pillars: (a) SEM image of film etched using oxygen plasma (b) illustration of the partial re-entrant structure of the produced nano-pillar [57]**.**

Changing the geometry of woven fabrics is important to improve the liquid-resistant/repellent surface properties such as self-cleaning. A super-hydrophobic character is increasingly required to attain effective liquid repellence. To have a superhydrophobic surface, we need to create appropriate roughness, porosity, and wettability behaviour. They have become the critical point of comprehensive and intensive research activity because of the steadily growing interest in technical textiles and composites.

2.6.2 Identifying the Key Microscopic Geometrical and Structural Features that Provide Self-Cleaning Ability in Fabric Textile Surfaces.

Identifying the key microscopic geometrical and structural features in textile fabric self-cleaning surfaces implies that changing the geometry of the woven fabrics is important and can improve the liquid-resistant/repellent surface properties [10].

Commonly, as mentioned in previous studies, the self-cleaning ability can be attributed to material concerning many microscopic features such as porosity (P = %), surface roughness (Ra= μm), and wettability contact angle (WCA=°C). The porosity was defined as the ratio of void space within the boundaries of solid material to the total volume [117]. The structure of a textile contains pores between the fibres and the yarns. Pore dimension and distribution are a function of the fabric geometry [118], as shown in Figure 2-22.These features are mainly responsible for this ability. The Porosity is the

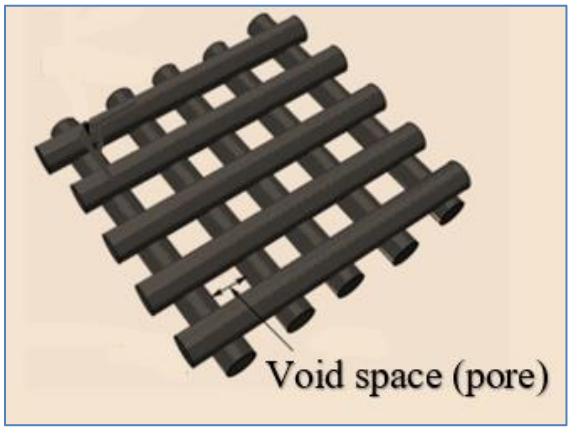

Figure 2-22. The porosity of textile fabrics [119]**.**

measurement of the void fraction in a surface. The structure of a textile contains pores between the fibres and the yarns. It is quite clear that pore dimension and distribution are a function of the fabric geometry [120]. Nevertheless, how fluid flows through a fabric is important in order to understand many of the physical and mechanical properties of it. When considering the fluid flow through textiles, the shape arrangement and size distribution of voids through which the fluid flows are of great importance [121].

The surface roughness is an important characteristic in a solid surface. It is a constituent of the surface texture. Any surface is made of three elements: roughness, waviness, and form with the wavelength of the surface particles [122]. It refers to the structural surface part, ranging from smooth to rough, depending on the material. These structures consist of a pattern and the main direction. A roughness value can be calculated on a profile (line) or a surface (area). The

profile roughness parameter (Ra, Rq) is more common, as shown in Figure 2-23 [123], [124]. The surface roughness can affect the water repellence for hydrophobic materials [125]. The water contact angle is dependent on the surface roughness, which is explained via two models: Cassie–Baxter and Wenzel. The Cassie–Baxter model explains the mixed wetting state with the Wenzel in which water in the surface holes traps the air, and because of which, the liquid and solid

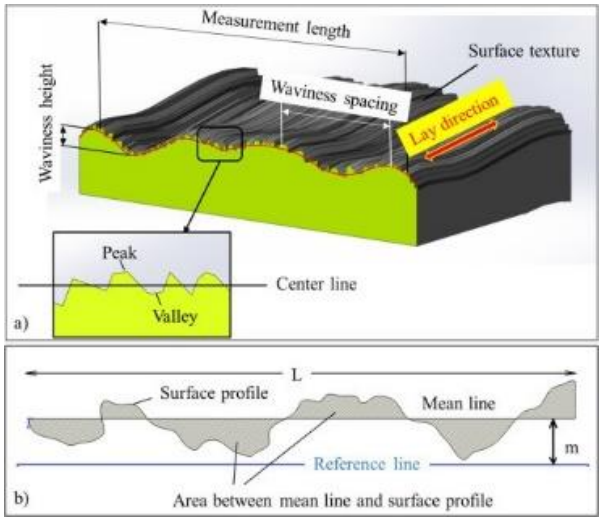

Figure 2-23. Terminology illustration of (a) surface texture (b) surface roughness (Ra) [123]**.**

interface area is reduced and the same between water and air is increased. This results in the formation of spherical droplets with lower hysteresis, and the hysteresis could be further reduced by increasing the roughness [126]. Surface roughness influences the observance of surface dust particles. It reduces the contact area between the surface and the particles (assuming the particles are larger than the surface holes), so it can be picked up by water [4]. We hypothesized that printing inputs such as line width and layer height have an apparent direct influence on roughness: there are more comprehensive lines and thicker layers; there are changes in print temperature; speed also affects roughness; and the print orientation angle can affect how the final part looks and feels [127].

The wettability of a solid surface with a liquid is controlled by its chemical properties and surface microstructure. It is described as the ability of a liquid to wet a surface; it is determined with the help of contact angle measurement. The three-phase contact point of solid–liquid-air interface is defined as the contact angle [128]. The surface contact angle is defined as the angle formed by the solid surface and the angle to the water droplet as shown in Figure 2-24 [129]. It is one of the most influential parameters during water droplet impact on a solid substrate [130],[131]. The wetting behaviour of a solid surface is controlled by both surface roughness and the geometric structure of the surface.

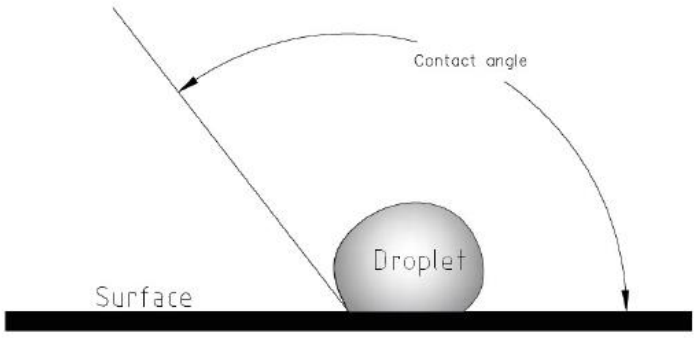

Figure 2-24. The image and measurement of contact angle of a water droplet on fabric surface [129]**.**

This research mainly focuses on improving the design of fabrics with self-cleaning properties by controlling the fabrication of parameters during manufacturing. Due to the benefits of additive printing, also known as 3D printing, in controlling the fabrication parameters compared to traditional manufacturing methods, 3D printing has enormous potential for manufacturing self-cleaning materials.

2.7 Analysing the Possibility to Create a Self-Cleaning Surface Using a 3D Printer

2.7.1 The 3D printing technology

Many methods have been developed for the preparation of hydrophobic coatings; however, these preparation methods for hydrophobic surfaces are complicated

and expensive. Three-dimensional printing (3DP) creates three-dimensional items effectively, and layer by layer using computer-aided design (CAD), computer-assisted manufacturing (CAM), or other digital design [132]. The application of 3D printing technology has increased dramatically over the past few years and is found in many different industrial sectors [133]. It is a fast-developing additive manufacturing technology that can provide cost efficiency and flexibility in product development and production [134],[135]. There are various 3D printing technologies based on polymerization, binding, or melting techniques. 3D printing technologies can be categorized into three basic processes: the polymers can be 3D printed via polymerization, powder-bed-based, and extrusion-based methods. During the polymerization process, a liquid photopolymer (monomer) is layer by layer solidified or cured using an energy source such as a laser beam or UV rays using a slicing technique. In the second approach powder-bed based process, successive layers of powder are coated with a bonding agent, such as an adhesive, which causes the layers to adhere to one another and, collectively, create the portion. In the third, extrusion-based method, a wire-shaped filament is heated by induction to build the component layer by layer as it is deposited onto the printing platform along a path predetermined by G-code [136]. The most affordable and widely used 3D printing technique today is fused deposition modelling (FDM). FDM printing uses material extrusion and is based on melting [137]. It is popular because of its open-source and simple system configuration, which has been widely used in the polymers field [138]. The process for this printer is extrusion-based so that the thermoplastic filaments are heated in the extruder, and the extrusion nozzle is used to deposit the heated filaments on the construction platform. The applied thermoplastic quickly solidifies since the construction platform has a lower temperature. The second layer of material is deposited by the extruder's nozzle as the platform goes down. This process is repeated until the printing is finished [139]. Stereolithography (SLA) was the first 3D printing method have been developed using the polymerization process. The first layer of liquid resin is hardened by the ultraviolet lasers. Following this, a layer of liquid resin is added

gradually by lowering the platform where the solidified resin layer was previously positioned. Once the resin is solidified by the laser, the platform shifts down to a certain height depending on the thickness of the printing layer and solidifies the next layer of resin. This procedure is repeated up to the object's completion [140]. Selective laser sintering (SLS) uses powder-bed-based as a laser to liquidate powder in order to create 3D printed objects, where the item takes on a solid shape after cooling. The process of SLS uses the powder as a material, a liquidating temperature and carbon dioxide (CO_2) laser power. SLS-based printing involves first creating a layer of powder, followed by laser sintering the material, which causes lowering of the supporting plate as the layer thickness increases. The procedure is then repeated with a fresh coating of powder. This process continues until all of the layers are sintered, and the desired product is printed. One of the main benefits of using SLS is that leftover powder can be reused to reduces waste [141]. Fused Filament Fabrication (FFF) is an extrusion-based process in which a continuous filament of thermoplastic material is extruded through a heated nozzle controlled via G-code, which is placed layer-by-layer on a platform to form the module. The movement of the extruder is consistently in the X–Y directions only, with the build platform moving in the Z direction, as shown in Figure 2-25 [136].

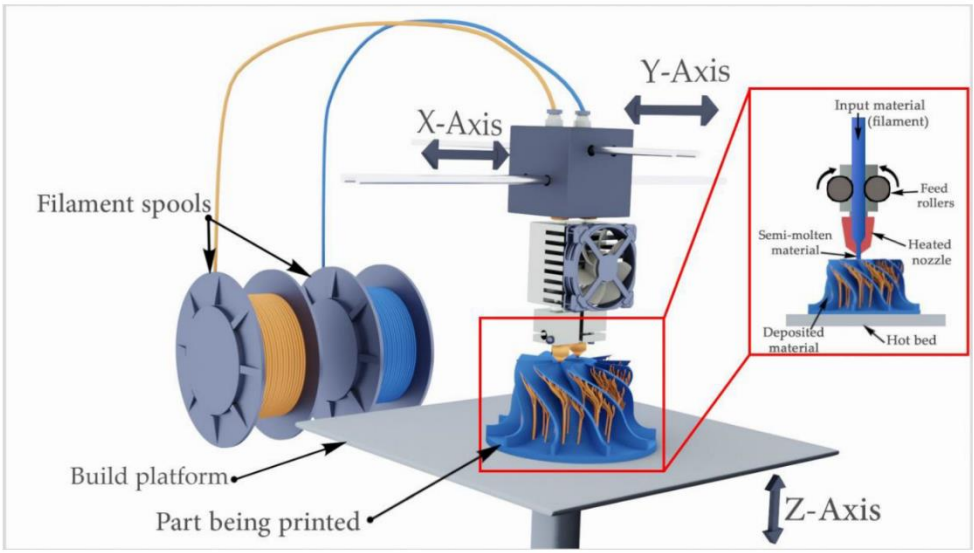

Figure 2-25. A schematic of the fused filament fabrication (FFF) process [136]

These printers work with the thermoplastic polymers by melting and extruding them through a nozzle to the printing plate [142]. The polymers have been the dominating materials used in 3D printing in the last five years. They have a wide range of properties, which is why they are used in a variety of applications ranging from adhesives to medical and advanced technologies in large industries. The thermoplastic polymers are PLA polylactic acid, ABS acrylonitrile butadiene styrene, PLA Polylactide, PETG polyethylene terephthalate glycol-modified, and nylon polyamide [140] [138]. The most widely used polymer for 3D printing with FDM technique is PLA polylactic acid [133]. Thermoplastic elastomers are categorised into six categories based on their chemistry: TPU thermoplastic polyurethanes, TPV thermoplastic vulcanizates, TPS styrenic block copolymers, TPO polyolefinic rubber blends, TPE thermoplastic polyetherimide and TPC thermoplastic polyether ester. Each category produces parts with different properties and shows different chemical compositions [143]. In spite of this kind of chemical alternatives, soft PLA enables printing of lace-like, glossy, and smooth fabric structures. Because ABS is rigid and strong, using it gives materials more movement and makes it perfect for joints. The main reason PLA and soft PLA are used is because they have greater mechanical qualities than ABS and PLA. The physical and mechanical qualities of knitted and woven items as well as garment parts are improved when Ninjaflex, BendLay (butadiene), and TPE thermoplastic elastomer are combined with PLA and soft PLA. Manufacturers are now implementing PLA, ABS, or PC as support materials. When compared to synthetic polymer-based filament, this kind of filament offers greater strength, durability and flexibility [144]. 3D printing is a computer-aided design (CAD)/computer-aided manufacturing (CAM) technology in which a component or the entire substance is manufactured layer by layer using liquid or stiff materials based on a 3D digital model. It has two major phases: pre-processing and post-processing. The product's pre-processing begins with the model's design using the required software (e.g., Rhino, Catia V5, AutoCAD, Inventor, 3Ds Max, etc.) [144]. Following this, an STL (Standard Tessellation Language) version of the project is created. The next stage is to choose a reference plane

from the STL file, and the item will then be separated into layers parallel to the selected reference flat. It will allow controlling of the printing parameters and data on temperature, lining, speed, and positioning, among other things. The accuracy of the print will increase with layer height, and each of these layers is represented by a file called G-CODE. This code contains the instructions necessary to create each layer, and the STL file can be downloaded to the printer [130], as shown in Figure 2-26.

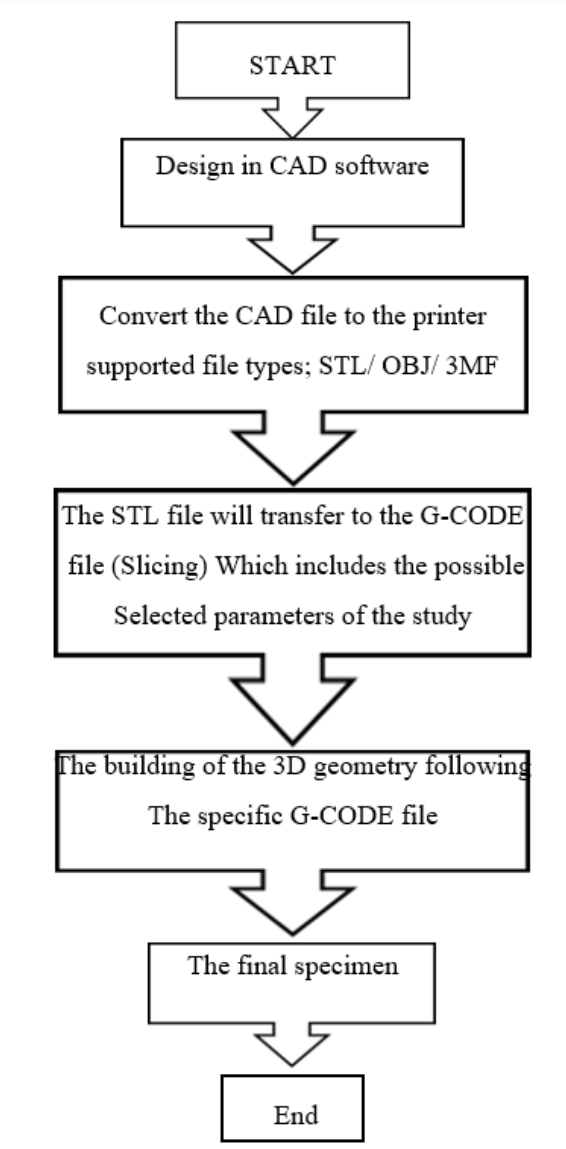

Figure 2-26. The printing processes.

In the post-process, the object's surface finish is improved by sanding, polishing, further dyeing, or painting and the undesired print edges are eliminated [144].

2.7.2 The 3D-printed of textiles

The use of 3D printing technology can increase fashion design's creativity options. 3D printing has only recently become established in the fashion and textile industries, where many technologies are employed to produce patterned elements, fashion accessories, different textile structures, and functionalized textiles. For instance, the fashion industry employs 3D technology to create advanced inventions such as 3D printed shoes, clothing, and accessories that are created by a large number of famous designers [133]. The concept of using 3DP technology to create useful fabrics has received a lot of attention in recent time. It can be used to create smart textiles and protective apparel while keeping the comfort and wearability of the fabrics [140]. Retailers and designers believe that creating fashion products using 3D printing technology help to improve product design by providing customers with personalised and unique products. The benefits of developing a product using 3D printing technology include on-demand custom fit and styling. Meanwhile, by utilising 3D printing technology, it is possible to reduce supply chain costs. Finally, 3D printing technology can quickly create and deliver products in small quantities [145]. In recent years, fully 3D-printed garments have been created and brought to market. Most of these garments are stiff and solid, making them unsuitable for everyday use. Various flexible-structure fabrics have recently been developed, offering improved, comfortable, and practical 3D-printed garments [140]. Beecroft demonstrated the ability to print single-faced and double-faced weft-knitted structures using Selective Laser Sintering (SLS) of Nylon powder PA12. When printed at different thicknesses, these structures exhibit mechanical properties such as flexibility, strength, and stretch, which could make them viable solutions for use in the technical textile industry [146]. Takahashi and Kim established a new low-cost 3D printing technique for textile fabrication using a consumer-grade FDM 3D printer as show in Figure 2-27. Given various parameter options, the process allows them to weave a thin fibre across a series of pillars within the fabricated

textile's design space. They presented a system allowing end users to design textiles by experimenting with various parameters. It can be used in real-world fabrication, allowing users to introduce thin threads as a new design medium for their 3D models [134]. Melnikova et al. developed a lace-structure fabric inspired

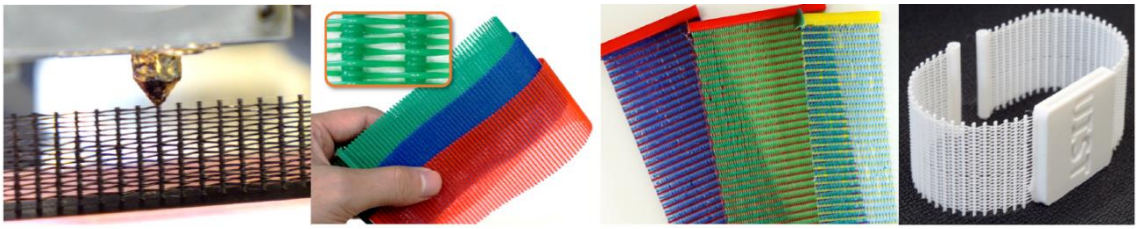

Figure 2-27. 3D printed fabric. Our technique can fabricate a textile that is woven using the movements of the nozzle of an FDM 3D printer [134]**.**

by Plauen lace, using FDM printing PLA. These materials can create innovative patterns and construction techniques for clothes and other fields, allowing new designs and functionalities that conventional textile fabrics are unable to achieve [147]. Spahiu et al. employed FilaFlex material and FDW printing to create flexible geometric fabrics. They presented an alternative use for the less expensive FDM technology, which may be used to produce clothing in this industry. The finished dress is simple to wear because of the elasticity of the FilaFlex material [148]. There have been limited performance tests of the 3DP textiles (e.g. draping, breathability, and tensile strength) performed in previous studies. There is a lack of combined test standard, making it difficult to compare the measurements and characteristics of the different 3DP textiles. As a result, the development of a consent test method for 3D-printed textile-based structures should be considered [140]. Mikkonen et al. mentioned that 3D-printed flexible materials can be viewed as usable, fabric-like materials even without complex micro- or meso-structures that create the feeling of flexibility. A practical garment was printed and constructed using flexible materials and rugged connectors to show its applicability as shown in Figure 2-28. The standard they used provided guidelines for evaluating flexible 3D printed materials [149].

Figure 2-28. The full corset printed with flexible materials [149]**.**

The improvement of 3DP technology and research can help produce more 3D printing fabric with comfort and softness, and more materials can be used in more functional applications. This technology is also environmentally friendly as it reduces waste and the need for mass production, making it a more sustainable industry option [150]. Therefore, any new technique that can produce textiles, including 3DP, must be able to build fabric-like porous structures and accurately simulate the fundamental characteristics of the textiles, such as softness, flexibility, strength, and porosity. One of the key parameters of textile products is the link between structural features and their properties. The dimensional qualities of the basic fibres and intermediaries, such as yarns and fabrics, are fundamental factors in textile products [151].

2.7.3 The advances in self-cleaning 3D-printed structures

Three-dimensional (3D) printing is developing the way we create products [152]. Through the rapid advancement of this technology, the printing procedure must

significantly improve efficiency with ideal print settings and without making repeated unintentional mistakes to produce higher "quality" pieces. Previous studies have mostly emphasised dimensional accuracy, surface detail, and bridging as quality values [153]. All 3D printing technologies use the same process of adding and joining materials to create an object that is modelled numerically. Controlling the surface layers' features allows an exciting property to achieved, such as increasing the hydrophobicity or hydrophilicity of the surfaces [152]. Superhydrophobic surfaces demonstrate high water repellence, low adhesion and self-cleaning properties [154]. Several studies showed that the surface properties could affect their wettability, and the surface quality is affected by process parameters of FDM 3D-printed [155], [156]. Research has demonstrated that the wettability of parts is affected by their surface qualities, and the surface quality of FDM 3D-printed parts is affected by the printing parameters [157], [158], [159]. Barrios and Romero declared that controlling the height of the nozzle and the amount of material extrusion, expressive textures, layer thickness, and filling method can have a significant effect on the surface roughness of the 3D-printed parts [160], [161]. New 3D printing methods have extended the capability of 3D printers and offer a new area of usage. Many efforts have explored the possibility of fabricating textiles using a 3D printer. Different textures can be printed by controlling the nozzle's height and the amount of material extrusion [162], [163]. However, several factors, such as layer thickness, build orientation, bed/nozzle temperature, feed rate, extruder width effect, etc., affect FDM technology's accuracy. The adjustment of these factors will have an impact on other properties of 3D objects such as surface roughness, wettability, and dimensional accuracy. Modi and Prakash examined wettability of 3D printed PLA parts at different raster angles of 0°, 30º, 60º & 90º. Contact angle measurements were made and, 0º raster angle achieved the lowest contact angle of 39.5º while a 90º raster angle had the largest contact angle of 94.0º [129].

Surface roughness, porosity, and wettability are the critical features of a self-cleaning surface. The input printing parameters can control these three features if FDM-based 3D printing is used to fabricate textile fabrics. The present study

uses different combinations of printing parameters and examines their relationship with the obtained features. If a surface can attain the required surface roughness and a possible porosity level, its wettability can be affected by these two parameters. Once wettability reaches a certain angle, the surfaces can be considered superhydrophobic or hydrophobic. So, the basic principle for any self-cleaning surface requires suitable surface roughness to generate an acceptable contact angle for a water droplet to float on the surface instead of being absorbed [152]. The effects of printing parameters on surface roughness have been studied by different authors. Buj-Corral et al. addressed the printing orientation angle influences on the surface roughness accomplished in lateral walls in fused deposition modelling (FDM) [164]. Pérez et al. have found that layer height and wall thickness had the greatest influence on surface roughness, and they considered layer height, temperature, printing path, printing speed, as well as wall thickness as well [165]. As for the influence of print orientation on roughness, Chaudhari et al. examined the surface finish of ABS parts that were printed with different layer thickness, infill, orientation, and postprocessing operation. Roughness was most affected by infill and postprocessing [166]. Asadi-Eydivand et al, successfully created 3D printed cylindrical calcium sulphate-based porous surface with three different pore sizes and fabricated with different setting parameters. The three key parameters chosen for the printing process of porous specimens were build orientation, the delay time of applying the new layer, and layer thickness (height) [167].

The 3D printing of textile fabrics of different materials provides control over the values of possible roughness and porosity levels with ease compared to the conventional weaving process [168]. The roughness can be changed via changes in the printing parameters, such as decreasing the layer height which can affect the surface texture, leading to increased printing time and lower surface roughness [169], [170]. Similarly, the porosity changes as the void spaces become affected by increasing the layer height or extruder width, but it can be minimized. As the surface roughness is affected, the surface's wettability was also affected. Printing orientation also affects surface roughness as the

measuring files showed differences in the roughness values [171], [164]. Changes in layer height have also provided highly variable results considering materials rather than surface properties. These parameters jointly govern how much heat is put in per unit of time and hence to what extent the melted material can settle [172].

2.8 Conclusion

In this review, all the previous efforts to create self-cleaning textiles by creating proper surface roughness or decreasing the surface energy using low surface energy chemicals or nanotechnology are compiled. Their key working elements have been discussed in detail. The development of different methods and techniques in recent years, such as the dip-coating (sol–gel) method, spin coating, spray coating and electro-spraying, chemical etching, CVD, HTT, electrospinning, LBL self-assembly, and wet chemical synthesis, has been reviewed. The preparation of these methods in the existing literature aimed to develop self-cleaning textiles with the help of coatings. They maintain different chemicals and processes; some are affordable and easy to handle, while others are complicated, expensive, and must be used only in a laboratory due to chemical usage. Several chemical solutions were used along with nanotechnology to enhance the coatings for desirable surface roughness or lower surface energy, as the nano-layer of anatase TiO_2 and other NPs are successfully applied on the textile fabric surface or the fibre itself.

These coatings create a different surface on the fabric, and hence the changes in the microscopic features of this surface control the self-cleaning ability. The use of these organic solvents and chemicals can be a cause of environmental health hazards. Therefore, the development of user-friendly and cost-effective methods to structure self-cleaning surfaces can be an inspiration for excellent ideas. Instead of using an additional coating, the microscopic features of the fabric itself can also influence the surface roughness and low surface energy and provide self-cleaning ability at the woven structural level. Although the influence of the microscopic features at the fabric woven structural level has been studied

in the past, a comprehensive effort is still required to evaluate the actual quantitative influence on the self-cleaning fabric phenomenon.

Researchers examined the woven level by focusing on strength and durability, along with other properties. They used microscopic features to increase the mechanical strength of the fabric. However, they did not change the microscopic features at the woven level to evaluate the self-cleaning ability. Changing the shape of the surface to obtain self-cleaning properties has been done in other areas, such as polymers, where the geometry of the microscopic features of the top of the specimen surface were changed to create the self-cleaning ability. However, the same can be used to employ the same concept of geometrical changes and obtain self-cleaning textile fabric surfaces.

Key microscopic features, such as surface roughness, porosity, and wettability of a textile fabric, have still not been comprehensively investigated for their influence on fabric self-cleaning ability. Significantly, the interdependencies between these features with overall fabric geometry at the woven level have not been explored quantitatively. Qualitative observations have been made mainly in the past literature. However, the mass production of fabrics with self-cleaning ability requires extensive empirical studies. These studies must involve parametric analysis on varying the values of the microscopic features and their quantitative influence on the desired self-cleaning feature. So, more exciting applications in self-cleaning surfaces need to be focused upon intensely in the coming years to use the surface property for more comprehensive industrial applications.

3 METHODOLOGY

3.1 Introduction

The purpose of this research is to establish the context of self-cleaning ability by controlling the fabrication parameters of the fabric at the microscopic level. The literature review in the previous chapter highlighted various approaches to create self-cleaning textiles, which often involve modifying surface properties through coatings or nanotechnology. These coatings or treatments can alter the surface roughness, reduce surface energy, and impact the microscopic features of the fabric, such as porosity and wettability. These modifications have been explored to achieve self-cleaning functionality in textiles. However, the study identifies that the microscopic features of the fabric can not only impact the mechanical strength of the fabric but also play a crucial role in determining its self-cleaning ability. By investigating the impact of these microscopic features on the self-cleaning ability of the fabric, the research aims to contribute to the development of self-cleaning textiles with improved functionality and performance. The focus on fabricating self-cleaning ability at the woven structural level, rather than relying on external coatings, provides a unique and potentially more sustainable approach to achieving self-cleaning properties in textiles.

Thus, the methodology outlined in this chapter aims to achieve the following objectives:

- To identify the microscopic features and their influence on the self-cleaning surface.
- To examine the possibility of making 3D printed self-cleaning textile fabric by changing the structural woven pattern with the help of the microscopic features.
- To model the self-cleaning ability and fabric printing parameters.
- To evaluate the optimum printing parameters for self-cleaning printed textile fabric.

The methodology diagram is explained in Figure 3-1.

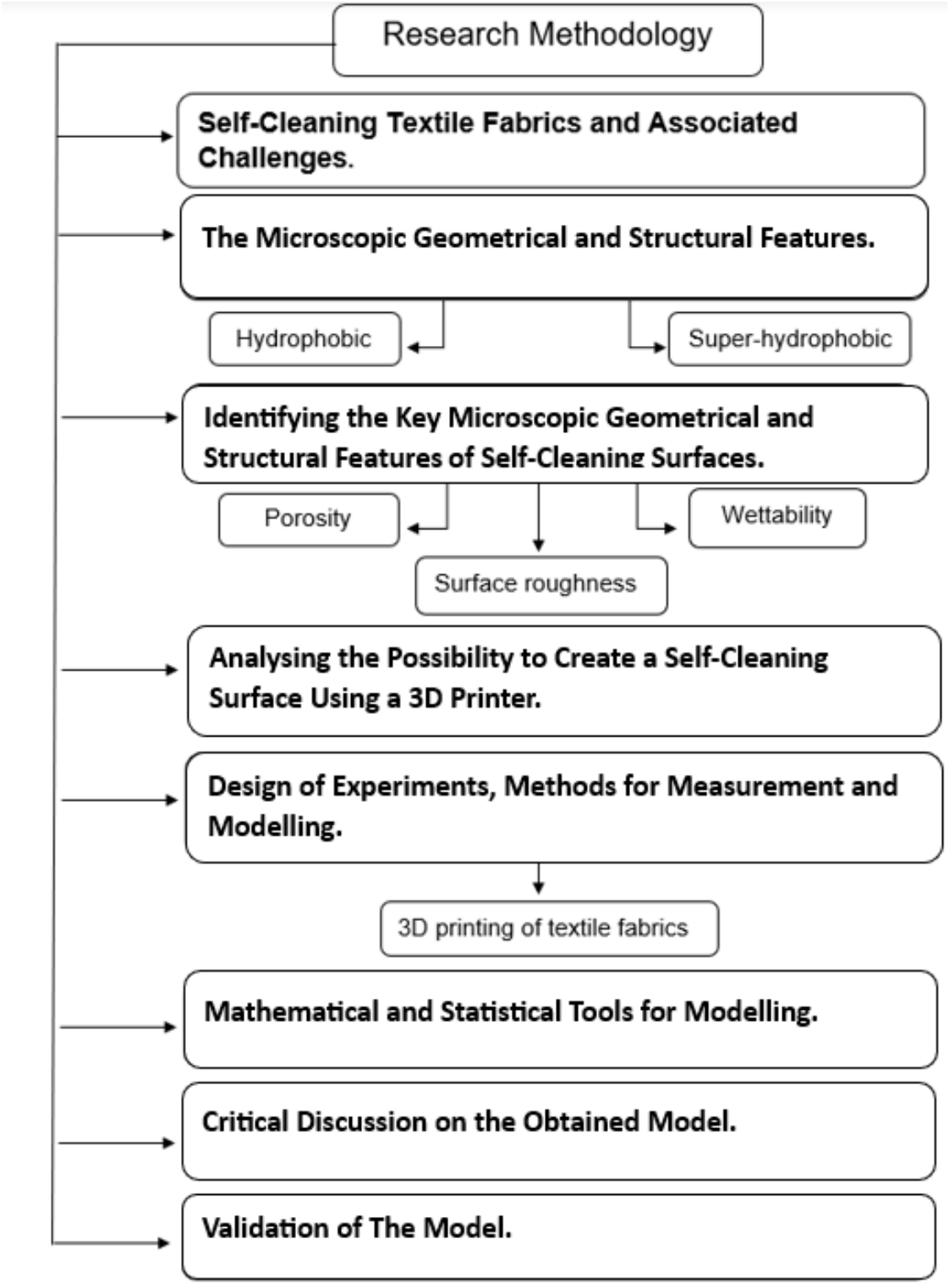

Figure 3-1 Methodology diagram.

3.2 Self-Cleaning Textile Fabrics and Associated Challenges

To achieve the objectives mentioned above, an enhanced review of the literature was carried out in chapter 2. All the previous efforts to create self-cleaning textiles were either by creating proper surface roughness or decreasing the surface energy using low surface energy chemicals or nanotechnology. These coatings create a different surface on the fabric, and hence the changes in the microscopic features of this surface control the self-cleaning ability. The use of these organic solvents and chemicals can cause environmental health hazards. Therefore, the development of user-friendly and cost-effective methods to structure self-cleaning surfaces can be an inspiration for excellent ideas. Instead of using an additional coating, the microscopic features of the fabric itself can also influence the surface roughness and low surface energy and provide self-cleaning ability at the woven structural level. Researchers examined the woven level by focusing on strength, durability, and other properties. They used microscopic features to increase the mechanical strength of the fabric. However, they did not change the microscopic features at the woven level to evaluate the self-cleaning ability. Key microscopic features, such as surface roughness, porosity, and wettability of a textile fabric, have still not been comprehensively investigated for their influence on fabric self-cleaning ability.

A further literature review is conducted in the following chapter to assess more relevant discussions to evaluate self-cleaning ability by studying self-cleaning surfaces' structural features, e.g. hydrophobic and superhydrophobic. It identifies the key structural features that provide self-cleaning ability on a surface and analysing the possibility of implementing the identified structural features on a textile fabric to fabricate a 3DP self-cleaning textile.

3.3 Design of Experiments

A quantitative methodology was used in developing an experimental scheme for this research to test the implementation of the identified features on different types of textile fabric. To this end, a fused filament fabrication (FFF) technology-

based 3D printer was used due to factors such as affordability, cost-effectiveness, and material availability. Computer-aided design (CAD) software was used to design the sample, which was then transmitted to a (FFF) fused filament fabrication printer for printing. Three types of flexible filaments (TPU, TPE, and TPC) were used to create 3DP textile fabrics. A total of 162 3D printed samples of polymeric textile fabric were produced, which included 54 samples of each of the three filaments at different 3D parameters: layer height (LH), extruder width (EW), and two different angular printing orientations (O). Further, the microscopic features (porosity, roughness, and wettability), which are mainly responsible for this ability, were measured and recorded to evaluate and compare the best values for self-cleaning between the three chosen materials. The data were analysed to define the optimal self-cleaning number as shown in Figure 3-2.

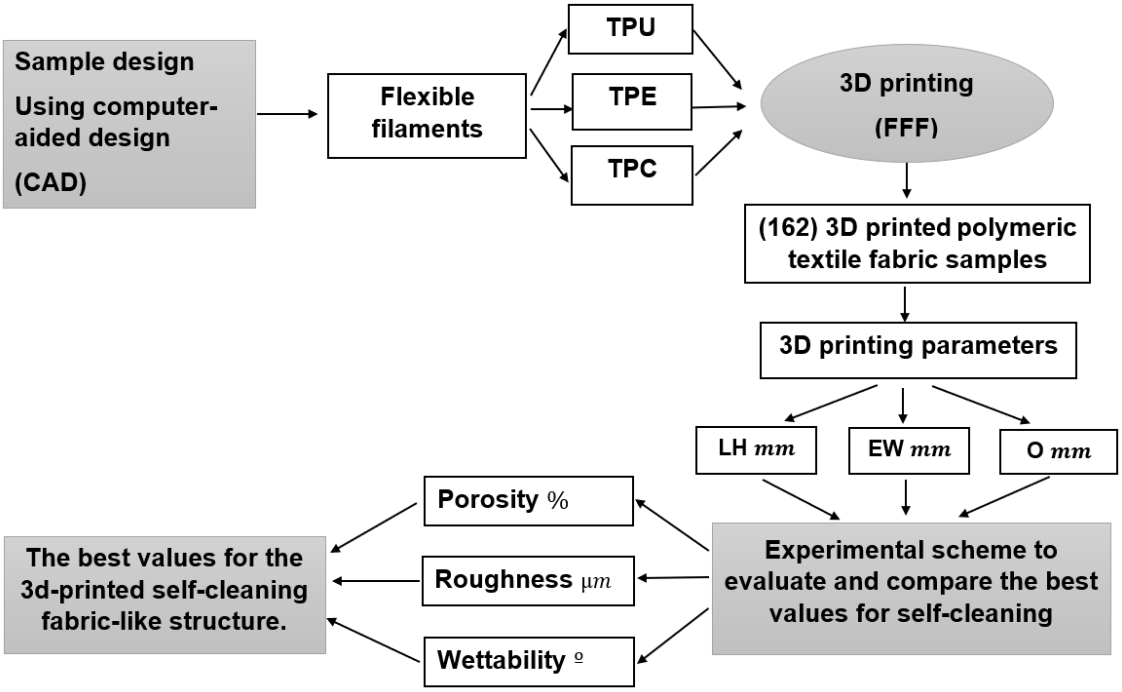

Figure 3-2. The making of 3D printed self-cleaning textile polymeric fabrics.

3.4 Mathematical and Statistical Tools for Modelling

In the research study, a second-degree polynomial response surface methodology (RSM) model is employed to determine the regression model and correlation between the input parameters and the response variables. The regression model is used to understand the relationship between the input parameters and the self-cleaning attribute features, namely porosity, roughness, and wettability.

The RSM model allows for the examination of complex relationships and interactions between the input parameters and the response variables. By fitting a second-degree polynomial model, the study aims to capture both linear and non-linear effects, as well as possible interaction effects, between the input parameters and the self-cleaning attributes.

The regression models for each self-cleaning attribute feature (porosity, roughness, and wettability) are determined separately for the three materials: thermoplastic polyurethane (TPU 98A), thermoplastic elastomer (TPE filaflex), and thermoplastic co-Polyester (TPC flex45). This allows for material-specific analyses and insights into how the input parameters influence the self-cleaning attributes in each material.

The regression models obtained from the RSM analysis provide mathematical equations that express the relationships between the input parameters and the self-cleaning attributes. These equations can be used to predict the values of the self-cleaning attributes based on the given input parameters. Additionally, the correlation analysis helps quantify the strength and direction of the relationships between the input parameters and the self-cleaning attributes.

By applying the second-degree polynomial RSM model and presenting the regression models for each self-cleaning attribute feature across the three materials, the study aims to provide an understanding of the factors that influence the self-cleaning characteristics of the fabricated fabrics. This information can

further guide the optimization of the input parameters to achieve desired self-cleaning attributes in future fabrications.

3.5 Critical Discussion on the Obtained Model

In the study, the aim is to identify the optimal combination of printing parameters that can achieve the best self-cleaning ability for the three materials: thermoplastic polyurethane (TPU 98A), thermoplastic elastomer (TPE Filaflex), and thermoplastic co-polyester (TPC flex45).

An optimization process will be conducted to determine the optimal values of the printing parameters that inherit the highest self-cleaning ability. The optimization process will be guided by the developed models and correlations between the printing parameters and the self-cleaning attributes, such as porosity, roughness, and wettability. By adjusting the printing parameters based on the optimization model, the study aims to achieve the best possible self-cleaning ability for the printed fabric specimens. The aim is to find the combination of printing parameters that results in high wettability, low porosity, and high roughness, as these factors contribute to a higher self-cleaning number.

The devised method and optimization model will enable the estimation of the self-cleaning ability of the printed fabric when the inputs of the printing parameters are known. By inputting specific values for the printing parameters into the model, the self-cleaning ability of the fabric can be predicted. This allows for the assessment and comparison of different combinations of printing parameters to determine the optimal settings for achieving the desired self-cleaning ability. This approach provides a systematic methodology for achieving improved self-cleaning ability in printed textile fabric surfaces.

3.6 Validation of The Model

The validation of the analytical model is an important step in assessing its accuracy and reliability. In this research, the validation process involves printing additional specimens for the three materials (thermoplastic polyurethane,

thermoplastic elastomer, and thermoplastic co-polyester) using different printing parameters that were not previously tested in the experimental scheme.

The purpose of printing these additional specimens is to compare the experimental results obtained from these new configurations with the regression model of each self-cleaning attribute feature, namely porosity, roughness, and wettability. The accuracy and effectiveness of the analytical model can be evaluated and validated.

The validation process consists of the following steps:

Printing Specimens: Two specimens are printed for each material using the different printing parameters that were not tested in the initial experimental scheme. These parameters are selected based on the optimization model or by exploring different combinations to cover a wide range of possibilities.

Experimental Measurements: The printed specimens are then subjected to experimental measurements to determine their actual self-cleaning attribute features, including porosity, roughness, and wettability. These measurements can be conducted using suitable techniques and instruments specific to each attribute.

Regression Model Comparison: The experimental results obtained from the newly printed specimens are compared with the regression model developed for each self-cleaning attribute feature. The model predictions for porosity, roughness, and wettability are compared to the corresponding experimental measurements.

Accuracy Assessment: The comparison between the experimental results and the regression model predictions allows for an assessment of the accuracy and reliability of the analytical model. Statistical measures, such as mean absolute error, root mean square error, or coefficient of determination (R-squared), can be used to quantify the level of agreement between the model predictions and experimental measurements.

By printing additional specimens with different printing parameters and comparing the experimental results with the regression model predictions, the validation process provides a comprehensive evaluation of the analytical model's performance. This validation step ensures that the model accurately captures the relationship between the printing parameters and the self-cleaning attribute features for the three materials under consideration.

The successful validation of the analytical model strengthens confidence in its reliability and allows for more accurate predictions of the self-cleaning attribute features based on the input parameters. It demonstrates the effectiveness of the research in providing a robust framework for optimizing the printing parameters and achieving the desired self-cleaning ability in printed fabric specimens.

4 DESIGN OF EXPERIMENTS, METHODS FOR MEASUREMENT AND MODELLING

4.1 Introduction

The fabrication of 3D printed textile fabrics using a low-cost fused filament fabrication (FFF) technique has been conducted in this research. The specific design of the fabric specimens, the chosen test parameters, and the experimental setup have been determined to examine the self-cleaning features of the printed fabrics. The control the self-cleaning microscopic features in the printed fabrics, key printing parameters such as orientation angle, layer height, and extruder width are adjusted. The combination of these parameters is controlled to achieve the best self-cleaning textile fabric surface.

The layer height (LH) parameter is varied at values of 0.15 mm, 0.13 mm, and 0.10 mm, while the extruder width (EW) is adjusted to 0.5 mm, 0.4 mm, and 0.3 mm. Two different angular printing orientations (O) of 45° and 90° are considered. These variations in the printing parameters allow for the exploration of different fabrication conditions and their impact on the self-cleaning properties of the printed specimens.

Additionally, three different thermoplastic flexible filaments are used in the printing process: thermoplastic polyurethane (TPU 98A), thermoplastic elastomers (TPE filaflex), and thermoplastic co-polyester (TPC flex45). These materials offer flexibility and softness similar to conventional textile fabrics, making them suitable for this study.

Furthermore, the optimization of the printing parameters will be modelled to identify the optimum self-cleaning properties for the printed specimens. By applying optimization techniques, the researchers aim to determine the combination of printing parameters that maximizes the self-cleaning performance of the fabricated fabrics.

For the validation of the developed model, a set of experimental methods will be employed. This validation process involves printing additional specimens with different printing parameter combinations that were not previously tested. The experimental measurements of self-cleaning features, such as surface roughness, wettability contact angle, and porosity, will be analysed for these specimens. The experimental results will then be compared with the predicted values from the optimization model, assessing the reliability and accuracy of the model in predicting self-cleaning properties.

By conducting these experiments and validation procedures, the research aims to gain insights into the optimal printing parameters for achieving self-cleaning properties in 3D-printed textile fabrics. The combination of modelling and experimental validation provides a comprehensive approach to understanding and optimizing the self-cleaning features of the fabricated specimens.

4.2 Design of Experiment

The experimental part of the study was divided into three main parts:

I. Specimen Design and Printing: The specimens were designed and printed using three different sets of printing parameters and three different materials. The selected parameter values ensured high printing quality, while the other parameters remained constant across all samples. This allowed for consistent comparison and evaluation of the self-cleaning ability. The printed samples were then subjected to testing based on an experimental scheme specifically designed to assess their self-cleaning ability.

II. Measurement of Microscopic Features: The microscopic features, namely porosity, roughness, and wettability, which play a crucial role in determining the self-cleaning ability, were measured and recorded for each sample. This evaluation aimed to identify and compare the optimal values of these features that contribute to effective self-cleaning among the three chosen materials. The measurements provided valuable data to analyse and understand the relationship

between the printing parameters and the microscopic features related to self-cleaning.

III. Data Analysis and Optimization: The collected data were analysed to determine the optimal self-cleaning number. Analytical calculations were performed using the experimental outputs to establish the relationship between the changes in printing parameters and the variations in microscopic features. The purpose was to identify the printing parameter values that would result in the most beneficial self-cleaning properties. Additionally, an optimization model was developed to further explore and define the optimum self-cleaning properties based on the printing parameters. This optimization model allowed for the identification of the best combination of printing parameters to achieve the desired self-cleaning attributes.

The experimental scheme provided a systematic approach to evaluate and compare the self-cleaning ability of the printed specimens, assess the influence of the printing parameters on microscopic features, and establish an optimized set of parameters for achieving optimal self-cleaning properties. The results of the experimental scheme were utilized in analytical calculations and modelling to establish the relationship between the printing parameters and the microscopic features and to validate the effectiveness and accuracy of the model.

The detailed experimental scheme, which outlines the specific steps, methods, and measurements employed in the study as shown in Figure 4-1.

4.3 The 3D Printing Parameters

This study focuses on three printing parameters (layer height (LH), extruder width (EW), and raster orientation angle (O)) and the possibility of developing a 3D printed self-cleaning textile fabric. It identifies the significance of the fabric's microscopic features, such as porosity, surface roughness, and wettability, along with the aesthetic appearance after optimizing these features. These microscopic features were obtained and controlled by using different sets of printing parameters as shown in Table 4-1.

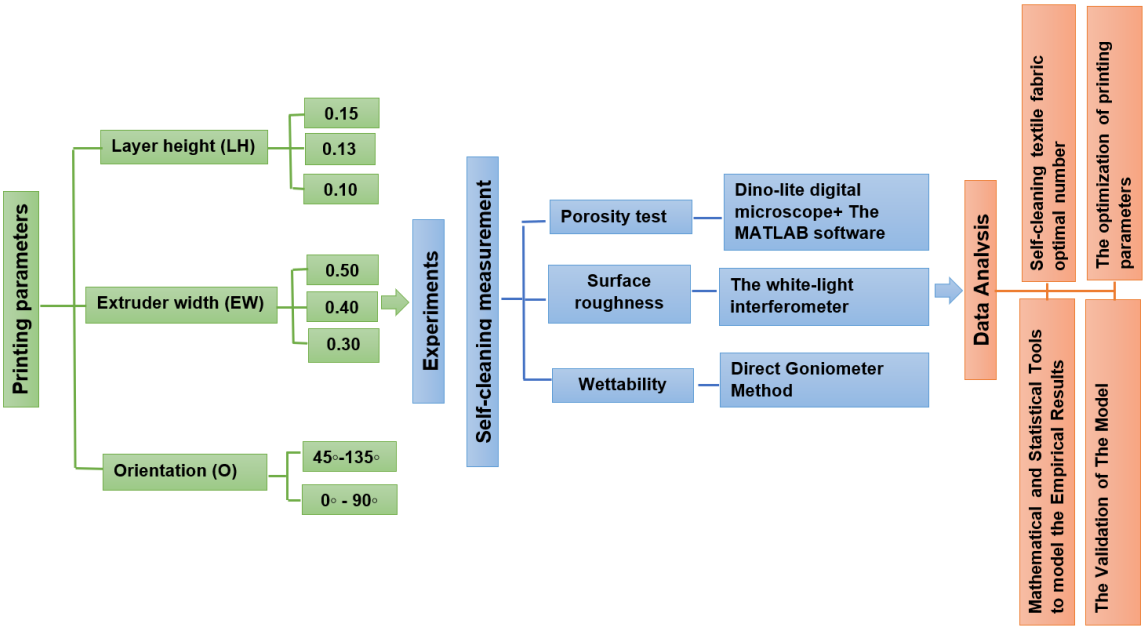

Figure 4-1. The design of the experiments.

Table 4-1 Printing parameters.

Layer Height (LH) mm	**Extruder Width (EW)** mm	**Orientation (O)** **Degree** °
0.15	0.50	0° (first layer) - 90° (second layer), 45° (first layer) - (second layer) 135°
0.13	0.40	0° (first layer) - 90° (second layer), 45° (first layer) - (second layer) 135°
0.10	0.30	0° (first layer) - 90° (second layer), 45° (first layer) - (second layer) 135°

Further, the influence of these features on mechanical strength at the fabric woven-structure level was tested, along with their effect on self-cleaning ability. The fundamental definitions of printing parameters, the microscopic features, and their interrelationship are provided below to comprehend this influence and self-cleaning ability.

I. Layer height (LH) mm: The height of each layer in the printed specimen. It influences the number of layers printed for a given thickness of specimen, as shown in Figure 4-2. A fixed number of layers with different values of layer height will provide different values of fabric thickness.

For layer height, the lowest value of 0.10 mm was chosen as it is the minimum recommended by the software options of the ideaMaker, the printer software. A higher value was determined as 0.13 mm, which was selected expecting an increase in the microscopic features that affect the self-cleaning property. The last value of 0.15 mm was the highest was chosen to provide a fabric-like structure while still ensuring that the surface does not become overly stiff. Going beyond this threshold would result in a surface that deviates too much from the characteristics of a fabric.

II. Extruder width (EW) mm: The width of the printed material. It is dependent on the nozzle size of the selected printer. The influence of extruder width on self-cleaning features can only be evaluated if the overall fabric dimensions remain constant, as shown in Figure 4-2.

For extruder width, the lowest value of 0.30 mm was chosen as it is the minimum recommended by the software options of the ideaMaker. If a lower value were adjusted, it would affect the fabric quality. A higher value was determined as 0.40 mm, which was selected expecting an increase in the microscopic features that affect the self-cleaning property. The last value of 0.50 mm was the maximum value recommended by the software.

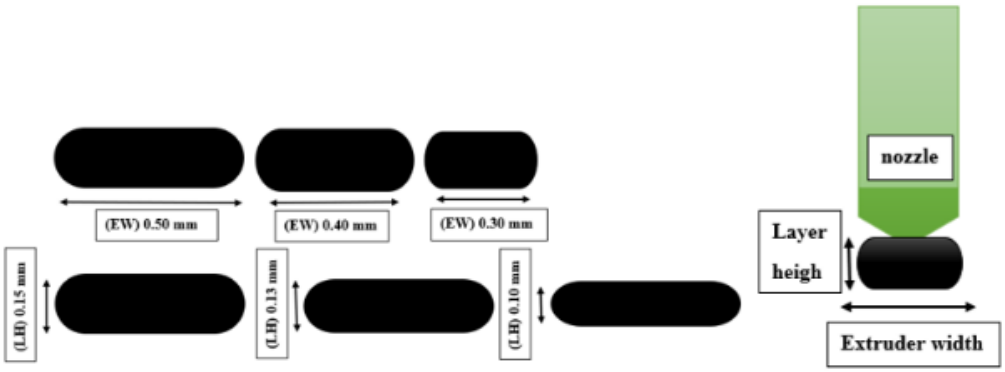

Figure 4-2 Layer height and extruder width definition.

III. Orientation angle (O) °: The path on which the nozzle moves on each layer of the FFF 3D printer part as in Figure 4-3.

Adding to the various printing parameters, orientation angle seems to have an impact on the surface quality [165]. Therefore, it was rational to consider the orientation as a main factor along with the other two parameters (layer height and extruder width). The orientation of the printed layers is certainly an important factor to consider in achieving a fabric-like structure with the desired texture and characteristics. To simulate a woven-like structure as closely as possible and to create the desired softness, strength, flexibility, and porous structure, two orientation combinations were selected. These combinations aim to replicate the layered structure found in woven fabrics and enhance the fabric's overall texture. Considering the orientation parameter as a significant factor in conjunction with the other printing parameters demonstrates the comprehensive approach taken in this study to achieve a printed fabric with the desired qualities. By mimicking a woven structure and optimizing the printing parameters accordingly, the research aims to develop 3D-printed fabrics that closely resemble traditional woven textiles in terms of their appearance and characteristics as shown in Figure 4-3.

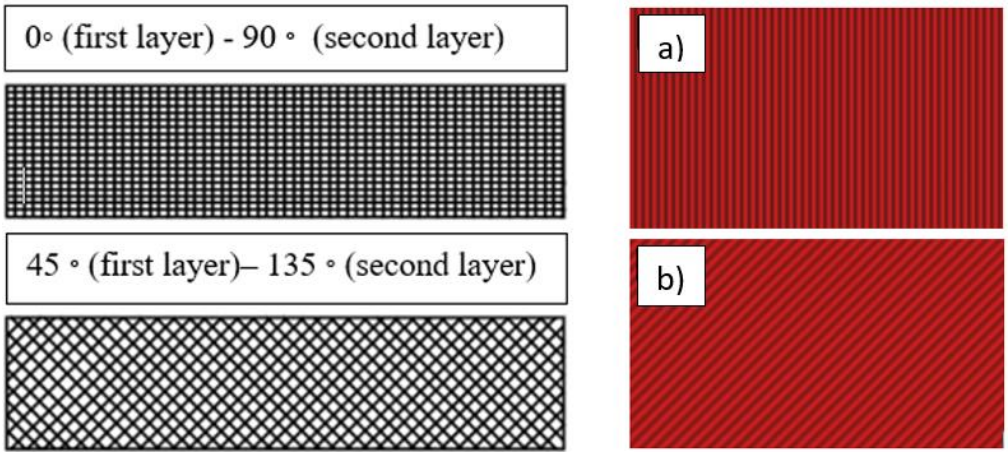

Figure 4-3. Scheme showing two samples printed flat and loaded in the x/y direction 45° - 135°,0º - 90°. a) XY (90°) and, b) XY (45°).

The aforementioned printing parameters were adjusted in the 3D printer software in this research. Other parameters such as nozzle temperature ($°C$), print speed (mm/s), and infill density ($\%$) were selected based on the recommendation of the printer OEM (i.e. original equipment manufacturer). These parameters mainly depend on the hardware capacity and quality. In the presented research, printing parameters including LH, EW, and O are analysed to develop fabrics with self-cleaning ability. Parameters, mainly dependent on hardware, are kept on the values advised by the printer OEM manual. The choice to adhere to the recommendations provided by the printer OEM for the hardware-dependent parameters helps maintain consistency and standardization in the printing process, allowing for reliable and comparable results across the fabricated specimens.

4.4 FFF Materials

The structures were fabricated by using a Raise3D pro-2 printer with different types of filaments for FFF-based such as flexible filaments (thermoplastic polyurethane (TPU 98A), thermoplastic elastomer (TPE filaflex), thermoplastic co-polyester (TPC flex 45)). The filament materials mentioned in Table 4-2, they were chosen for their fabric-like properties, such as flexibility and softness. The research aimed to explore the potential of these filaments as suitable replacements for conventional textile fabric materials in the fabrication of structures. The choice of filaments with fabric-like properties opens up possibilities for creating flexible and soft structures using additive manufacturing techniques. It allows to produce objects that can mimic the properties and behaviours of textile fabrics, offering potential applications in areas such as wearable technology, soft properties, and custom-made textile-like products.

The specific filament materials mentioned, TPU 98A, TPE filaflex, and TPC flex 45, were likely selected based on their specific mechanical properties, printability, and suitability for the desired application. Each filament material may have distinct characteristics that make it suitable for different purposes or offer different levels of flexibility and softness.

Overall, the study's choice of these filament materials with fabric-like properties demonstrates the exploration of alternative materials and the potential for additive manufacturing to create structures that exhibit textile-like properties.

Table 4-2. The flexible filaments specifications and properties of the (FFF)-based.

Properties/filament	TPU 98A	TPE fila flex	TPC flex 45
Chemical name/blend	Thermoplastic polyurethane	Thermoplastic elastomer	Thermoplastic co-polyester
Cost per kilo($£/kg$)	22 – 40	20 - 30	30 - 60
Supplier	RS Components	RS Components	RS Components
Diameter (mm)	1.75	1.75	1.75
Printing temperature ($°C$)	205 – 230 (Test method: Print lab)	210 – 240 (Test method: Print lab)	210 – 250 (Test method: Print lab)
Density ($g/m3$)	1.16 (Test method: ISO 1183)	1.09 (Test method: ISO 1183)	1.14 (Test method: ISO 1183)
Tensile strength at yield (MPa)	50 (Test method: ISO 527)	45 (Test method: ISO 527)	24 (Test method: ISO 527)

4.5 Sample Preparation

Two layers were printed in two orientation angles of 45°and 90°. The cross-section of the filament is a flat rectangular measuring 6 x 10 cm printed under different sets of parameters as shown in Figure 4-4. To design the fabric specimen, the researchers employed Autodesk Inventor 2020 CAD software,

which allowed them to create a 3D model in the STL file format. The STL file was then imported into the Idea Maker 4.2.0 software, which was used for configuring the printing process. During the printing process, most parameters were set to their default values as recommended by the software. However, certain specific parameters were adjusted as per the requirements of the study.

Overall, the combination of CAD software, printer software, and the adjustment of specific printing parameters allowed the investigation of different settings' impact on the fabric's microscopic features and self-cleaning properties, contributing to a better understanding of the printing process and its influence on the final product. These parameters were likely chosen based on their potential influence on porosity, surface roughness, wettability, and overall fabric performance, their values are provided in in Table 4-3.

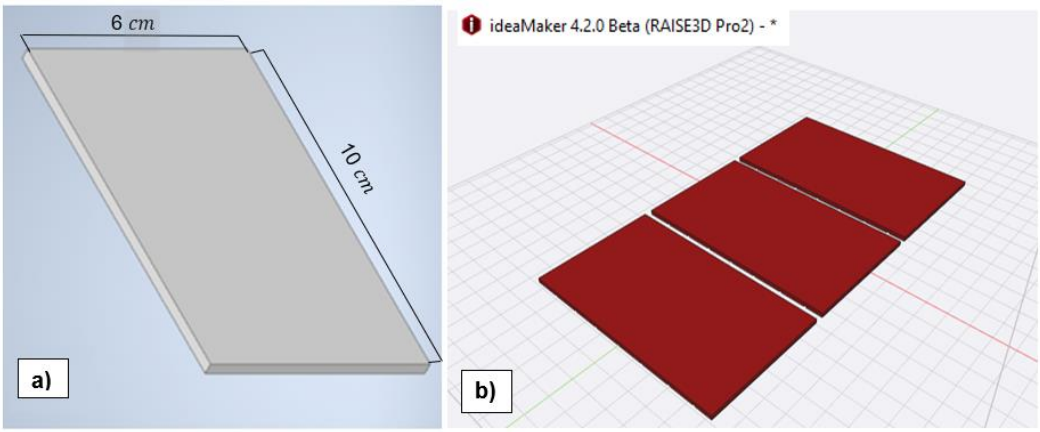

Figure 4-4. a) The CAD model of the specimen b) The printed samples preview in IdeaMaker.

Table 4-3. The 3D parameters were used to produce the samples.

Filament	Layer hight (mm)	Number of layers	Extruder width (mm)	Orientation degree (°)	Printed samples
TPU 98A	0.15		0.50	45	3
				90	3

		2	0.40	45	3
				90	3
			0.30	45	3
				90	3
	0.13	2	0.50	45	3
				90	3
			0.40	45	3
				90	3
			0.30	45	3
				90	3
	0.10	2	0.50	45	3
				90	3
			0.40	45	3
				90	3
			0.30	45	3
				90	3
TPE Filaflex	0.15	2	0.50	45	3
				90	3
			0.40	45	3
				90	3
			0.30	45	3

				90	3
	0.13	2	0.50	45	3
				90	3
			0.40	45	3
				90	3
			0.30	45	3
				90	3
	0.10	2	0.50	45	3
				90	3
			0.40	45	3
				90	3
			0.30	45	3
				90	3
TPC 45 flex	0.15	2	0.50	45	3
				90	3
			0.40	45	3
				90	3
			0.30	45	3
				90	3
	0.13		0.50	45	3
				90	3

		2	0.40	45	3
				90	3
			0.30	45	3
				90	3
	0.10	2	0.50	45	3
				90	3
			0.40	45	3
				90	3
			0.30	45	3
				90	3
Total printed samples					162

The final samples for self-cleaning textiles were set and tested through a specific measurement as in Figure 4-5.

Figure 4-5. The self-cleaning 3D printed textile-like structures with both orientation angle 45 ° - 90 ° for each material.

4.5.1 The Measurement Method for Porosity:

The main advantage of using digital image analysis to assess the porosity of the textile specimen is that there is greater accuracy and higher duplicability. First, digital images of part of the specimens were taken by Dino-lite digital microscope (a). As the image in (b) was in colour, it has been transferred into grayscale. The images of the fabrics with known magnifications were imported into a computer and converted into binary image (c). Then the porous area and the total area of the fabric were extracted. They were calculated by MATLAB software, as shown in Figure 4-6 (d).

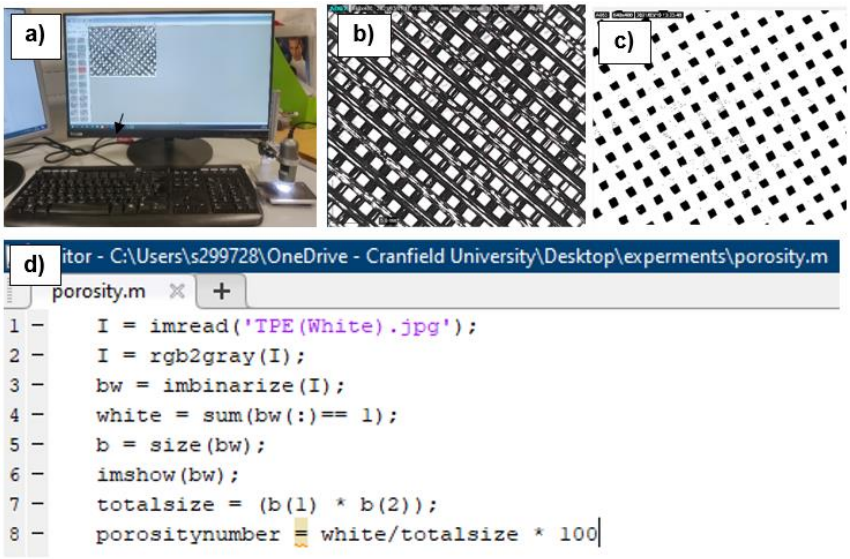

Figure 4-6. a) Fabric under the dino-lite microscope with led and upload picture to the application b) Image from the application c) Binary image converted by MATLAB d) The MATLAB code to calculate the porous.

4.5.2 The Measurement Method of Surface Roughness

In this study, the measurement was evaluated by the white-light interferometer (a). The surface roughness definition is presented as the average of the standard deviation, which shows that a higher peak means higher roughness. If the peaks are higher, the water droplets will be moving on the surface and will not go inside the pores. Physical sample surface roughness parameters (Ra and Rq) were first

obtained (b) and (c). The surface roughness Ra was measured quantitatively in μm from the filtered profiles as shown in Figure 4-7 and Figure 4-8 (a) and (b).

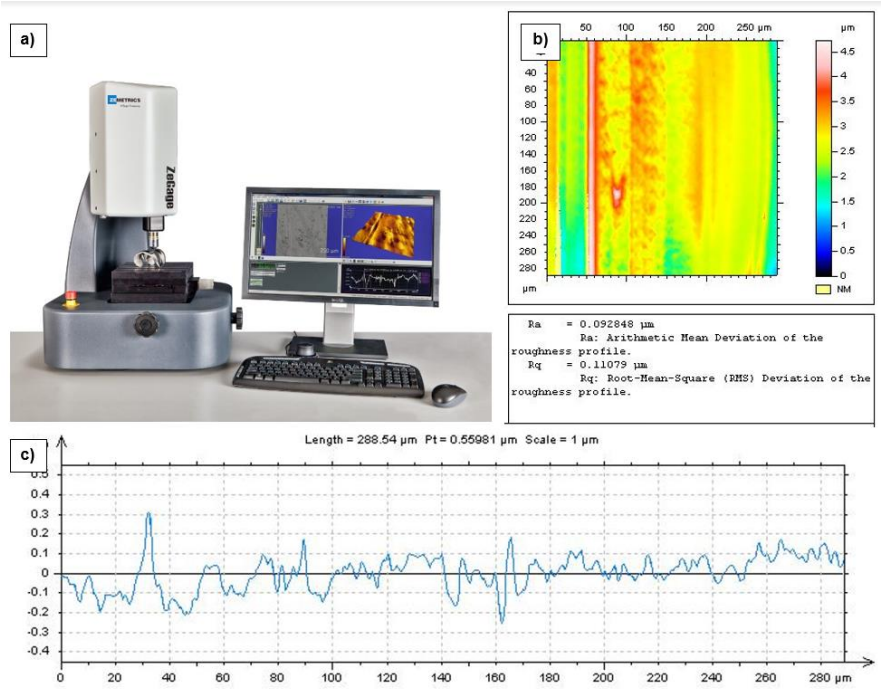

Figure 4-7. a) the sample measured with the white-light Interfor-meter b) The surface roughness Ra-Rq measurement in μm from the filtered profiles.

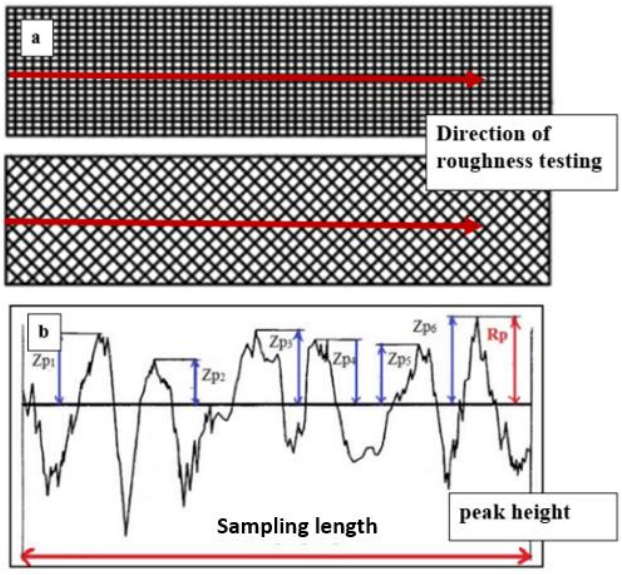

Figure 4-8. a) The measurement direction of roughness testing b) the peak height profile.

4.5.3 The Measurement Method of Wettability

The tools and techniques used to measure the contact angle of liquid drops with solid surfaces are also being developed from very basic to some advanced techniques, such as the Direct Goniometric Method, which is the most commonly used method for measuring liquid contact angles on solid surfaces. The instrument consists of four essential components: (1) a horizontal surface to mount a liquid or solid sample; (2) a micropipette to form a liquid droplet on the surface; (3) an illuminating source; and (4) a telescope assembled with a protractor eyepiece as shown in Figure 4-9 (a). The angle measured through the droplet at the interference of the three phases, i.e. solid, liquid and vapour, is referred to as the water contact angle (WCA) (b) and (c) [87].

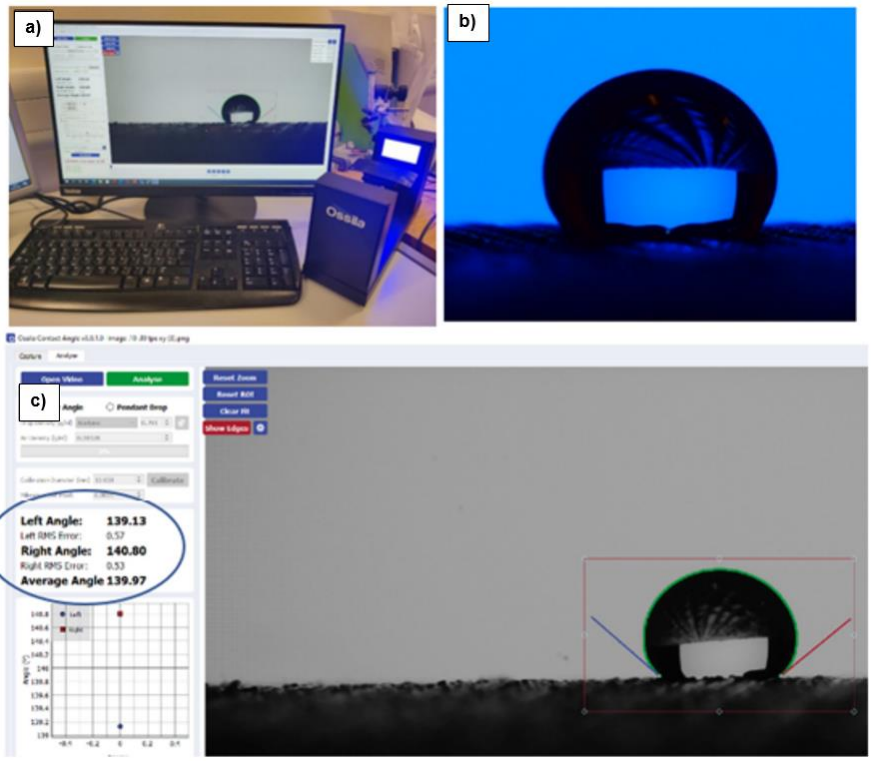

Figure 4-9. a) Ossila Contact Angle Goniometer setup b) Image of water droplet on the fabric taken from the Ossila Contact Angle application (c) Image of (CA) analysis by the Ossila Contact Angle application.

4.5.4 The Unit Cell Measure

The unit cell for the three filaments TPU 98A – TPE fila flex – TPC 45 flex was measured under a Dino-lite digital microscope with 50x magnification as shown in Figure 4-10. The unit cell measurements are provided in Table 4-4.

Table 4-4. The unit cell measurements.

Name	TPU 98A	TPE fila flex	TPC 45 flex
Porosity (P1) length (mm)	0.044	0.035	0.047
Porosity (P2) width (mm)	0.044	0.035	0.047
Water Droplet (WD)	Circumference (mm)	Circumference (mm)	Circumference (mm)
	1.867	1.928	1.932
	Area (mm)	Area (mm)	Area (mm)
	0.277	0.296	0.297
	Radius (mm)	Radius (mm)	Radius (mm)
	0.297	0.307	0.307
	Diameter (mm)	Diameter (mm)	Diameter (mm)
	0.594	0.614	0.615

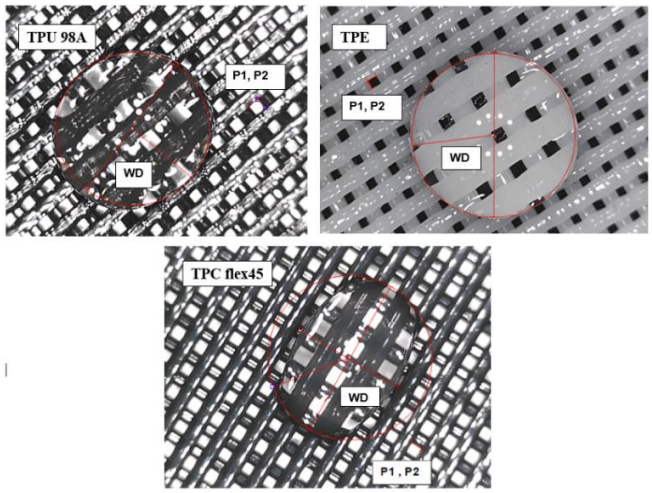

Figure 4-10. The unit cell measurement for the porosity and the water droplet for TPU, TPE, and TPC.

4.5.5 Data Process

4.5.5.1 The Relationship Between the Printing Parameters and the Microscopic Features

Mathematical and statistical tools are used to model the empirical results and develop a relationship between the microscopic features, and the printing parameters. Multiple linear regression (MLR) is suitable for modelling the relationship between the features and the parameters. It will allow us to understand the relationships between the microscopic features (porosity, roughness, and wettability) values and the different printing parameters for the three materials: thermoplastic polyurethane (TPU 98A), thermoplastic elastomer (TPE Filaflex), and thermoplastic co-polyester (TPC flex45). Therefore, their effect on the self-cleaning ability is shown in the equation:

$$\boldsymbol{y = b_0 + b_1 x_1 + b_2 x_2 + b_3 x_3} \quad \textbf{(4-1)}$$

where y *is* the microscopic feature (porosity, roughness, and wettability), and x_1 represents the layer height, x_2 represents the extruder width, x_3 represents the orientation angle, and b_{0-3} is the estimated regression coefficient that quantifies the association between the parameters x and the dependent variable y.

The printing parameters are converted from the original values in Table 4-1 above into standardized dimensionless values to eliminate the effects of differences in properties, such as dimension and order of scale between different variables, thus making the effect sizes of different variables comparable as shown in Table 4-5.

Table 4-5. Standardized value for different parameters.

Layer height (LH) $\boldsymbol{mm}$	**Extruder width (EW)** $\boldsymbol{mm}$	**Orientation angle (O)** º	**Standardized value**
0.10	0.30	0°	-1

0.13	0.40	45 º	0
0.15	0.50	90 º	1

4.5.5.2 The Self-Cleaning Number

The principle of self-cleaning ability is based on the formation of a spherical water droplet on the surface, which can effectively remove dirt particles by utilizing the surface properties [32]. In this context, wettability is considered as the most influential parameter in determining the self-cleaning ability of a textile fabric. When the contact angle between the water droplet and the solid surface is $\leq$ 90°, the solid surface is referred to as hydrophobic. In this case, the water droplet tends to roll off the surface, indicating a minimum self-cleaning ability. On the other hand, when the contact angle is $\leq$ 90°, the surface becomes hydrophilic, meaning the water droplet is absorbed by the surface rather than rolling off. For surfaces with a contact angle approaching or $\geq$ 150°, they are termed superhydrophobic surfaces. These surfaces exhibit the best self-cleaning ability as the water droplet easily rolls off, carrying away dirt particles and leaving the surface clean [109]. The wettability, defined by the contact angle of a water droplet with the surface, may not directly reflect the surface's self-cleaning ability. The self-cleaning number is introduced to overcome this limitation and provide a more representative measure.

To quantify and represent the self-cleaning ability numerically, the concept of the self-cleaning number is introduced. The self-cleaning number is derived based on the wettability parameter, and it provides a scale ranging from 0 to 100. A self-cleaning number of 0 indicates no self-cleaning ability, while a self-cleaning number of 100 represents the highest level of self-cleaning ability. By using wettability and the associated contact angle, the optimal self-cleaning number can be determined. This allows for a more accurate characterization and evaluation of the self-cleaning performance of different surfaces or materials, particularly in relation to their wettability properties. However, as much as the self-cleaning number is higher than it means the surface has more ability to self-clean.

The self-cleaning number was evaluated based on the linear equation. This equation assumes a linear relationship between the wettability (X) and the self-cleaning number (Y), with the values of Y ranging from 0 to 100.

Tan (Θ) = $\frac{100}{60}$

Θ = tan^{-1} ($\frac{10}{60}$)

$(Y - Y_1) = \frac{(y_2 - y_1)}{(X_2 - X_1)}(X - X_1)$

As Y= is the self-cleaning no, (Y1 = 0), (Y2 =100), (X1 = 90) and (X2=150).

Self-cleaning number = 1.6 (X – 90)

As X = wettability

$$\boldsymbol{Self - cleaning\ number = 1.6 * (wettability - 90)} \quad \textbf{(4-2)}$$

5 RESULT AND DISCUSSION

5.1 Introduction

This chapter discusses the influence of the chosen printing parameters (layer height, extruder width, and orientation angle) on the microscopic features, which were evaluated by plotting them separately concerning affecting self-cleaning ability. The 162 prepared samples were printed and tested based on an experimental scheme to evaluate the self-cleaning ability. The microscopic features (porosity, roughness, and wettability), which are mainly responsible for this ability, were measured and recorded to evaluate and compare the best values for self-cleaning between the three chosen materials (TPU 98A), (TPE filaflex), and (TPC flex45). The aim was to identify the parameter combinations that yield the best self-cleaning results.

Furthermore, the collected experimental data were subjected to analytical calculations to establish the relationships between variations in the printing parameters and the resulting microscopic features. This analysis helps in understanding how changes in layer height, extruder width, and orientation angle impact the porosity, roughness, and wettability of the printed samples.

By examining these relationships and evaluating the self-cleaning number, a more comprehensive understanding of the influence of printing parameters on the self-cleaning ability of the materials is obtained. This information can be valuable for optimizing the printing process and achieving the desired self-cleaning characteristics in future applications.

5.1.1 The Influence of Printing Parameters on Porosity

This study investigated the layer height effects for the three materials (TPU 98A, TPE filaflex, and TPC 45 flex). The porosity is defined as the ratio of the volume of voids within a structure to the total volume, and it can take values as a percentage ranging from 0% to 100% [172]. It determines the number and size of the holes within the textile fabric and must be as low as possible. From the

results obtained, the layer height has a minimum influential effect on the gap sizes (porosity). Increasing the layer height can increase the porosity by about 5 % for the three materials, which can be considered as a slight change. The (TPU 98A) obtained porosity values between 54 % and 57 % for layer height 0.10 mm. It increased as the layer height increased, e.g. for layer height 0.13 mm the values were between 57 % and 60 %. For the highest layer height 0.15, it increased more between 59% and 62 %. The porosity number was almost the same regarding layer height as the range changed slightly when the layer height increased. The average value remained the same about 3% increase.

For (TPC 45flex), the obtained value was slightly higher than the TPU values; it showed the same variation in the layer height in porosity for layer heights of about 5 %. For (LH) 0.10 mm the values started from 57 % to 62 %. For (LH) 0.13 mm it increased more, between 59 % and 64 %. As for the highest (LH) 0.15 mm , the increased was from 61% to 66 %. A comparison of the influence of the layer height on the porosity values of TPE with TPU and TPC showed a significant difference showed a significant difference in porosity numbers by approximately 40 % or more. The filament itself showed a slight change in porosity values, around 4 % to 5 % at higher and lower layers. For (LH) 0.10 mm the values started from 8 % to 12 %. For (LH) 0.13 mm it increased more between 11 % and 16 %. As for the highest (LH) 0.15 mm, it increased from 14% to 18 %. The results are represented in the diagram shown in Figure 5-1.

For the three different materials (TPU 98A, TPE filaflex, and TPC 45flex), the extruder width influencing the porosity number remained constant when it increased. The porosity numbers are higher than the layer height; therefore, the extruder width affects the porosity values more. Increasing the extruder width can increase the porosity by almost 10 % for the three materials, which can be considered a substantial change. The TPU 98A obtained porosity values between 53% and 63% for EW 0.30 mm. It increased when the extruder width increased

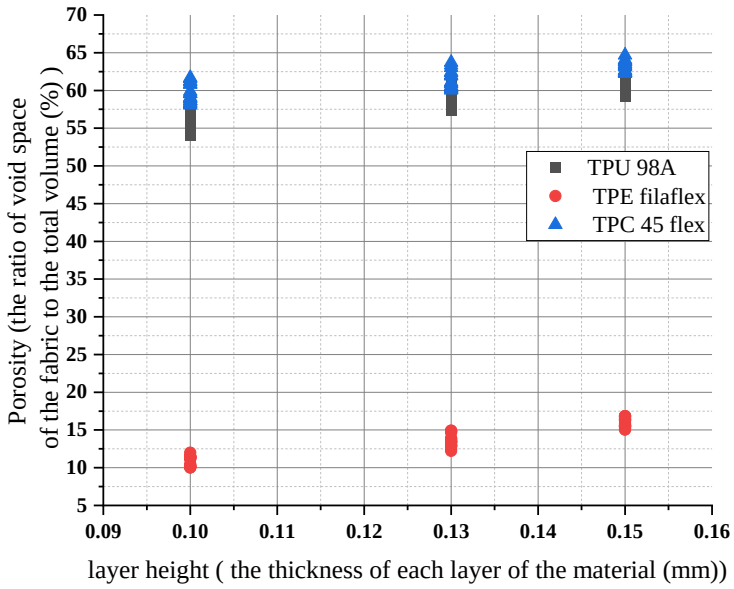

Figure 5-1. Layer height influences on porosity for the three materials.

far more at EW 0.40 mm; the values increased from 56 % and 63 %. For the highest extruder width, 0.50, it increased slightly more between 57% and 64 %. The porosity number was almost the same at 0.40 mm and 0.50 mm, as the range changed slightly when EW increased. For TPC 45flex, the obtained result was slightly higher than the TPU values, and it showed the same variation in the EW in porosity, almost 10 %. For EW 0.30 mm and EW 0.40 mm, the values were almost the same, starting from 57 % to 65 %, while for the highest EW 0.50 mm, it increased from 58 % and 66 %. Comparison between extruder width influences for TPE porosity values with TPU and TPC showed a significant difference in porosity numbers of approximately 30 % or more. The TPE porosity values were the lowest among the other materials. For EW 0.30 mm, EW 0.40 mm, and EW 0.50 mm the values were similar starting from 9% to 17%, as shown in Figure 5-2.

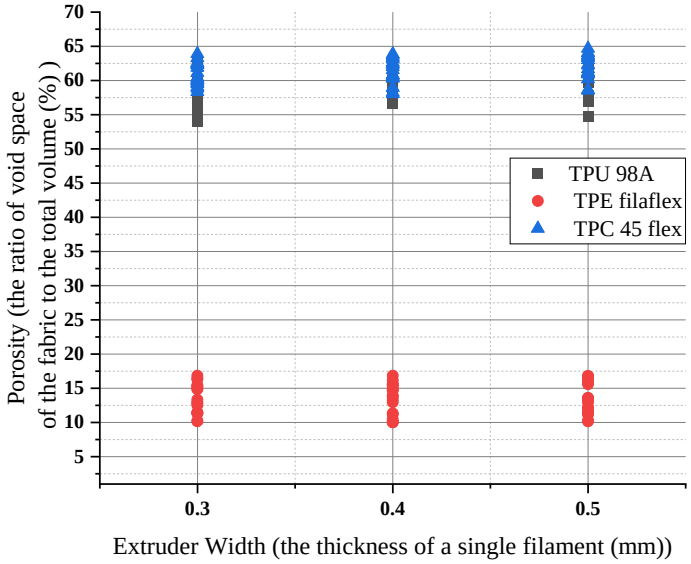

Figure 5-2. Extruder width influences on porosity numbers for the three materials

Orientation had no impact on the porosity numbers for the three materials. The porosity numbers changed from 45 to 90 orientations but remained constant. For (TPU), the porosity number for both orientations had the same increasing range of almost 10%, from 55% to 63%, and from 57% to 66% for the (TPC). However, the (TPE) porosity values were the lowest of the other materials. They showed a considerable change in porosity of almost 40% in both orientations, from 9% to 18%, as shown in Figure 5-3.

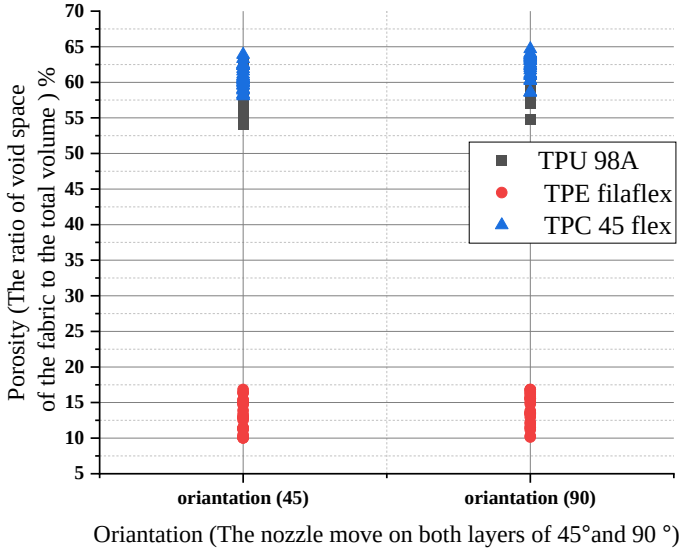

Figure 5-3. Orientation influences on porosity numbers for the three materials.

Therefore, it can be found that the changes in porosity numbers were dependent on the material itself rather than the layer height changes, as the difference was only 5%. The higher porosity can be achieved as the layer height increases from (LH) 0.10 mm to (LH) 0.15 mm for all three materials. It was observed after printing the samples that compared to TPU and TPC, TPE is typically lighter, softer, and more flexible with higher elasticity which leads to less porosity and pore size, as the density (g/m^3) for the (TPU and TPC) was 1.14, and 1.16 (g/m^3) respectively, and the (TPE) was 1.09 (g/m^3). Changing the layer height can affect the surface texture and quality. It was found that the changes in porosity numbers were dependent on the material itself rather than the extruder width changes being similar to the layer height. Higher porosity can be achieved as the extruder width increases from (EW) 0.30 mm to (EW) 0.50 mm for the TPU while the range remains constant for the TPC and TPE. Increasing the extruder width did not affect the porosity number, but it changed with the other parameters. The (TPE) porosity values were the lowest among the other materials. It meant that the value changed considerably for the same material. Individually, layer height and extruder width did not impact the porosity number, but if they were combined, they could affect it. The total porosity of the material shifted almost 10 % as it would create an impact on surface roughness which would also affect the wettability.

5.1.2 The Parameters Influence on Surface Roughness

The differences in the surface roughness behaviour profiles of printed fabric at different layers of height for the three different materials (TPU 98A, TPE filaflex, and TPC 45flex) showed a variation of values as the range changed when the layer height increased. It is common in textiles to use Mean Absolute Deviation (MAD), calculated below along with Ra. It is the most valuable and standard parameter for analysing the surface structure [174]. For TPU 98A, it was shown that 0.10 mm of layer height had the lowest surface roughness between 0.06 - 0.17 μm, whereas the maximum roughness occurred at 0.15 mm of layer height, between 0.29 - 0.45 μm. For the LH 0.013 mm the values are 0.18 – 0.31 μm.

The average amount of the increase remained the same approximately 0.17 μm for the same layer height. As for increasing the layer height, the values increased between 0.11 – 0.14 μm. For TPC 45flex, the result showed that the surface roughness of LH 0.10 mm of layer height had the lowest value of the three materials 0.04 – 0.15 μm, and maximum roughness occurred at 0.15 mm of layer height 0.22 – 0.40 μm. For the LH 0.013 the values were 0.12 – 0.25 μm. The average increase for each layer height increased from 0.11 μm reached 0.18 μm as the layer height changed. As for increasing the layer height, the values increased between 0.11 – 0.14 μm for the same LH. However, the TPE showed the highest roughness values of 0.15 mm of layer height 0.44 - 0.65 μm, whereas it decreased at 0.10 mm of layer height 0.16 - 35 μm. For the LH 0.013 mm the values were 0.34 – 0.45 μm. The average amount of the increase remained the same approximately 0.20 μm for the same layer height. The results are represented in the diagram shown in Figure 5-4.

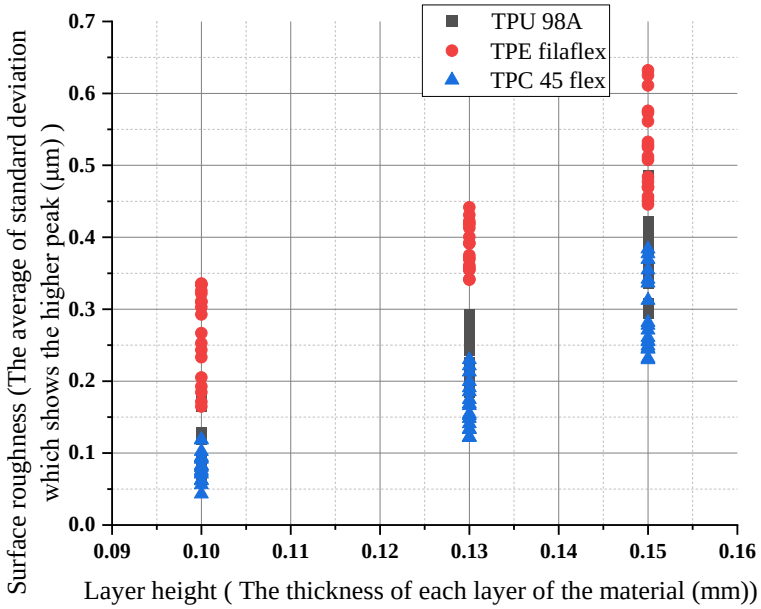

Figure 5-4. Layer height influences on surface roughness for the three materials.

For the extruder width effect on the samples, the TPU 98A result showed that EW 0.30 mm had the lowest surface roughness between 0.06 - 0.17 μm, whereas the maximum roughness occurred at EW of 0.50 mm between 0.29 - 0.45 μm. For the EW 0.40 mm the values are 0.18 - 0.31 μm. The average amount of increase

remained the same, approximately 0.17 μm for the same extruder width. As for increasing the extruder width the values increased between 0.11 – 0.14 μm. For TPC 45flex, the result showed that the surface roughness of EW 0.30 mm had the lowest value of the three materials 0.04 – 0.15 μm, and maximum roughness occurred at EW)0.50 mm 0.22 – 0.40 μm. For the EW 0.013 mm the values were 0.12 – 0.25 μm. The average increase for each extruder width increased from 0.11 μm reached 0.18 μm as it changed. As for increasing the (EW), the values increased between 0.11 – 0.14 μm for the same one. However, the (TPE) showed the highest roughness values of EW 0.50 mm (0.44 - 0.65 μm), whereas it decreased at EW)of 0.30 mm between 0.16 - 35 μm. For the EW 0.40 mm the values were 0.34 – 0.45 μm. The average amount of the increase remained the same approximately 0.20 μm for the same extruder width. The results are represented in the diagram in Figure 5-5.

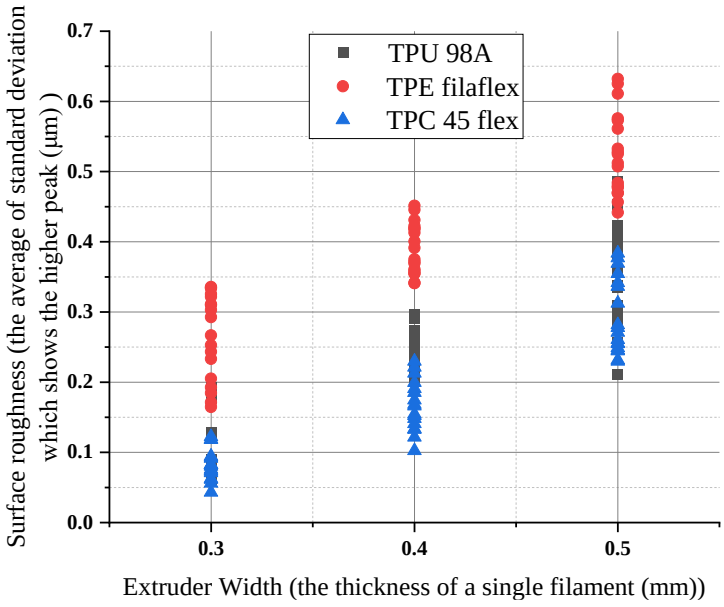

Figure 5-5. Extruder width influences on surface roughness for the three materials.

For the same material there was a significant change with the two different orientation angles 45º - 90º of approximately 0.20 μm. The surface roughness profile at a 45° measuring direction with narrower peaks to valleys distribution increased in the measuring direction angle of 90°. Between the 45° and 90° measuring direction, the surface roughness change remained relatively constant,

with a minor variation of 0.06–0.45 μm for the three materials. They showed the highest roughness values in a printing orientation of 90°, and the values decreased in a printing orientation of 45°, the TPU 98A result showed that O 45º had the lowest surface roughness between 0.06 - 0.28 μm, whereas the maximum roughness occurred at O of 90º between 0.19 - 0.49 μm . For TPC 45flex, the result showed that the surface roughness of O 45º had the lowest value of the three materials 0.04 – 0.25 μm) and maximum roughness occurred at O 90º 0.20 – 0.40 μm. However, the TPE showed the lowest roughness values of O) at 45º 0.16 - 0.46 μm, whereas it increased at O of 90º between 0.34 – 0.65 μm. The average amount of the increase remained the same approximately 0.20 μm, as shown in Figure 5-6.

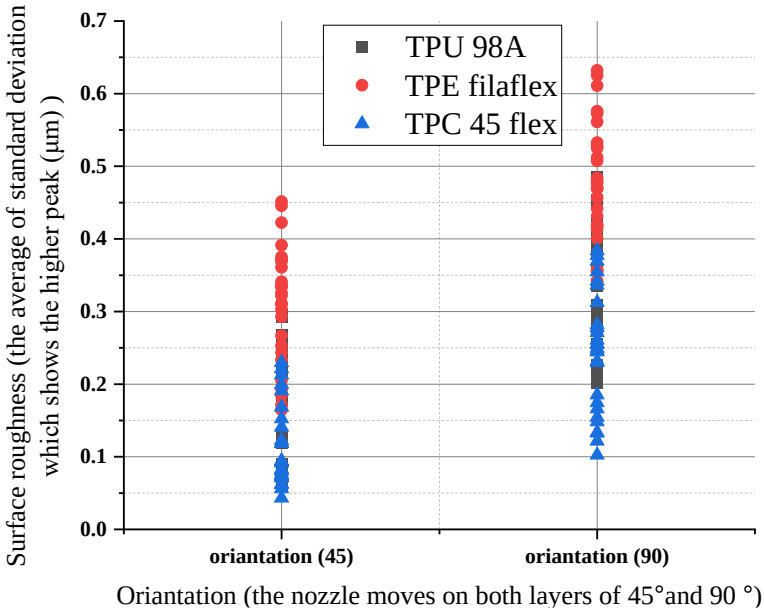

Figure 5-6. Orientation influences on surface roughness for the three materials.

Therefore, one possible way to justify the differences in the effect of the various parameters would be the changes in the material density. These can cause a difference in roughness between the three chosen materials, which was approximately 0.65 μm . For changes in individual print parameters, our results offered acceptance margins for producing a specific desired surface roughness. They suggest that manufacturers, whether private users or companies have considerable room for adjusting printing parameters within the current range that

affects the physically perceived surface roughness, as the printing parameter significantly impacts surface roughness. A proper layer height results in better surface quality, whereas increasing layer height at certain levels increases surface roughness values. Changing the print layer height and extruder width produced samples that spanned relatively RQ ranges between 0.04 - 0.65 μm for the three materials. The fabric's surface with the highest layer height had the highest roughness values for the three materials as the surface became rougher. The average value of the increase remains the same.

5.1.3 The Parameters Influence on Wettability Contact Angle

The wettability of the surface varies according to many parameters such as materials, printing orientation, infill density, etc. The connection between surface roughness and wettability indicates that an accurate surface roughness improves the water repellence for hydrophobic materials, and the water contact angle is dependent on it [129]. For TPU 98A, increasing layer height can cause an increase in wettability. It was shown that 0.10 mm of LH had the lowest wettability between 117º-123º, whereas the maximum WCA accrued at 0.15 mm of layer height 124º-136º. The values for the LH of 0.13 mm were 122º-125º. For TPC 45flex, the result showed that the wettability of LH 0.10 mm had the lowest value of the three materials 112º -120º, and the wettability increased at 0.15 mm of layer height 124º- 136º. For the LH 0.13 mm, the values were 119º-126º. However, the TPE showed the highest values of the three materials of LH 0.15 mm between 149º-143º, while the WCA for 0.10 mm of layer height 124º-136º was decreased. For LH 0.13 mm, the values were 134º-143º. The results are represented in the diagram in Figure 5-7.

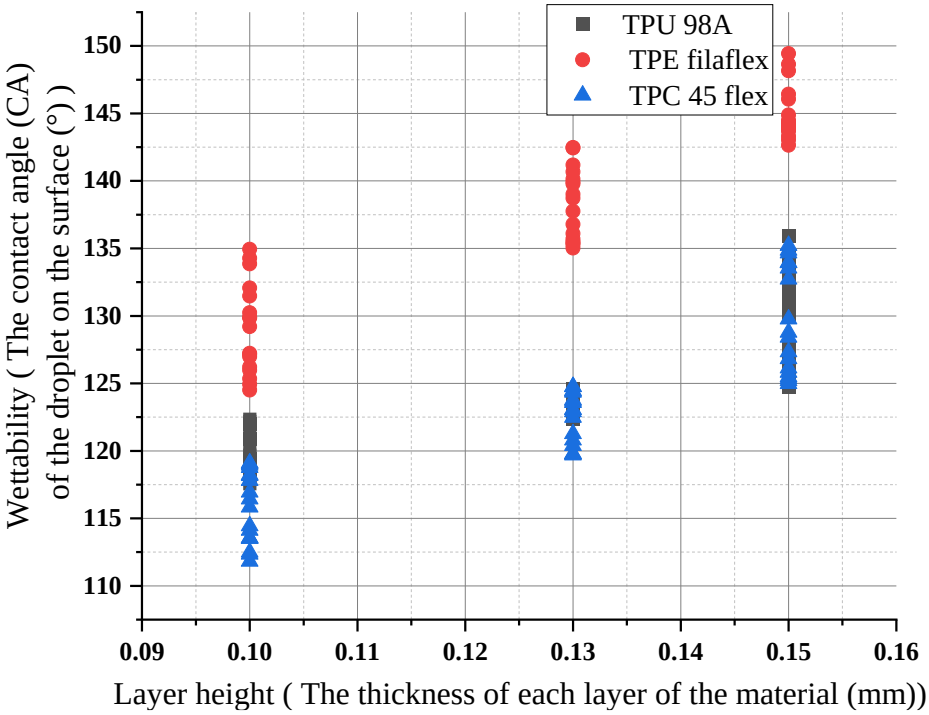

Figure 5-7. Layer height influences on wettability for the three materials

Similarly, increasing the extruder width resulted in increasing the WCA. For TPU 98A the result showed that 0.10 mm of EW had the lowest wettability between 116º-122º, whereas the maximum WCA accrued at 0.15 mm of extruder width 123º-135º. The values for the EW of 0.13 mm were 121º-124º. For TPC 45flex, the result showed that the wettability of EW 0.10 mm had the lowest value of the three materials 111º -120º, and the wettability contact angle increased at 0.15 mm of extruder width 124º- 136º. For the EW 0.13 mm, the values were 118º-125º. However, the TPE showed the highest values of the three materials of EW)0.15 mm between 148º-142º, while the WCA values for 0.10 mm of layer height 123º-134° were decreased. For EW 0.13 mm, the values were 133º-142º, as shown in the diagram in Figure 5-8.

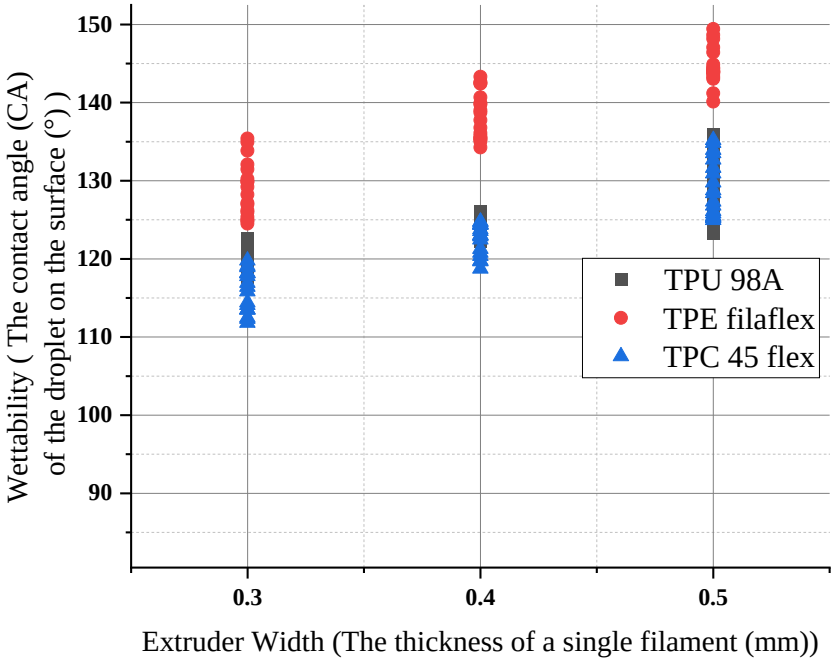

Figure 5-8. Extruder width influences on wettability for the three materials

There is a change for the same material with the two different orientation angles (45°–90°). Hence between 45° and 90°, the wettability changes according to the changes in surface roughness [175],[87],[129]. The three materials (TPU 98A), (TPC 45flex), and (TPE) showed that the highest wettability values were in a printing orientation of 90°, while the values decreased at a printing orientation of 45°. For the same material there was a significant change with the two different orientation angles (45º - 90º) of approximately 10º. They showed the highest roughness values in a printing orientation of 90 °, and the values decreased in a printing orientation of 45°, the TPU 98A result showed that at O 45º had the lowest WCA between 117º - 125º, whereas the maximum roughness occurred at O of 90º between 124º - 136º. For TPC 45flex, the result showed that the wettability contact angle of O 45º had the lowest value of the three materials 112º–126º, and maximum roughness occurred at O)90º 122º – 136º. However, the TPE showed the lowest roughness values of O at 45º (124º - 143º), whereas it increased at O of 90 º between 134º – 149º. as shown in Figure 5-9.

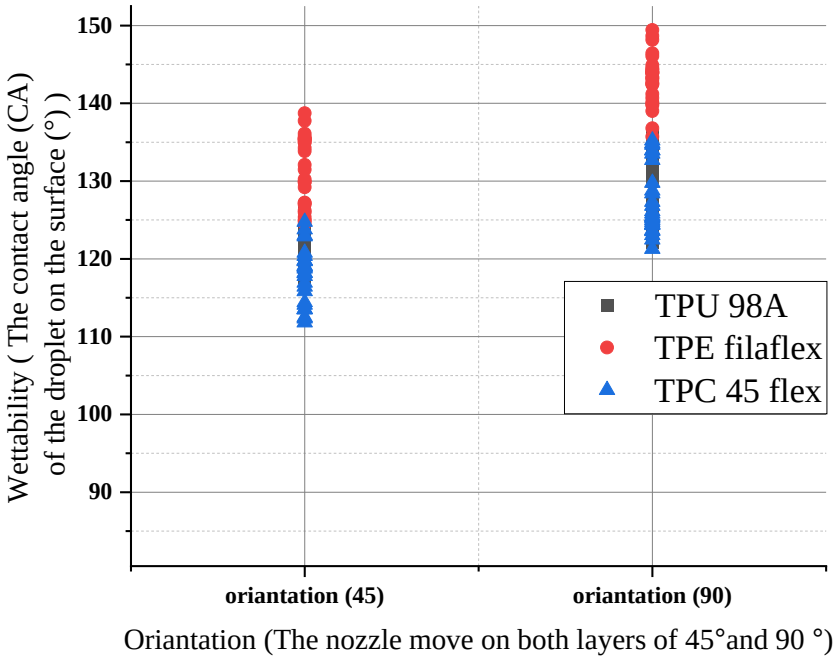

Figure 5-9. Orientation influences on wettability for the three materials

The experimental results showed that TPE has a better water contact angle WCA than the other two materials. Changing the print layer height and extruder width produced samples that spanned relatively RQ ranges between 0.04 – 0.65 μm, yet there were significant differences in the wetting ability. This indicated that layer height, extruder width and orientation changes caused an increase in wettability contact angle. The average value of the increase remained the same at 10º. Therefore, the connection between the roughness and wettability caused a higher value in wettability contact angle for the three materials.

5.1.3.1 Water Absorption and Fabric Wettability

The principle that can be applied to this work is that if the raw material (TPU 98A, TPE filaflex or TPC 45flex) is hydrophilic, the printed porous material will automatically absorb water with time to generate a liquid infused layer and the contact angle of the droplet will diminish after some time. To validate this phenomenon, we conduct additional experiments to demonstrate the stability of contact angles on porous textile fabric made from these three materials.

The fabrication of the porous surface required a combination of the printing parameters. The pore size can influence the behaviour of liquids in porous textiles and control the flow pattern of that liquid moving through a porous material. In this study, the flow of the water droplet through the printed textiles is caused by the surface movement, as the person wearing the fabric will be moving most of the time. This constant movement should provide the floating action as soon as the droplet comes to the surface. If the droplets are retained on the fabric surface, they will gradually be absorbed.

While there is an absorption principle, the researchers hypothesize that due to the self-cleaning wettability angle and the continuously changing surface position, there will be minimal time for absorption to occur. The wettability angle is a critical parameter that describes how the material is expected to exhibit self-cleaning properties. Additional experiments have been conducted to observe the behaviour of wettability over time.

- **(TPU 98A).**

Specifically, for the TPU 98A, the contact angle experiences slight changes when the textile surface remains static, as shown in Figure 5 10. The figure demonstrates the contact angle transition as follows: (a) initially, the contact angle of the droplet on the surface measures 112.18°, (b) after 5 minutes, the contact angle decreases to 77.25°, and (c) after 10 minutes, the contact angle further decreases to 59.95°. As time progresses, the water droplet will gradually be absorbed into the porous material. Additionally, the implications of the contact angle changes and water absorption behaviour on the self-cleaning properties and functionality of the printed porous materials were discussed.

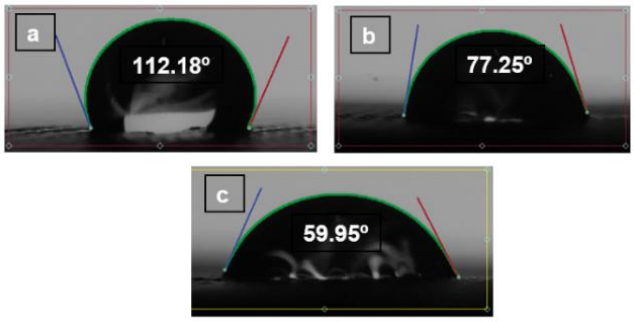

Figure 5-10. (a) The contact angle on the TPU (b) The contact angle after 5 minutes and (c) The contact angle on after 10 minutes.

- **(TPE filaflex).**

The observation on the TPE filaflex was that the contact angle changes slightly if the textile surface remains without movement as it shown in Figure 5-11. The figure indicates the change in contact angle for TPE filaflex over time when the textile surface remains stationary. The figure shows the following transitions: a) Initially, when a droplet is placed on the surface, the contact angle is measured to be 120.46°. This suggests that the surface has a relatively high hydrophobicity, causing the water droplet to bead up and form a high contact angle; b) After 5 minutes, the contact angle decreases to 80.21°. This decrease in contact angle indicates that the water droplet is starting to spread and access the porous structure of the fabric. The fabric may have a certain degree of water absorption capability, allowing the droplet to be partially absorbed; c) After 10 minutes, the contact angle further decreases to 64.46°. This suggests that the water droplet has continued to spread and penetrate deeper into the porous structure of the fabric. The absorption of the droplet within the fabric's pores leads to a lower contact angle.

These observations indicate that the TPE filaflex fabric has some degree of hydrophobicity initially, resulting in a high contact angle. However, over time, the water droplet is absorbed by the porous structure of the fabric, causing the contact angle to decrease as the droplet spreads and penetrates deeper. This behaviour suggests that the fabric has some water absorption properties.

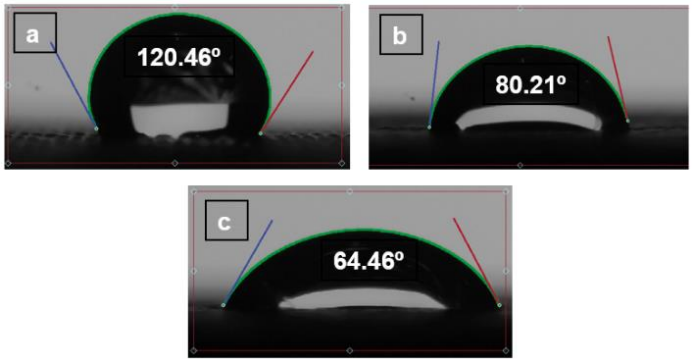

Figure 5-11 (a) The contact angle on the TPE (b) The contact angle after 5 minutes and (c) The contact angle after 10 minutes.

- **(TPC 45flex).**

The observations for the TPC 45flex were that the contact angle changes slightly if the textile surface remains without movement as shown in Figure 5-12. The figure illustrates the change in contact angle for TPC 45flex over time when the textile surface remains stationary. The figure depicts the following transitions: a) Initially, when a droplet is placed on the surface, the contact angle is measured to be 94.45°. This indicates that the surface possesses a certain level of hydrophobicity, causing the water droplet to form a relatively high contact angle; b) After 5 minutes, the contact angle decreases to 75.95°. This reduction in contact angle suggests that the water droplet is starting to spread and access the porous structure of the fabric. The fabric likely has some water absorption capacity, allowing the droplet to be partially absorbed; c) After 10 minutes, the contact angle further decreases to 49.29°. This implies that the water droplet continues to spread and penetrate deeper into the porous structure of the fabric. The absorption of the droplet within the fabric's pores leads to a lower contact angle.

These observations indicate that the TPC 45flex fabric exhibits a certain level of hydrophobicity initially, resulting in a relatively high contact angle. However, with the passage of time, the water droplet is absorbed by the porous structure of the fabric, leading to a decrease in the contact angle as the droplet spreads and

passes through further. This behaviour suggests that the fabric possesses some water absorption properties.

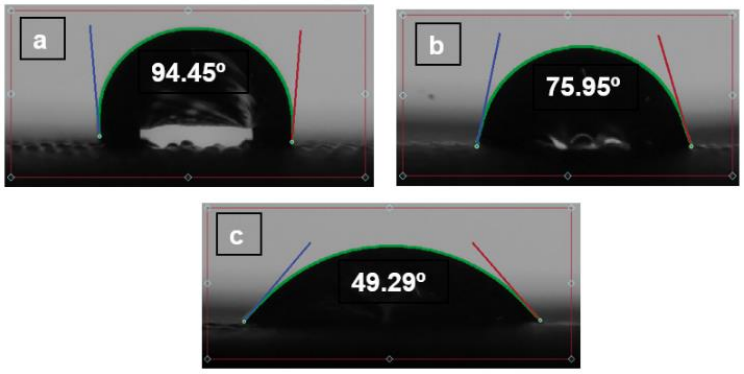

Figure 5-12. (a) The contact angle on the TPC. (b) The contact angle after 5 minutes and (c) The contact angle on after 10 minutes.

5.2 The Relationship Between the Printing Parameters and the Microscopic Features

The application of a second-degree polynomial response surface methodology (RSM) model allows for the determination of regression models and the correlation between input parameters and the response variables. In this case, the regression models for self-cleaning attributes, namely porosity, surface roughness, and wettability, were developed for the three different materials: TPU 98A, TPE filaflex, and TPC 45flex. These regression equations were fitted using MATLAB based on Equation (4-1).

- **(TPU 98A).**

$$\boldsymbol{Porosity = 48.12 + 0.03x_1 + 44.03x_2 + 8.19x_3} \quad \textbf{(5-1)}$$

$$\boldsymbol{Roughness = -0.23 + 0.001x_1 + 1.20x_2 + 0.62x_3} \quad \textbf{(5-2)}$$

$$\boldsymbol{Wettability = 100.51 + 0.17x_1 + 137.22x_2 + 3.306x_3} \quad \textbf{(5-3)}$$

The regression measurements for the three parameters (x_1, x_2, x_3) in the regression equations have positive values for all three features: porosity, roughness, and wettability. This indicates that as the building orientation changes from 45° to 90°, the values of these features increase. Similarly, for the layer height and extruder width, the regression measurements for porosity (44.03 and 8.19), roughness (1.20 and 0.63), and wettability (137.22 and 3.306) suggest that as these parameters increase, the porosity and roughness values also increase. These regression equations provide a mathematical representation of the relationship between the input parameters (building orientation, layer height, and extruder width) and the self-cleaning attributes (porosity, surface roughness, and wettability) for TPU 98A. They can be used to predict the values of these features based on specific combinations of printing parameters.

- **(TPE filaflex).**

$$\boldsymbol{Porosity = 3.14 + 0.03x_1 + 25.88x_2 + 13.06x_3} \quad \textbf{(5-4)}$$

$$\boldsymbol{Roughness = -0.062 + 0.001x_1 + 1.29x_2 + 1.13x_3} \quad \textbf{(5-5)}$$

$$\boldsymbol{Wettability = 39.15 + 0.098x_1 + 139.11x_2 + 135.87x_3} \quad \textbf{(5-6)}$$

The regression measurements for the building orientation parameter (x_3) in the regression equations have positive values (0.03, 0.0014, and 0.098) for porosity, roughness, and wettability, respectively. This indicates that as the building orientation changes from 45° to 90°, the values of these features increase. Similarly, the regression coefficients for layer height (x_1) and extruder width (x_2) are positive values. For porosity, roughness, and wettability, the layer height regression coefficients are 25.88, 1.29, and 139.11, respectively, while the extruder width regression coefficients are 13.06, 1.13, and 135.87, respectively. This implies that increasing the layer height or extruder width will increase the corresponding feature values.

- **(TPC flex45).**

$$\boldsymbol{Porosity = 53.17 + 0.03x_1 + 25.03x_2 + 8.25x_3} \quad \textbf{(5-7)}$$

$$\boldsymbol{Roughness = -0.29 + 0.0009x_1 + 0.66x_2 + 0.81x_3} \quad \textbf{(5-8)}$$

$$\boldsymbol{Wettability = 93.02 + 0.11x_1 + 22.61x_2 + 45.21x_3} \quad \textbf{(5-9)}$$

The regression measurements for the building orientation parameter (x_1) in the regression equations have positive values (0.03 and 0.0009) for porosity and roughness, respectively. This indicates that as the building orientation increases from 45° to 90°, the values of these features increase. Similarly, the regression coefficients for layer height (x_2) and extruder width (x_3) are positive values. For porosity and roughness, the layer height regression coefficients are 25.03 and 0.66, respectively, while the extruder width regression coefficients are 8.25 and 0.81, respectively. This implies that increasing the layer height or extruder width will increase the corresponding feature values.

These regression equations and their coefficients provide a mathematical model to predict the values of porosity, surface roughness, and wettability based on the input parameters (building orientation, layer height, and extruder width) for TPE filaflex and TPC flex45 materials.

Therefore, for porosity in all materials, the most influential parameter is layer height. Layer height has a consistent influence of about 5% increase in porosity from its minimum to maximum values in all materials. Extruder width and orientation have very little or no influence on porosity, as per the experimental observations for all materials. For surface roughness all the three printing parameters have an equal influence. Layer height, extruder width and orientation have a consistent influence of about an approximately 0.20 μm increase in roughness from their minimum to maximum values in all materials. Changing the layer height and extruder width gave samples that have RQ ranges between 0.04 - 0.65 μm for the three materials. For wettability, the layer height, extruder width,

and orientation have varying degrees of influence on wettability, depending on the material being used.

5.3 The Self-Cleaning Number

Based on the information provided, the self-cleaning ability of the three materials (TPU 98A, TPE filaflex, and TPC 45flex) was evaluated using the self-cleaning number. The self-cleaning number is determined based on a linear equation (4-2), where a wettability value of 90° corresponds to a self-cleaning number scale of 0 (indicating no self-cleaning ability), and a wettability value of 180° corresponds to a self-cleaning number scale of 100 (indicating optimal self-cleaning ability).

I. TPU 98A: The self-cleaning number varied between 44.11 and 73.49. The lowest self-cleaning number (44.11) was achieved with a wettability value obtained from a combination of printing parameters: 0.10 mm layer height (LH), 0.3 mm extruder width (EW), and 45° printing orientation (O). The highest self-cleaning number (73.49) was achieved with a wettability value obtained from a combination of printing parameters: 0.15 mm LH, 0.5 mm EW, and 90° O.

II. TPE filaflex: The self-cleaning number varied between 55.22 and 94.90. The lowest self-cleaning number (55.22) was achieved with a wettability value obtained from a combination of printing parameters: 0.10 mm LH, 0.3 mm EW, and 45° O. The highest self-cleaning number (94.90) was achieved with a wettability value obtained from a combination of printing parameters: 0.15 mm LH, 0.5 mm EW, and 90° O.

III. TPC 45flex: The self-cleaning number varied between 34.91 and 72.33. The lowest self-cleaning number (34.91) was achieved with a wettability value obtained from a combination of printing parameters: 0.10 mm LH, 0.3 mm EW, and 45° O. The highest self-cleaning number (72.33) was achieved with a wettability value obtained from a combination of printing parameters: 0.15 mm LH, 0.5 mm EW, and 90° O.

Comparing the three materials, TPE filaflex exhibited the best self-cleaning result, with the highest self-cleaning number of 94.90. This result was obtained using a combination of printing parameters: 0.15 mm LH, 0.5 mm EW, and 90° O. This indicates that TPE filaflex showed the highest level of self-cleaning ability of the three materials studied.

It is important to note that these results are based on the specific combinations of printing parameters mentioned and may vary with different parameter values. Additionally, the self-cleaning number provides a relative measure of self-cleaning ability within the studied range but does not provide absolute quantification of the material's self-cleaning performance.

5.4 Mechanical Strength Test

The mechanical strength of 3D printed polymeric textile fabrics was evaluated through tensile testing. The samples chosen for the test were based on the ones that provided the highest self-cleaning numbers for each of the three materials: TPU, TPE, and TPC. The tensile test was conducted using an Instron machine with a speed of 0,5 mm/min at load 5 N, following the ISO 527 standard testing method as shown in Figure 5-13.

Figure 5-13. An Instron machine for the mechanical strength.

The chosen samples depended on the ones that provided the highest self-cleaning number for the three materials in Section 5.3. For TPU 98A, the highest

self-cleaning number was achieved with a layer height (LH) of 0.15 mm, an extruder width (EW) of 0.5 mm, and an orientation (O) of 90°. The tensile strength test procedure for TPU is illustrated in Figure 5-14.

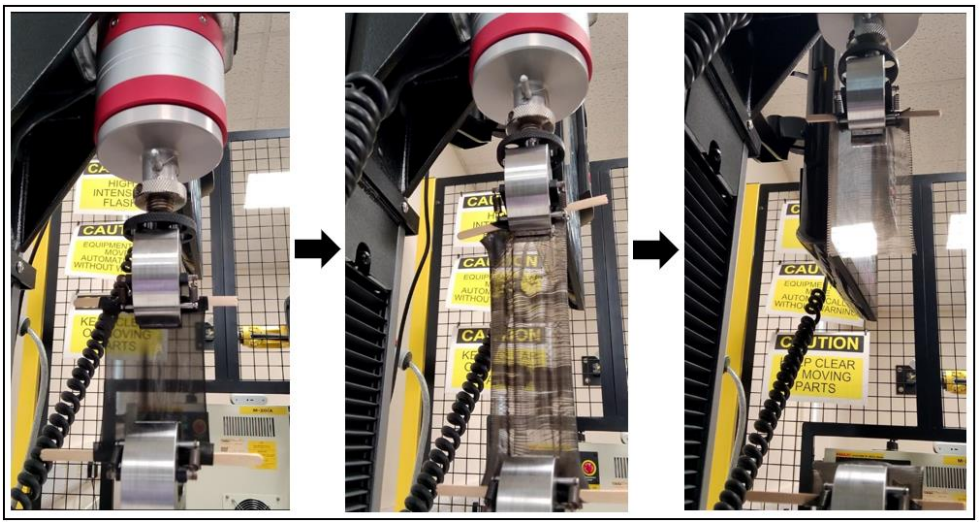

Figure 5-14. Procedure for (TPU 98A) tensile strength test.

For TPE filaflex, the highest self-cleaning number was obtained with a layer height (LH) of 0.15 mm, an extruder width (EW) of 0.5 mm, and an orientation (O) of 90°. The tensile strength test procedure for TPE is shown in Figure 5-15.

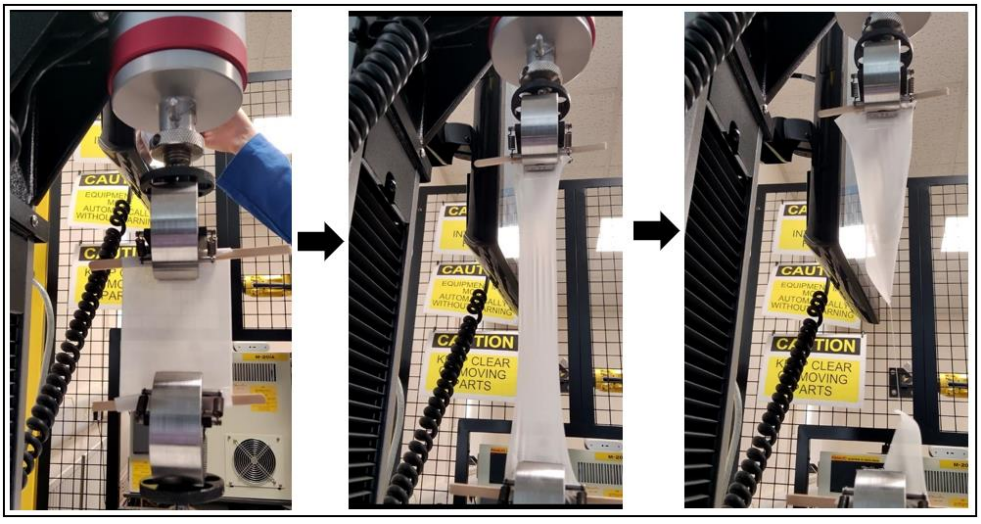

Figure 5-15. Procedure for (TPE filaflex) tensile strength test.

For TPC 45flex, the highest self-cleaning number was achieved with a layer height (LH) of 0.15 mm, an extruder width (EW) of 0.5 mm, and an orientation (O) of 90°. The tensile strength test procedure for TPC is depicted in Figure 5-16.

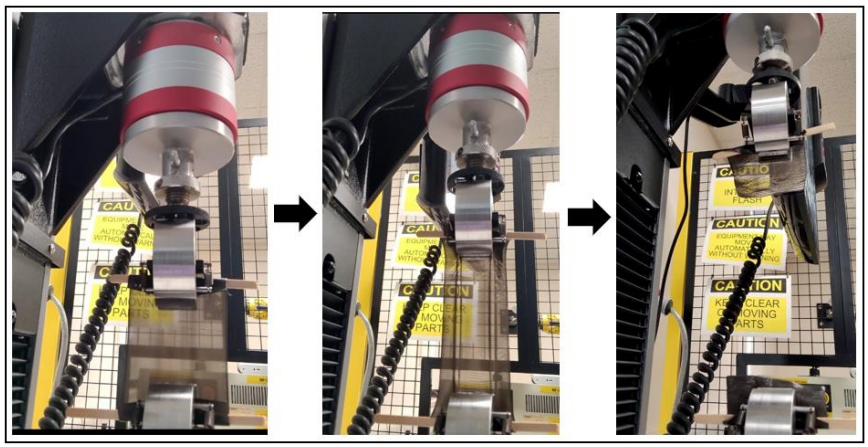

Figure 5-16. Procedure for (TPC) tensile strength test.

The results of the tensile strength tests showed that TPE filaflex exhibited the highest tensile strength, reaching over 122 mm displacement with a force of approximately 120 N, as shown in Figure 5-17. On the other hand, TPU and TPC demonstrated lower tensile strength. TPU had a tensile strength of 105 mm displacement with a force of 80 N, while TPC had a tensile strength of 85 mm displacement with a force of 60 N, which was the lowest of the three materials. These findings indicate that TPE filaflex is the most mechanically strong material of the three tested, while TPU and TPC exhibit reduced tensile strength. The higher tensile strength of TPE can be attributed to its excellent mechanical characteristics and flexibility, allowing it to withstand more force and stretch to standard extension while returning to its original shape.

The force displacement test conducted in the study aimed to evaluate and compare the mechanical strength of the three materials (TPU, TPE, and TPC) used in 3D printed polymeric textile fabrics. The test provided insights into the behaviour of the materials under applied force and displacement.

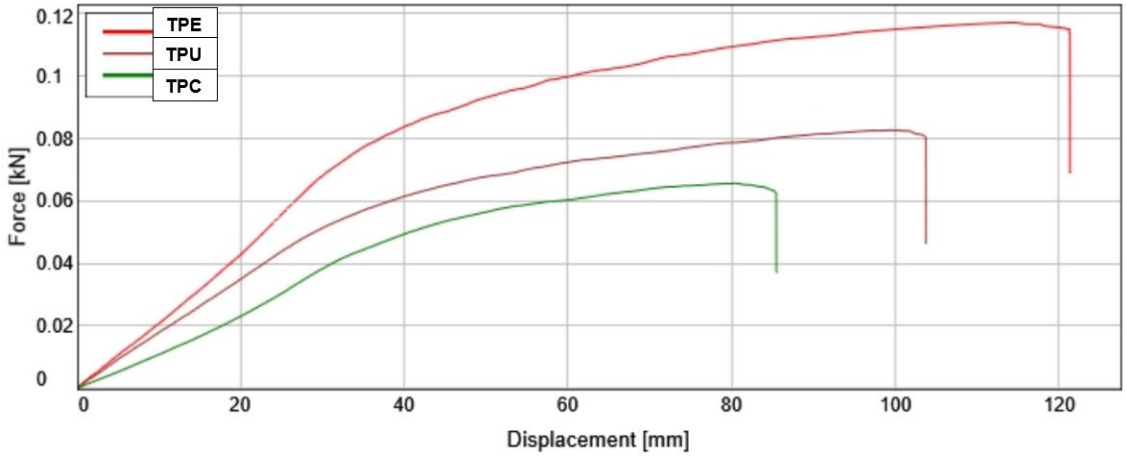

Figure 5-17. The mechanical strength results.

The observed results from the force displacement test can indeed provide valuable information regarding the mechanical strength of the materials. The displacement at which the material starts to deform, the maximum force it can withstand before failure, and its overall stiffness or flexibility can be determined from these tests. These observations can help in assessing the suitability of the materials for specific applications that require certain mechanical properties.

5.5 Conclusion

This chapter provides an experimental study performed on FFF-based using three different thermoplastic flexible filament printing materials: thermoplastic polyurethane (TPU 98A), thermoplastic elastomers (TPE filaflex), and thermoplastic co-polyester (TPC flex45) to fabricate 3D printed polymeric textile fabrics.

• It was found that the printing parameters have a very significant effect on the self-cleaning properties, when optimizing the selection of the process parameter combination of layer height, extruder width, and printing orientation. The results showed that changing layer height and extruder width combined can affect the porosity, surface roughness, and wettability. The highest layer height has a rougher impact on the surface texture.

• The changes in porosity numbers are dependent on the material itself rather than the layer height changes. It shows porosity values obtained between 9% and 18% for the chosen layer height. It slightly changes by about 2% to 5% at higher and lower layer height.

• The lowest surface roughness occurs on the 0.10 mm of layer height for TPC with 112 ° wettability contact angle, whereas the highest occurs on the 0.15 mm of layer height for TPE with 149 ° wettability contact angle. Changing the print layer height and extruder width produce samples that span relatively roughness ranges between 0.04 – 0.65 μm.

• The experimental results showed TPE has a better self-cleaning ability than the other two materials. It showed several scale values varying between 55.22 which is the lowest value with wettability of 0.10 mm LH, 0.3 mm EW and 45 ° O and 94.90 which is the highest value of 0.15 mm LH, 0.5 mm EW and 90 ° O for self-cleaning number. The results of the tensile test revealed that the TPE showed the highest tensile strength of more than 122 mm displacement with the highest force of almost 120 N, due to the flexibility of the fabric.

• Printing different layer heights can affect the printing time and divide a 3D model into more layers affecting the quality of the printed fabric. Extruder width was found to be much more critical related to surface printed quality, as lowering the width deteriorated the printed surface causing more threads to be printed to cover the surface. A desirable structural geometry and fibre orientation are achievable with reasonable and accurate control of printing parameters.

• The study successfully created a linear regression model to demonstrate the relationship between 3D printing parameters of (layer height, extruder width, and orientation) and the self-cleaning microscopic features of the 3D printed polymeric textile fabrics.

6 THE OPTIMIZATION OF PRINTING PARAMETERS

The optimization of printing parameters was conducted with the aim of achieving the highest self-cleaning ability for the printed specimens. A method and optimization model were developed, which can be utilized to estimate the self-cleaning ability of printed fabric when the inputs of the printing parameters are known. Through the optimization process, it was discovered that even better self-cleaning behaviour can be achieved by considering various combinations of the printing parameters. Specifically, it was observed that high wettability, low porosity, and high roughness contribute to a higher self-cleaning number, indicating improved self-cleaning ability.

The possible combinations of the printing parameters for optimal self-cleaning ability of all the three materials are discussed below. These parameter combinations have been identified as providing optimal self-cleaning ability for each respective material. However, it's important to note that these combinations are specific to the study and may not be universally applicable. The optimal parameter values for self-cleaning can vary depending on the specific material properties, printing technology, and desired outcomes.

Further research and experimentation are recommended to validate and refine these findings, considering the specific requirements and characteristics of the materials being used.

- **TPU 98A**

Equations (5-1), (5-2) and (5-3) above in chapter 5 were used to find out the optimal self-cleaning ability for the TPU fabrics. Printing parameters were plotted with self-cleaning attributes as shown in Figure 6-1, Figure 6-2 and Figure 6-3. based on the information provided, it appears that the minimum possible porosity was achieved with any orientation and lower values of extruder width 0 to 0.2 mm and layer height 0.25 mm to 0.3 mm of 62%. On the other hand, the maximum roughness was obtained with any orientation and higher values of extruder width 0.9 to 1 mm and layer height 0.45 mm to 0.5 mm. Similar trends were observed

for wettability, where maximum wettability seemed independent of extruder width, as long as the contact angle was above 150° reaching 180°. The wetting angle is typically measured as the angle between the liquid droplet and the solid surface and should not exceed 180°. To achieve the optimum self-cleaning ability, it is recommended to select a decent value of roughness while minimizing the porosity percentage. In the case of TPU, the optimum self-cleaning can be attained at any given orientation, although with a compromise on desired roughness and porosity percentage. The plots of roughness and porosity suggest that a good compromise can be achieved if the fabric is printed with an extruder width ranging from 0.4 to 0.5 mm, at layer height from 0.2 to 0.3 mm.

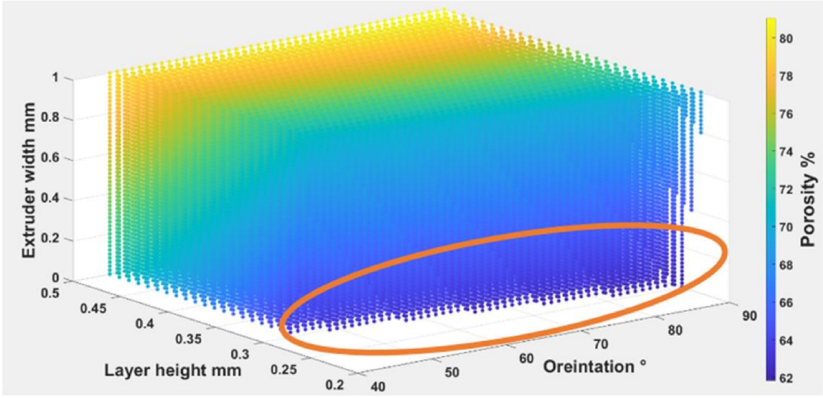

Figure 6-1. The possible combination of the printing parameters range for (O), (LH), (EW) to achieve the best self-cleaning performance for porosity.

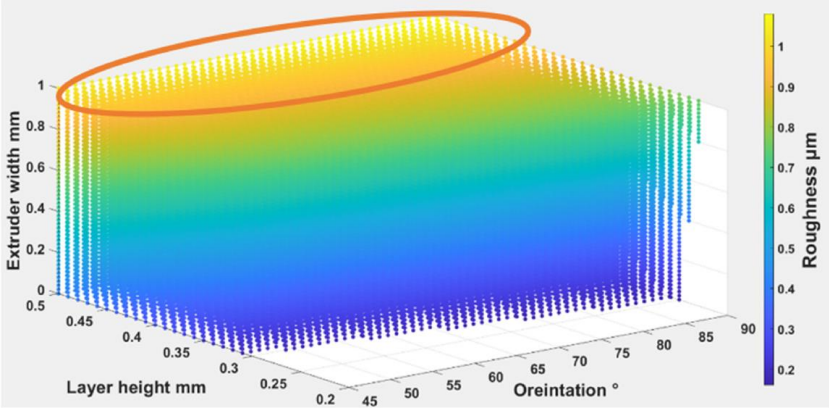

Figure 6-2. The possible combination of the printing parameters range for (O), (LH), (EW) to achieve the best self-cleaning performance for roughness.

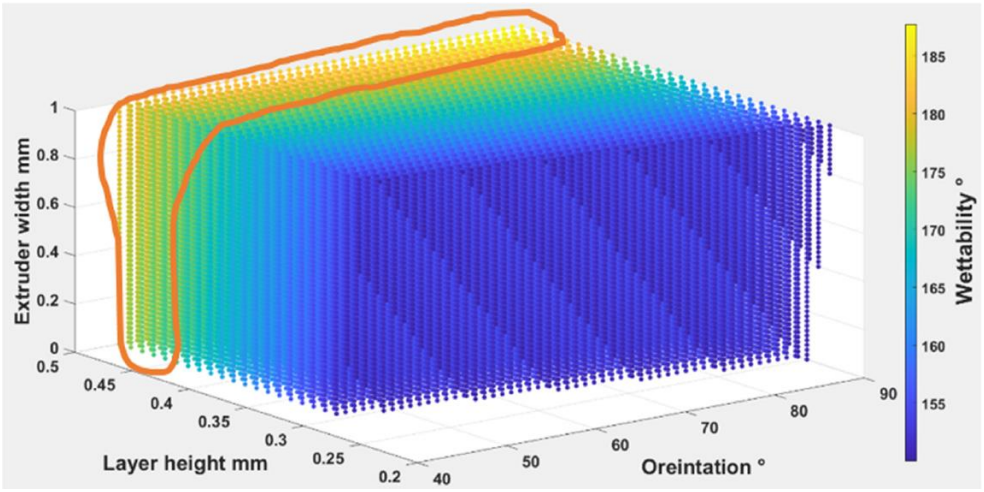

Figure 6-3. The possible combination of the printing parameters range for (O), (LH), (EW) to achieve the best self-cleaning performance for wettability.

It is important to note that these findings are based on the available information provided, and further experimentation and analysis may be required to validate and optimize the printing parameters for achieving the desired self-cleaning ability. Additionally, the specific requirements and characteristics of the materials being used should be taken into consideration when determining the optimal printing parameters.

- **TPE filaflex**

Equations (5-4), (5-5) and (5-6) were used to find out the optimal self-cleaning ability for the TPU fabrics. Printing parameters were plotted with self-cleaning attributes as shown in Figure 6-4, Figure 6-5 and Figure 6-6. Based on the information provided, it appears that the minimum possible porosity can be achieved with any orientation and lower values of extruder width 0 to 0.2 mm and layer height 0.25 mm to 0.3 mm. On the other hand, maximum roughness of 1 μm can be obtained with any orientation and higher values of extruder width 0.9 mm to 1 mm and layer height 0.45 mm to 0.5 mm. The trend for wettability, in terms of orientation and layer height, seems to be similar. It is worth noting that maximum wettability appears to be independent of extruder width, as long as the contact angle is above 150° and reaching 180°. The wetting angle is typically measured as the angle between the liquid droplet and the solid surface and

should not exceed 180°. To achieve the optimum self-cleaning ability, it is recommended to select a suitable value of roughness while minimizing the porosity percentage. In the case of TPE, the optimum self-cleaning ability can be attained at any given orientation, although there may be compromises in terms of desired roughness and porosity percentage. The plots of roughness and porosity indicate that a good compromise can be achieved by using an extruder width ranging from 0.4 mm to 0.5 mm, at layer height from 0.1 mm to 0.2 mm.

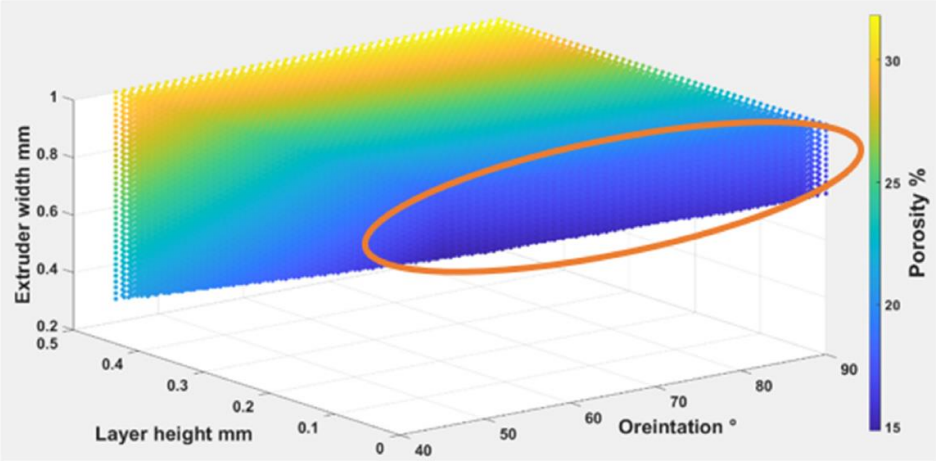

Figure 6-4. The possible combination of the printing parameters range for (O), (LH), (EW) to achieve the best self-cleaning performance for porosity.

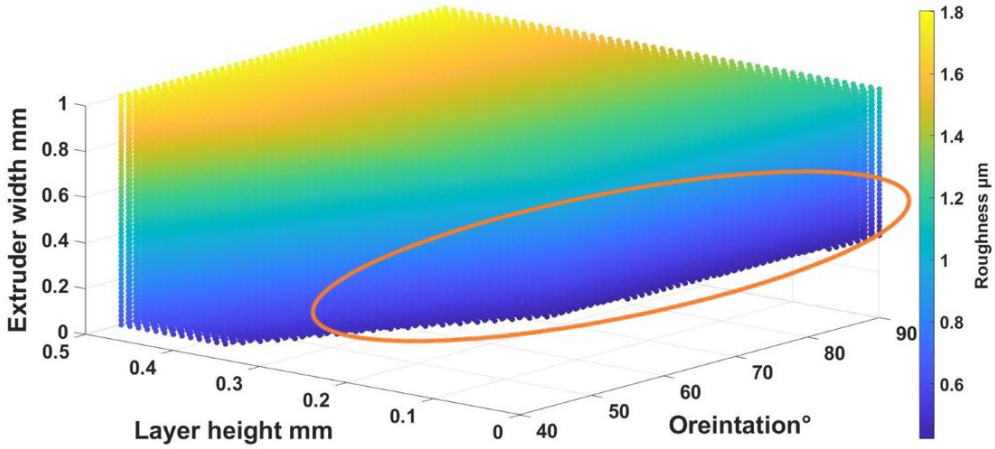

Figure 6-5. The possible combination of the printing parameters range for (O), (LH), (EW) to achieve the best self-cleaning performance for roughness.

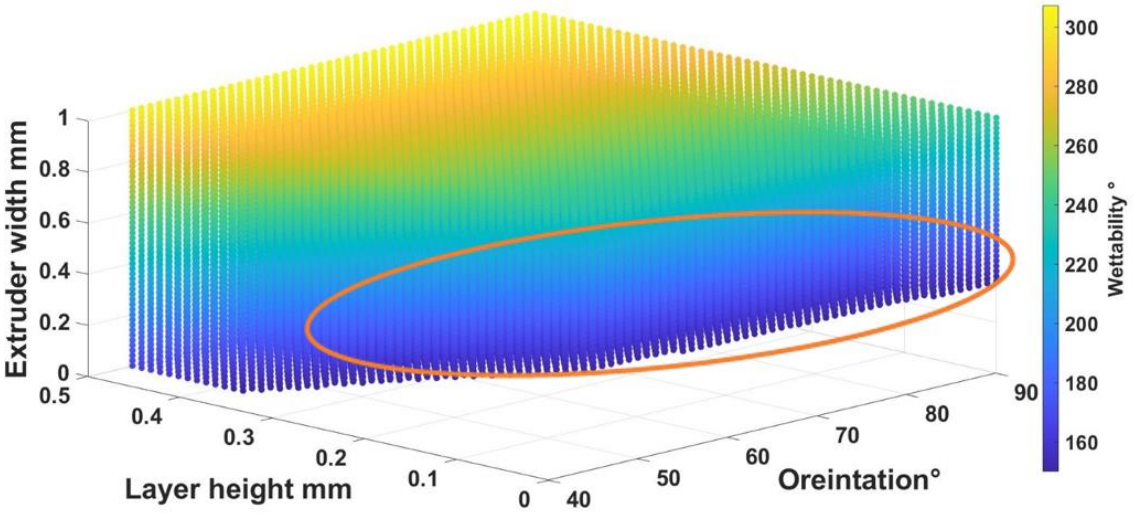

Figure 6-6. The possible combination of the printing parameters range for (O), (LH), (EW) to achieve the best self-cleaning performance for wettability.

The information provided is based on the given details. Further experimentation and analysis may be required to fully optimize the printing parameters and achieve the desired self-cleaning ability. Additionally, it is important to consider the specific characteristics and requirements of the materials being used when determining the optimal printing parameters.

- **TPC 45flex**

Equations (5-7), (5-8) and (5-9) were used to find out the optimal self-cleaning ability for the TPU fabrics. Printing parameters were plotted with self-cleaning attributes as shown in Figure 6-7, Figure 6-8 and Figure 6-9. The minimum possible porosity of 67% was available on any value of orientation and lower values of extruder width 0.1 mm to 0.2 mm and layer height 0.25 mm to 0.3 mm. Based on the information provided, it is evident that the minimum possible porosity can be achieved with any orientation and lower values of extruder width 0 to 0.2 mm and layer height 0.25 mm to 0.3 mm. Conversely, maximum roughness of 1 μm can be obtained with any orientation and higher values of extruder width 0.9 mm to 1 mm and layer height 0.45 mm to 0.5 mm. A similar trend can be observed for wettability concerning orientation and layer height. It is important to note that maximum wettability appears to be independent of extruder

width, as long as the contact angle exceeds 150 ° reaching 180°. The wetting angle is typically measured as the angle between the liquid droplet and the solid surface and should not exceed 180°. To achieve the optimum self-cleaning ability, it is recommended to select a suitable roughness value while minimizing the porosity percentage less than 100%. In the case of TPC, the optimum self-cleaning ability can be achieved at any given orientation, albeit with compromises in terms of desired roughness and porosity percentage. The plots of roughness and porosity suggest that a reasonable compromise can be made by utilizing an extruder width ranging from 0.4 mm to 0.5 mm, regardless of the layer height 0.1 mm to 0.2 mm.

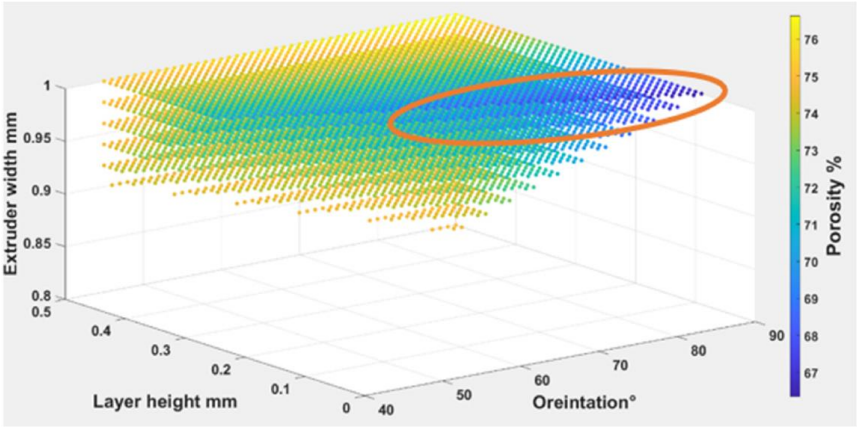

Figure 6-7. The possible combination of the printing parameters range for (O), (LH), (EW) to achieve the best self-cleaning performance for porosity.

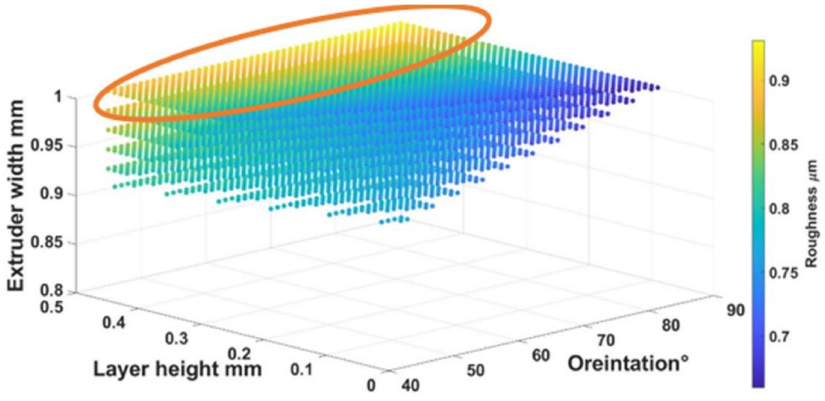

Figure 6-8. The possible combination of the printing parameters range for (O), (LH), (EW) to achieve the best self-cleaning performance for roughness.

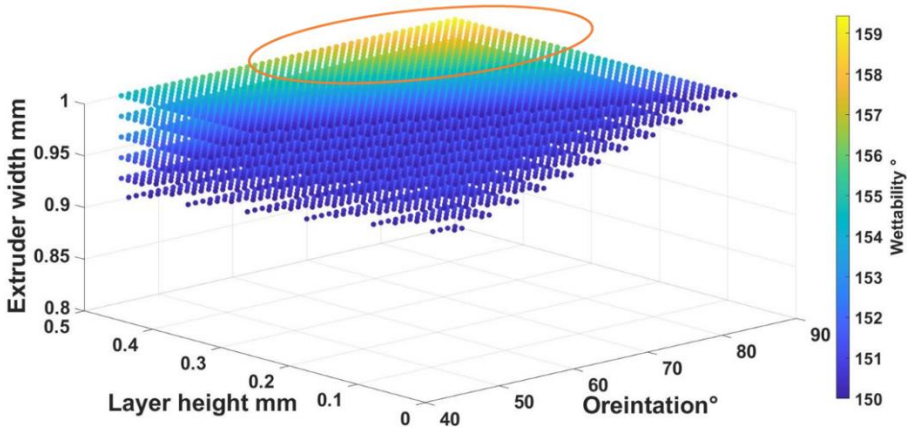

Figure 6-9. The possible combination of the printing parameters range for (O), (LH), (EW) to achieve the best self-cleaning performance for wettability.

However, it is important to consider that these findings are based on the information provided, and further experimentation and analysis may be necessary to fully optimize the printing parameters for the desired self-cleaning ability. Additionally, the specific characteristics and requirements of the TPC material should be considered when determining the optimal printing parameters for achieving the desired self-cleaning properties.

7 VALIDATION

The validation of the analytical approach was conducted through a set of experiments on two 3D printed polymeric textile fabric specimens for each of the three materials (TPU, TPE, and TPC). These experiments involved using different printing parameters that had not been previously tested in the experimental scheme outlined in the study as shown in Figure 7-2 and Figure 7-2. The experimental scheme for the validation experiments is presented, as shown in Table 7-1, and the results obtained from these experiments were compared with the analytical model provided in Chapters 4 and 5.

The purpose of this comparison was to assess the accuracy of the analytical model in predicting the experimental outcomes. To quantify the deviation between the measured values obtained experimentally and the values predicted by the analytical equations presented in Section 5.2, the experimental error was calculated. This error represents the difference between the measured values and the values obtained from the analytical model. By performing these validation experiments and calculating the experimental error, the researchers aimed to validate the analytical approach used in the study. The linear regression equations derived from the experimental data can be used to assess the accuracy of the analytical model and determine its reliability in predicting the behaviour of 3D printed polymeric textile fabrics.

Overall, this validation process provides a means to evaluate the effectiveness of the analytical model and its applicability. It helps establish confidence in the analytical approach and its potential for predicting and optimizing the properties of 3D printed polymeric textile fabrics.

Table 7-1. The 3D parameters used to produce the samples.

Layer height (LH) mm	Extruder width (EW) mm	Orientation angle (O) Degree ◦
0.14	0.60	70◦ (first layer) - 210◦ (second layer)

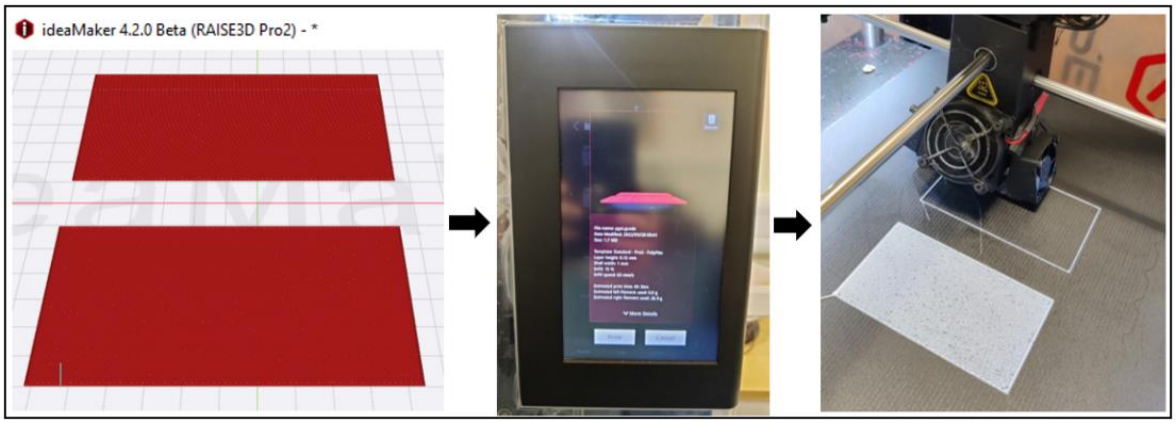

Figure 7-1. 3DP for validation samples.

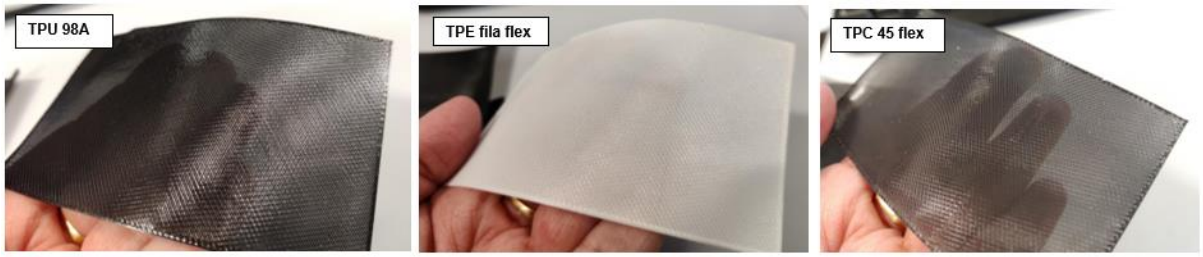

Figure 7-2. The 3D printed polymeric textile fabrics.

The contact angle to the water's droplet on the textile fabric surface was measured experimentally as shown in Figure 7-3 and Table 7-2.

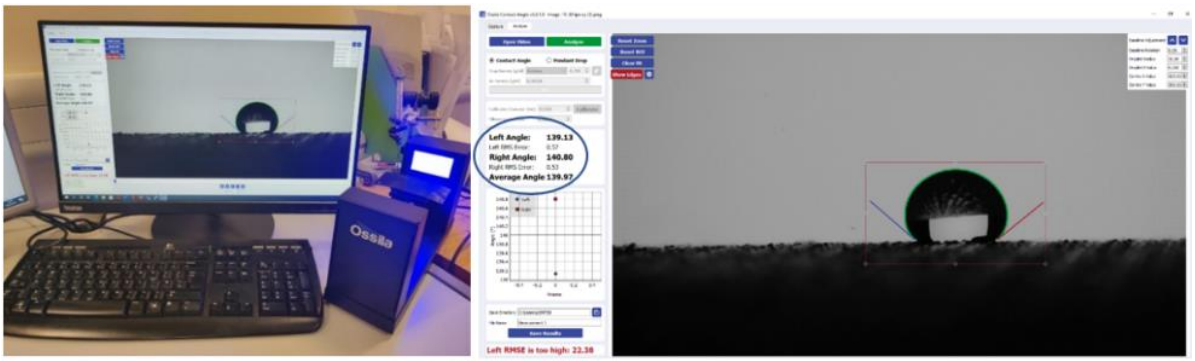

Figure 7-3. The contact angle measurement.

Table 7-2. (TPU flex 98) - (O) 70 ° (first layer) - 210 ° (second layer).

(LH) mm	(EW) mm	Sample 1	Sample 2

0.14	0.60	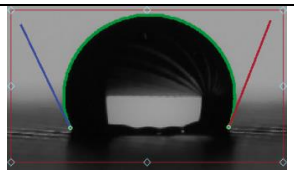 **Left Angle:** **136.94** Left RMS Error: 0.65 **Right Angle:** **130.94** Right RMS Error: 0.40 **Average Angle 133.94**	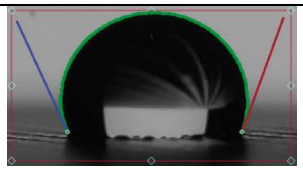 **Left Angle:** **134.03** Left RMS Error: 0.50 **Right Angle:** **131.78** Right RMS Error: 0.49 **Average Angle 132.08**

Based on equations (5-3), (5-6) and (5-9) for the three materials as shown in Table 7-3.

Table 7-3. The wettability measurement for the samples.

(TPU) - orientation 70◦					
Samples	(LH) mm	(EW) mm	Wettability Experimentally Degree °	Wettability Based on equation Degree °	Error (%)
1	0.14	0.60	133.94	133.7301	- 0.1573
2	0.14	0.60	132.08	133.7301	-1.0504
(TPE) - orientation 70°					
Samples	(LH) mm	(EW) mm	Wettability Experimentally Degree °	Wettability Based on equation Degree °	Error (%)
1	0.14	0.60	146.79	147.0002	- 0.1432
2	0.14	0.60	146.80	147.0002	- 0.1364
(TPC) - orientation 70◦					
Samples	(LH) mm	(EW) mm	Wettability Experimentally Degree °	Wettability Based on equation Degree °	Error (%)
1	0.14	0.60	131.52	130.8233	0.5297
2	0.14	0.60	130.34	130.8233	-0.3708

For the three materials, the porosity values experimentally were as shown in Figure 7-4.

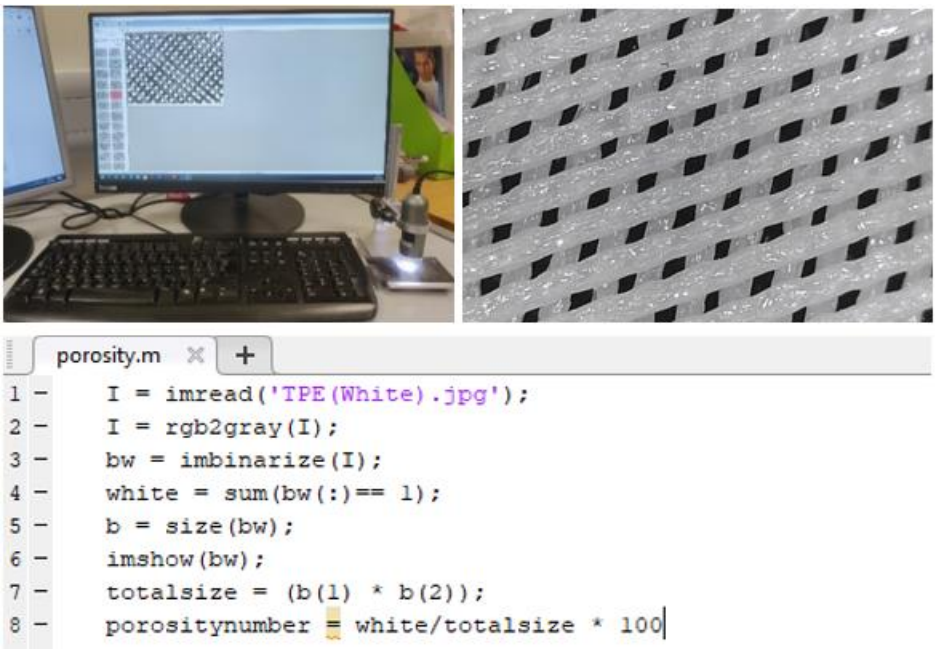

Figure 7-4. The porosity measurement.

For the three materials, the porosity values experimentally and based on equations (5-1), (5-4) and (5-7) were as shown in Table 7-4.

Table 7-4. The porosity measurement for the samples.

Samples	(O) Degree °	(LH) mm	(EW) mm	Porosity experimentally (%)	Porosity based on the equations (%)	Error (%)
TPU 1	70	0.14	0.6	60.5487	61.18675	-1.0538
TPU 2	70	0.14	0.6	61.3495	61.18675	0.2653
TPE 1	70	0.14	0.6	15.9889	16.5023	-3.2109
TPE 2	70	0.14	0.6	16.2713	16.5023	-1.4196
TPC 1	70	0.14	0.6	62.2025	63.46319	-1.0521
TPC 2	70	0.14	0.6	61.1086	63.46319	-2.5111

For the three materials, the surface roughness values were measured experimentally for each sample as shown in Figure 7-5 and Figure 7-6.

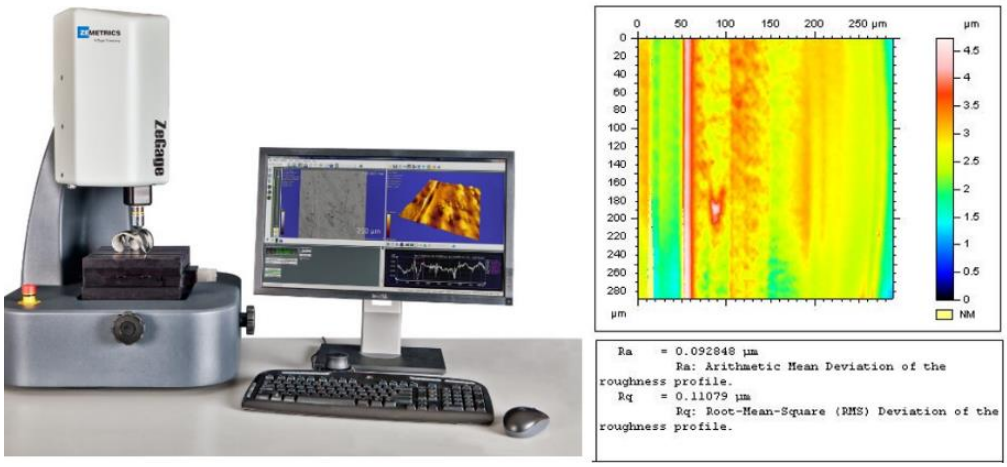

Figure 7-5. The surface roughness measurement.

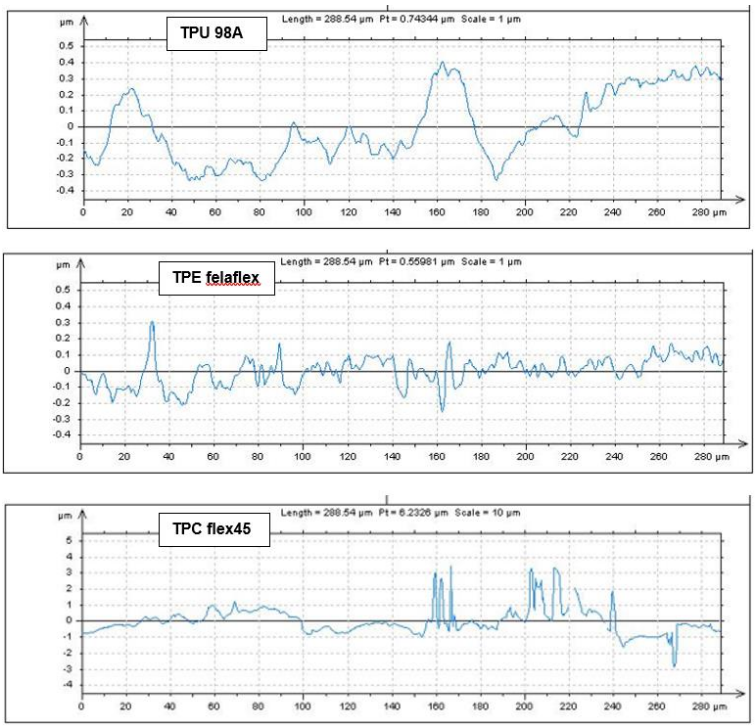

Figure 7-6. Surface Roughness profile for the three materials.

The surface roughness based on equations (5-2), (5-5) and (5-8) was as shown in Table 7-5.

Table 7-5. The surface roughness measurement for the samples.

Samples	(O) Degree ◦	(LH) mm	(EW) mm	Surface roughness Experimentally μm	Surface roughness Based on the equations μm	Error (%)
TPU 1	70	0.14	0.6	0.37949	0.383772	-1.1284
TPU 2	70	0.14	0.6	0.38049	0.383772	-0.8626
TPE 1	70	0.14	0.6	0.63273	0.64494	-1.9297
TPE 2	70	0.14	0.6	0.64253	0.64494	-0.3751
TPC 1	70	0.14	0.6	0.35156	0.357016	-1.5519
TPC 2	70	0.14	0.6	0.34996	0.357016	-2.0162

The analytical modelling is followed by a validation process, which involves performing experiments on two 3D printed polymeric textile fabric specimens for each of the three materials (TPU, TPE, and TPC). The experimental results are compared with the predictions obtained from the analytical the models for porosity, roughness, and wettability, as outlined in Table 7-3, Table 7-4 and Table 7-5 in the models prediction. The validation aims to assess the accuracy of the analytical models and determine the appropriate model equations for different parameters and materials. The criteria used for evaluating the model fit include comparing the predicted values with the experimental observations for porosity, roughness, and wettability. The errors between the predicted and experimental values are calculated to quantify the discrepancies.

The obtained model errors for the three materials fall within an expected range (0.5297 to -3.2109), indicating that the models provide reasonably accurate predictions. However, it is important to note that reducing the difference between the errors requires conducting further precise experimental research. This would help minimize the discrepancies between the analytical predictions and the experimental measurements.

In conclusion, the validation process involves comparing the experimental results with the predictions obtained from the analytical models, assessing the errors, and refining the models to improve their accuracy. By conducting accurate experimental research and minimizing the analytical-experimental differences, the overall reliability and effectiveness of the models can be enhanced.

7.1 The self-cleaning number for the validation

Given the significance of wettability in justifying the self-cleaning number, the self-cleaning ability is evaluated based on the linear equations derived from the wettability measurements. The self-cleaning number serves as an indicator of the surface's ability to self-clean. The validation process helps verify the accuracy of the self-cleaning number calculations based on the analytical models.

As we clarified that the wettability was the most important parameter to justify the self-cleaning number, the self-cleaning number was evaluated based on the linear equation (4-2) as shown in Table 7-6.

Table 7-6. The self-cleaning number for the samples.

Samples	(O) Degree °	(LH) mm	(EW) mm	Wettability Degree°	Self-cleaning number
TPU 1	70	0.14	0.6	133.52	69.632
TPU 2	70	0.14	0.6	132.34	67.744
TPE 1	70	0.14	0.6	146.79	90.864
TPE 2	70	0.14	0.6	146.8	90.88
TPC 1	70	0.14	0.6	131.52	66.432
TPC 2	70	0.14	0.6	130.34	64.544

7.2 Discussion on Experimental Error in Predictions of Porosity, Surface Roughness and Wettability for the Three Materials

In the evaluation of model fit for porosity, roughness, and wettability, the predicted values are compared with the corresponding experimental observations. The differences between the predicted and experimental values are then calculated to quantify the discrepancies. This will assist in improving future research along with the accuracy and reliability of the analytical models. The acceptable range of errors for the microscopic features may depend on the material being printed, the desired mechanical properties, and the intended application of the printed objects. Similarly, the chosen printing parameters, such as layer hights, extruder width and orientation can influence the acceptable range of errors. The error ranges obtained for porosity are shown in Figure 7-7.

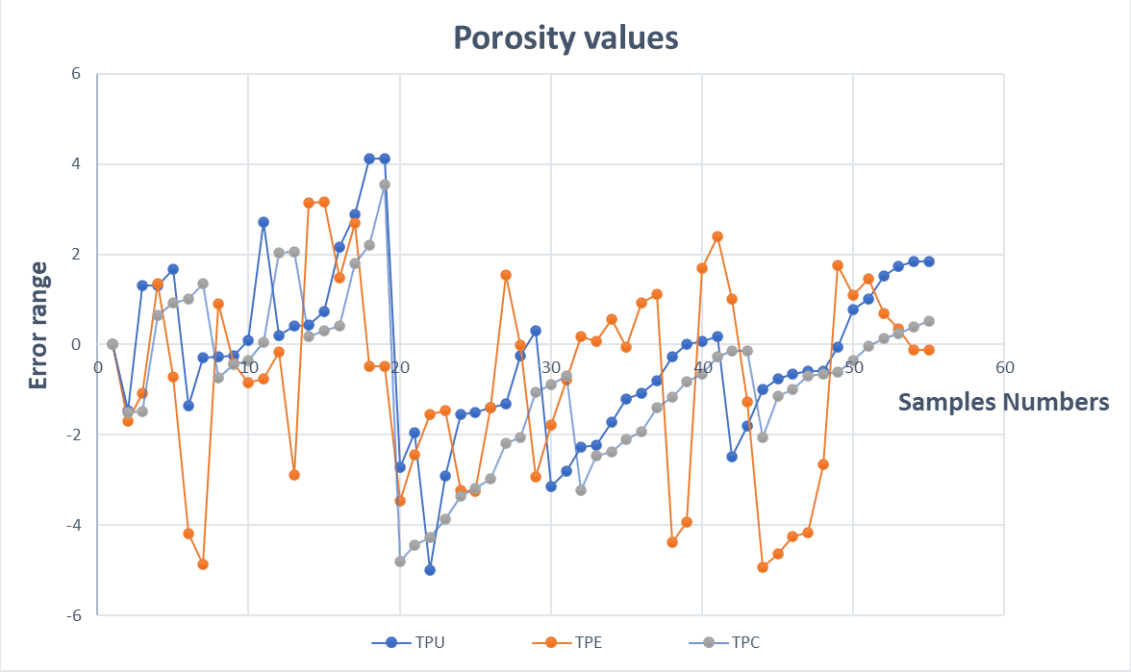

Figure 7-7. Error ranges for porosity for TPU, TPE and TPC.

When comparing the differences between the experimental and analytical results for porosity as shown in Figure 7-7, it is stated that the error ranges fall within an acceptable range considering the specific application of the study. The determination of what is considered as an acceptable range of errors can vary

depending on various factors, such as the nature of the materials or the chosen printing parameters. Stating that the error ranges are within an acceptable range suggests that the observed discrepancies between the experimental and analytical results for porosity do not significantly affect the overall validity or reliability of the study's conclusions. The differences may be relatively small and fall within the expected range of variability for the study. Based on the obtained model errors for the three materials, it is stated that the errors fall within an expected range of -4.9287 to 4.1225. This suggests that the models provide reasonably accurate predictions for porosity.

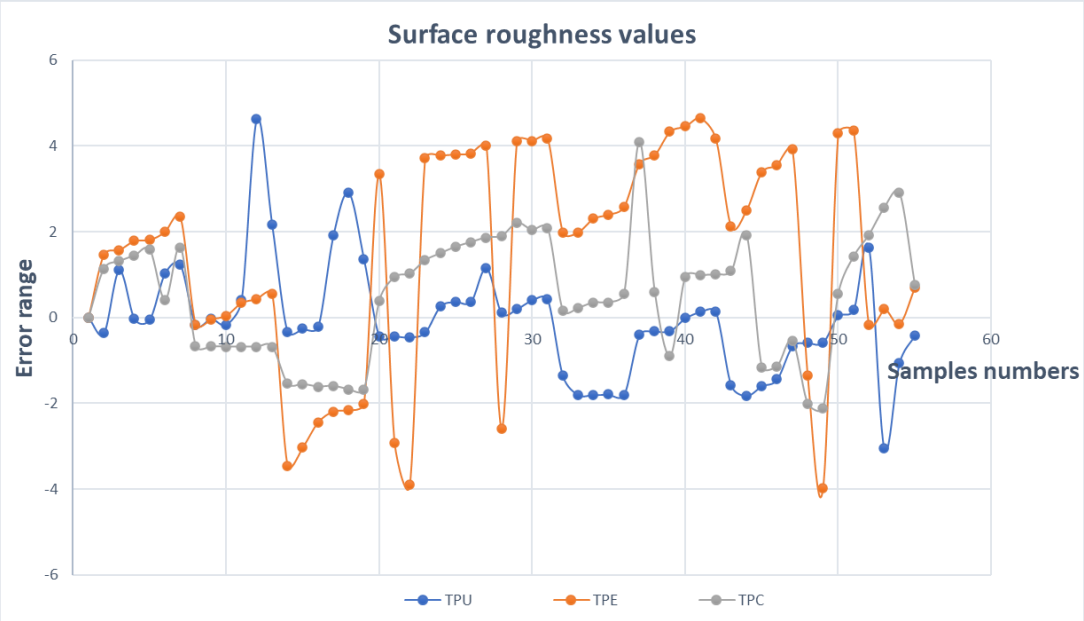

Figure 7-8 Error ranges for surface roughness for TPU, TPE and TPC.

When comparing the differences between the experimental and analytical results for surface roughness, it is stated that the error ranges shown in Figure 7-8 fall within an acceptable range considering the specific application of the study. This suggests that the observed discrepancies between the experimental and analytical results for roughness do not significantly impact the overall validity or reliability of the study's conclusions. The differences may be relatively small and fall within the expected range of variability for study.

Furthermore, it is stated that the obtained model errors for the three materials have an expected range of -3.9744 to 4.6296. This range indicates that the models provide reasonably accurate predictions for roughness.

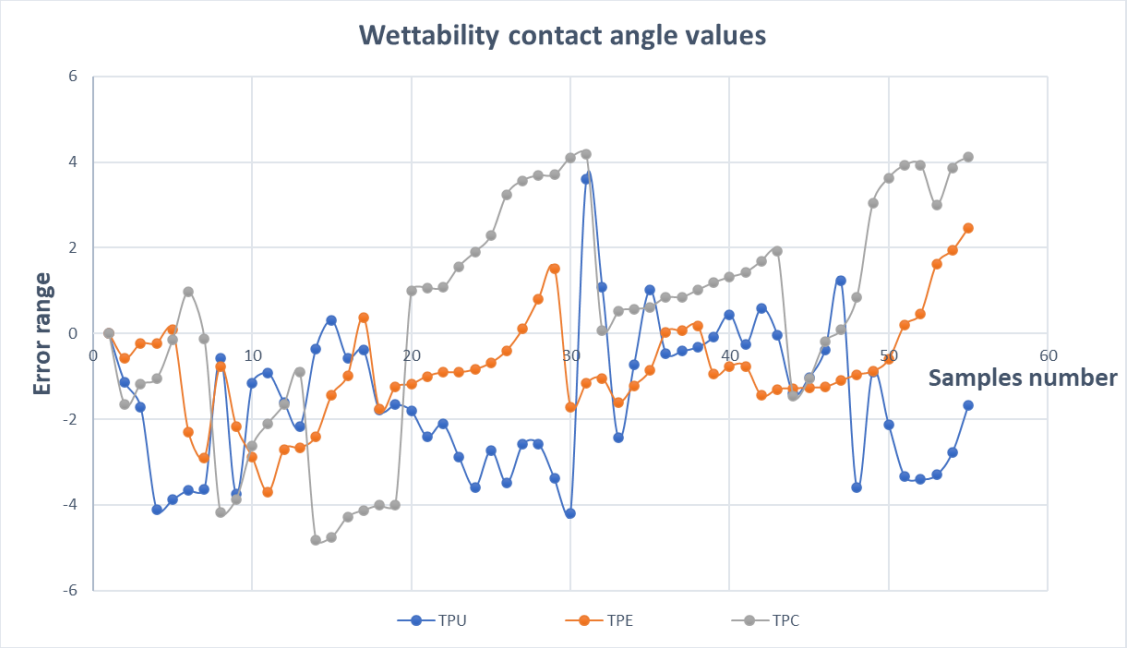

Figure 7-9 Error ranges for wettability for TPU, TPE and TPC.

Comparing the differences between the experimental and analytical results for wettability, it is stated that the error ranges shown in Figure 7-9 have an acceptable range considering the specific application of the study. The differences may be relatively small and fall within the expected range of variability for the study. Determining what is considered an acceptable range of errors for wettability can depend on the specific application or industry standards. Different applications or industries may have different requirements or specifications for wettability, and the acceptability of errors should be evaluated in that context. Additionally, it is stated that the obtained model errors for the three materials have an expected range of -4.8112 to 4.1864. This range indicates that the models provide reasonably accurate predictions for wettability within the specific application or context of the study.

However, although the error ranges falling within an acceptable range and provide the expected model error range, suggesting that the analytical models

offer reasonably accurate predictions for the microscopic features in the studied materials, it is crucial to emphasize the ongoing need for further validation and refinement of the models. Continued research and validation efforts are essential to enhance the accuracy and reliability of the analytical models for future studies. These efforts may involve comparing the models against additional experimental data, conducting sensitivity analyses to assess the model's response to different parameters, and incorporating more comprehensive or sophisticated modelling techniques. Therefore, the initial assessment of the error ranges and expected model error range indicates reasonably accurate predictions for the microscopic features; however, researchers should continue to validate and refine the models to enhance their accuracy and reliability for future studies.

Additionally, careful designing and executing of experiments can minimize the sources of error and uncertainty, leading to more accurate and reliable data. Conducting experimental research with precision is an effective method to reduce the difference between analytical predictions and experimental observations. Experimental research allows for direct measurements and observations of the studied phenomena, providing a level against which analytical models can be validated.

8 CONCLUSIONS

Additive manufacturing can contribute to sustainable manufacturing practices by reducing material waste. With the ability to precisely deposit materials, 3D printing minimizes material consumption compared to traditional manufacturing methods. Furthermore, filament materials used in FFF-based printing are often recyclable, contributing to a more environmentally friendly production process. This research focused on exploring the development of self-cleaning textile fabrics through the precise control of fabrication parameters at the microscopic level. The experimental investigation involved the use of three different thermoplastic flexible filaments for Fused Filament Fabrication (FFF) printing. The validation process encompassed the exploration of various printing parameters and their impact on the microscopic features influencing the self-cleaning ability of the fabrics. The research successfully achieved the objectives outlined in Section 1.3, and the key contributions of this study can be summarized as follows:

Fabrication Parameter Control: The research provided insights into the effective control of fabrication parameters during the printing process to optimize the self-cleaning properties of textile fabrics. By manipulating parameters such as layer height, extruder width, and orientation angle, the researchers were able to achieve desired levels of porosity, roughness, and wettability, which are crucial factors in self-cleaning performance.

Experimental Study: Through a systematic experimental study, the researchers examined the self-cleaning ability of the printed textile fabrics. By evaluating microscopic features such as porosity, roughness, and wettability, the study shed light on the relationship between these parameters and the fabrics' self-cleaning performance.

1- It can be found that the changes in porosity numbers were dependent on the material itself rather than the layer height changes, as the difference was only 5%. The (TPE) porosity values were the lowest among the other materials. The total porosity of the material shifted almost 10 % as it would create an impact on surface roughness which would also affect the wettability.

2- To justify the differences in the effect of the various parameters would be the changes in the material density. These can cause a difference in roughness between the three chosen materials, which was approximately 0.65 µm.

3-The experimental results showed that TPE has a better water contact angle WCA than the other two materials. Changing the print layer height and extruder width produced samples that spanned relatively RQ ranges between 0.04 – 0.65 µm. The connection between the roughness and wettability caused a higher value in wettability contact angle for the three materials.

4- Therefore, for porosity in all materials, the most influential parameter is layer height. Layer height has a consistent influence of about 5% increase in porosity from its minimum to maximum values in all materials. For surface roughness all the three printing parameters have an equal influence. For wettability, the layer height, extruder width, and orientation have varying degrees of influence on wettability, depending on the material being used.

5-These findings indicate that TPE filaflex is the most mechanically strong material of the three tested, while TPU and TPC exhibit reduced tensile strength. The higher tensile strength of TPE can be attributed to its excellent mechanical characteristics and flexibility.

6- Based on the obtained model errors for the three materials, for porosity, it is stated that the errors fall within an expected range of -4.9287 to 4.1225. For surface roughness, it is stated that the obtained model errors for the three materials have an expected range of -3.9744 to 4.6296. For wettability, it is stated that the obtained model errors for the three materials have an expected range of -4.8112 to 4.1864This suggests that the models provide reasonably accurate predictions for the three microscopic features.

Validation of Analytical Models: The research incorporated analytical models to predict and analyse the self-cleaning ability of the fabrics based on the microscopic features. The experimental validation process helped assess the

accuracy of these models and establish their reliability in predicting the self-cleaning performance of printed textile fabrics.

Novel Contributions: The research presented novel findings regarding the optimization of printing parameters, the influence of microscopic features on self-cleaning ability, and the correlation between fabrication parameters and self-cleaning performance. These contributions expand the knowledge base and provide valuable insights for the development of advanced self-cleaning textile fabrics.

Therefore, this research successfully explored the fabrication parameter control, conducted an experimental study, validated analytical models, and made novel contributions to the field of self-cleaning textile fabrics. The findings and insights gained from this study can serve as a foundation for further research and development in this area, opening new possibilities for the creation of innovative and functional textile materials. By exploring the use of filament materials with fabric-like properties, researchers aim to expand the applications of additive manufacturing beyond rigid structures and traditional materials. The integration of flexibility, softness, and customizability allows for producing objects that exhibit textile-like characteristics while benefiting from the design freedom and functional integration capabilities of 3D printing. The study objectives outlined in Section 1.3 were accomplished, and novel contributions are summarized below.

8.1 Achievement of Objectives

Objective 1 - To identify the microscopic features and their influence on the self-cleaning surface. (Achieved in Chapters 2 and 3)

Objective 1 of the research aimed to identify the microscopic features and their influence on the self-cleaning surface of textile fabrics. This objective was achieved through an extensive literature review, which explored the existing research on self-cleaning textile fabrics and identified the research gap in this area. The review highlighted that previous efforts to create self-cleaning textiles primarily focused on two approaches: creating appropriate surface roughness

and reducing surface energy using low surface energy chemicals or nanotechnology coatings. These approaches resulted in changes in the microscopic features of the fabric surface, which played a crucial role in determining the self-cleaning ability.

However, the use of organic solvents and chemicals in the coating process raised concerns about environmental health hazards. Therefore, there was a need to develop user-friendly and cost-effective methods for structuring self-cleaning surfaces without the need for additional coatings. This led to the exploration of the fabric's intrinsic microscopic features that could influence surface roughness and low surface energy, thereby providing self-cleaning ability at the woven structural level. By focusing on the fabric's own microscopic features, this research aimed to discover innovative approaches to achieve self-cleaning surfaces without relying on external coatings. Chapters 2 and 3 of the study provided a comprehensive understanding of the literature and research findings related to self-cleaning textile fabrics, laying the foundation for further exploration and experimentation in subsequent chapters.

Overall, Objective 1 successfully identified the microscopic features responsible for self-cleaning and emphasized the significance of developing fabric-level structural solutions for achieving self-cleaning surfaces, thereby reducing the reliance on additional coatings and potentially addressing environmental concerns.

Objective 2 - To examine the possibility of making 3D printed self-cleaning textile fabric by changing the structural woven pattern with the help of the microscopic features. (Achieved in Chapters 2.6 and 4).

Objective 2 of the research aimed to examine the possibility of creating 3D printed self-cleaning textile fabrics by utilizing the microscopic features and changing the structural woven pattern. This objective was achieved through the implementation of a design of experiments, which involved modelling empirical results, establishing relationships between self-cleaning ability, microscopic features, and printing parameters, and conducting an experimental scheme to

test the implementation of the identified features on different types of textile fabric. They focused on achieving Objective 2 by utilizing mathematical and statistical tools to model the empirical results. The critical review of the existing literature on self-cleaning textile fabrics provided the foundation for identifying the microscopic features and their relationship to self-cleaning. Based on this knowledge, an experimental scheme was developed to investigate the implementation of these features using 3D printing technology.

The research utilized a fused filament fabrication (FFF) technology-based 3D printer, chosen for its affordability, cost-effectiveness, and material availability. Three types of flexible filaments, namely TPU, TPE, and TPC, were selected to create 3D printed textile fabrics. A total of 162 samples were produced, with 54 samples for each filament, using different 3D printing parameters such as layer height (LH), extruder width (EW), and printing orientation (O). Computer-aided design (CAD) software was used to design the samples, which were then transmitted to the FFF printer for printing. The microscopic features, including porosity, roughness, and wettability, were measured and recorded to evaluate and compare the best values for self-cleaning among the three chosen materials. The collected data were analysed to determine the optimal self-cleaning number and establish the relationship between changes in printing parameters and microscopic features.

By successfully implementing the experimental scheme and analysing the data, Objective 2 was accomplished. Chapters 4 and 5 provided insights into the possibility of creating 3D printed self-cleaning textile fabrics by leveraging the identified microscopic features and manipulating the structural woven pattern using 3D printing technology. The study contributed to the development of knowledge and understanding in this field and paved the way for further exploration and applications of 3D printed self-cleaning textile fabrics.

Objective 3- To model the self-cleaning ability and fabric printing parameters. The research aimed to model the self-cleaning ability of the 3D printed polymeric

textile fabrics and establish a relationship with the fabric printing parameters. This objective was achieved in Chapters 5.

The research demonstrated that the selection of printing parameters, including layer height, extruder width, and printing orientation, has a significant impact on the self-cleaning properties of the 3D printed fabrics. By optimizing the combination of these process parameters, the study aimed to enhance the self-cleaning ability of the printed specimens.

Using statistical analysis and regression modelling, a linear regression model was developed to establish the relationship between the 3D printing parameters and the microscopic features responsible for self-cleaning. The model provided a quantitative understanding of how changes in printing parameters can influence the self-cleaning ability of the fabric.

The optimization of printing parameters was achieved by utilizing the developed model. By inputting the desired self-cleaning ability or target values for the microscopic features, the model can be used to estimate the optimal printing parameters required to achieve the desired self-cleaning performance. The devised method and optimization model presented in Chapter 6 provide a valuable tool for predicting and optimizing the self-cleaning ability of 3D printed polymeric textile fabrics. It allows for informed decision-making in the selection of printing parameters to achieve the desired self-cleaning properties. The model's applicability extends to cases where the printing parameters are known, providing a means to estimate the self-cleaning ability of the printed fabric.

Overall, Objective 3 was successfully accomplished through the modelling of the self-cleaning ability and fabric printing parameters, providing valuable insights and tools for enhancing the self-cleaning performance of 3D printed polymeric textile fabrics.

Objective 4 - To evaluate the optimum printing parameters for self-cleaning printed textile fabric. (Achieved in Chapters 6 and 7)

Critical discussion on the obtained model with the help of constraints and rules (as required to express self-cleaning of a printed fabric while keeping its aesthetic look) was used to establish the values of printing parameters where an optimum self-cleaning can be observed. Validation of the model was performed by testing printed fabrics on arbitrary values of printing parameters.

8.2 Contribution to Knowledge

The research presented in this study has made significant contributions to knowledge in several areas:

8.2.1 Influence of Microscopic Features on Self-Cleaning Ability

The study sheds light on the importance of microscopic features in achieving self-cleaning ability in textile fabrics. By identifying and understanding the role of surface properties such as porosity, roughness, and wettability, the research has provided valuable insights into the design and development of self-cleaning fabrics. This contribution is particularly significant in the disciplines of textile and fashion, where the understanding of microscopic features and their impact on self-cleaning ability has been limited.

8.2.2 Influence of the Printing Parameter on Microscopic Features

The research highlights the influence of printing parameters, such as layer height, extruder width, and orientation angle, on the microscopic features responsible for self-cleaning ability. By optimizing these parameters, the study demonstrates the potential to create 3D printed self-cleaning textile fabrics. This contribution has implications for various industries, including clothing, furniture, and household products, where self-cleaning textiles can find practical applications. The research also emphasizes the cost-effectiveness and sustainability of additive manufacturing technologies for producing such fabrics. This has been done according to the experiments and the result. The contribution that we have made in this study is making a model that can create a self-cleaning surface by putting the printing parameters as input.

8.2.3 Relationship Between Printing Parameters and Microscopic Features

The study establishes empirical relationships between the printing parameters and self-cleaning attributes of the printed fabrics. These relationships provide a valuable tool for estimating the self-cleaning ability of a printed surface based on the input printing parameters. The accuracy of these relationships has been validated through rigorous experiments, enhancing their reliability and applicability. This contribution enables designers and manufacturers to optimize printing parameters to achieve desired self-cleaning properties.

8.3 Future Work

Future research can build upon the findings of this study and explore additional avenues. This includes further investigation into fabricating self-cleaning textiles using different materials and printing parameters. Exploring the self-cleaning mechanism and developing numerical models to better understand and predict self-cleaning behaviour would be valuable. Additionally, expanding the study to incorporate computer models and innovative self-cleaning nano-systems can open new possibilities for fabricating advanced self-cleaning fabrics. Evaluating the self-cleaning mechanism in the field of polymers and exploring the use of other printing parameters not covered in this study are also potential areas for future research.

In conclusion, this research has contributed to the knowledge and understanding of self-cleaning textile fabrics by elucidating the influence of microscopic features, printing parameters, and their relationships. The findings provide a foundation for further advancements in the field and offer practical applications in various industries. Future research can explore additional materials, mechanisms, and modelling techniques to enhance the development and utilization of self-cleaning textiles.

REFERENCES

[1] X. C. Hua, Y. Wu, X. J. Guo, B. Y. Liu, H. Di Wang, and S. T. Jia, “Superhydrophobic, flame-retardant and conductive cotton fabrics via layer-by-layer assembly of carbon nanotubes for flexible sensing electronics,” *Cellulose*, vol. 27, no. 6, pp. 3455–3468, 2020, doi: 10.1007/s10570-020-03013-z.

[2] S. Roy, L. Zhai, J. W. Kim, H. C. Kim, and J. Kim, “A novel approach of developing sustainable cellulose coating for self-cleaning-healing fabric,” *Prog Org Coat*, vol. 140, no. March 2019, p. 105500, 2020, doi: 10.1016/j.porgcoat.2019.105500.

[3] S. R. Saad, N. Mahmed, M. M. A. B. Abdullah, and A. V. Sandu, “Self-Cleaning Technology in Fabric: A Review,” in *IOP Conference Series: Materials Science and Engineering*, Institute of Physics Publishing, Jun. 2016. doi: 10.1088/1757-899X/133/1/012028.

[4] I. Sas, R. E. Gorga, J. A. Joines, and K. A. Thoney, “Literature review on superhydrophobic self-cleaning surfaces produced by electrospinning,” *Journal of Polymer Science, Part B: Polymer Physics*, vol. 50, no. 12. pp. 824–845, Jun. 15, 2012. doi: 10.1002/polb.23070.

[5] S. S. Latthe *et al.*, “Self – cleaning superhydrophobic coatings: Potential industrial applications,” *Prog Org Coat*, vol. 128, no. December 2018, pp. 52–58, 2019, doi: 10.1016/j.porgcoat.2018.12.008.

[6] I. Ahmad and C. W. Kan, “A Review on Development and Applications of Bio-Inspired Superhydrophobic Textiles,” *Materials*, vol. 9, no. 11, 2016, doi: 10.3390/ma9110892.

[7] I. Ahmad, C. wai Kan, and Z. Yao, “Reactive Blue-25 dye/TiO 2 coated cotton fabrics with self-cleaning and UV blocking properties,” *Cellulose*, vol. 26, no. 4, pp. 2821–2832, Mar. 2019, doi: 10.1007/s10570-019-02279-2.

[8] H. J. Lee, J. Kim, and C. H. Park, “Fabrication of self-cleaning textiles by TiO2-carbon nanotube treatment,” *Textile Research Journal*, vol. 84, no. 3, pp. 267–278, 2014, doi: 10.1177/0040517513494258.

[9] H. Yang, F. Ji, Z. Li, and S. Tao, “Preparation of hydrophobic surface on PLA and ABS by fused deposition modeling,” *Polymers (Basel)*, vol. 12, no. 7, Jul. 2020, doi: 10.3390/polym12071539.

[10] A. A. Atwah and M. A. Khan, “Influence of microscopic features on the self-cleaning ability of textile fabrics,” 2021, doi: 10.1177/00405175211069881.

[11] S. P. Dalawai *et al.*, “Recent Advances in durability of superhydrophobic self-cleaning technology: A critical review,” *Progress in Organic Coatings*, vol. 138. Elsevier B.V., Jan. 01, 2020. doi: 10.1016/j.porgcoat.2019.105381.

[12] M. Yu *et al.*, “Laundering durability of photocatalyzed self-cleaning cotton fabric with TiO2 nanoparticles covalently immobilized,” *ACS Appl Mater Interfaces*, vol. 5, no. 9, pp. 3697–3703, May 2013, doi: 10.1021/am400304s.

[13] H. M. Ahmed, M. M. Abdellatif, S. Ibrahim, and F. H. H. Abdellatif, “Mini-emulsified Copolymer/Silica nanocomposite as effective binder and self-cleaning for textiles coating,” *Prog Org Coat*, vol. 129, no. January, pp. 52–58, 2019, doi: 10.1016/j.porgcoat.2019.01.002.

[14] C. Wei, B. Jin, Q. Zhang, X. Zhan, and F. Chen, “Anti-icing performance of super-wetting surfaces from icing-resistance to ice-phobic aspects: Robust hydrophobic or slippery surfaces,” *J Alloys Compd*, vol. 765, pp. 721–730, Oct. 2018, doi: 10.1016/j.jallcom.2018.06.041.

[15] M. Ghasemlou, F. Daver, E. P. Ivanova, and B. Adhikari, “Bio-inspired sustainable and durable superhydrophobic materials: From nature to market,” *J Mater Chem A Mater*, vol. 7, no. 28, pp. 16643–16670, 2019, doi: 10.1039/c9ta05185f.

[16] X. P. Li, Y. L. Sun, C. W. Luo, and Z. S. Chao, “UV-resistant hydrophobic CeO2 nanomaterial with photocatalytic depollution performance,” *Ceram Int*, vol. 44, no. 11, pp. 13439–13443, Aug. 2018, doi: 10.1016/j.ceramint.2018.04.132.

[17] X. M. Li, D. Reinhoudt, and M. Crego-Calama, “What do we need for a superhydrophobic surface? A review on the recent progress in the preparation of superhydrophobic surfaces,” *Chem Soc Rev*, vol. 36, no. 8, pp. 1350–1368, Jul. 2007, doi: 10.1039/b602486f.

[18] S. Afzal, W. A. Daoud, and S. J. Langford, “Photostable self-cleaning cotton by a copper(II) porphyrin/TiO2 visible-light photocatalytic system,” *ACS Appl Mater Interfaces*, vol. 5, no. 11, pp. 4753–4759, Jun. 2013, doi: 10.1021/am400002k.

[19] V. A. Ganesh, H. K. Raut, A. S. Nair, and S. Ramakrishna, “A review on self-cleaning coatings,” *Journal of Materials Chemistry*, vol. 21, no. 41. pp. 16304–16322, Nov. 07, 2011. doi: 10.1039/c1jm12523k.

[20] E. Busi, S. Maranghi, L. Corsi, and R. Basosi, “Environmental sustainability evaluation of innovative self-cleaning textiles,” *J Clean Prod*, vol. 133, pp. 439–450, 2016, doi: 10.1016/j.jclepro.2016.05.072.

[21] B. Bhushan and Y. C. Jung, “Natural and biomimetic artificial surfaces for superhydrophobicity, self-cleaning, low adhesion, and drag reduction,” *Progress in Materials Science*, vol. 56, no. 1. Elsevier Ltd, pp. 1–108, Jan. 01, 2011. doi: 10.1016/j.pmatsci.2010.04.003.

[22] C. Zhu, J. Shi, S. Xu, M. Ishimori, J. Sui, and H. Morikawa, “Design and characterization of self-cleaning cotton fabrics exploiting zinc oxide nanoparticle-triggered photocatalytic degradation,” *Cellulose*, vol. 24, no. 6, pp. 2657–2667, Jun. 2017, doi: 10.1007/s10570-017-1289-7.

[23] M. M. De Villiers, D. P. Otto, S. J. Strydom, and Y. M. Lvov, “Introduction to nanocoatings produced by layer-by-layer (LbL) self-assembly,” *Adv Drug*

Deliv Rev, vol. 63, no. 9, pp. 701–715, 2011, doi: 10.1016/j.addr.2011.05.011.

[24] F. Shams-Ghahfarokhi, A. Khoddami, Z. Mazrouei-Sebdani, J. Rahmatinejad, and H. Mohammadi, “A new technique to prepare a hydrophobic and thermal insulating polyester woven fabric using electro-spraying of nano-porous silica powder,” *Surf Coat Technol*, vol. 366, no. March, pp. 97–105, 2019, doi: 10.1016/j.surfcoat.2019.03.025.

[25] W. N. W. Ismail, “Sol–gel technology for innovative fabric finishing—A Review,” *J Solgel Sci Technol*, vol. 78, no. 3, pp. 698–707, 2016, doi: 10.1007/s10971-016-4027-y.

[26] R. G. A. S. Infirri, *LIGHT INDUCED TEXTILE SUBSTRATE WITH SWITCHABLE AND REVERSIBLE*. 2016.

[27] J. Lin *et al.*, “A facile dip-coating approach to prepare SiO2/fluoropolymer coating for superhydrophobic and superoleophobic fabrics with self-cleaning property,” *J Appl Polym Sci*, vol. 132, no. 1, Jan. 2015, doi: 10.1002/app.41458.

[28] M. Yang, W. Liu, C. Jiang, S. He, Y. Xie, and Z. Wang, “Fabrication of superhydrophobic cotton fabric with fluorinated TiO2 sol by a green and one-step sol-gel process,” *Carbohydr Polym*, vol. 197, pp. 75–82, Oct. 2018, doi: 10.1016/j.carbpol.2018.05.075.

[29] M. Yang *et al.*, “Facile construction of robust superhydrophobic cotton textiles for effective UV protection, self-cleaning and oil-water separation,” *Colloids Surf A Physicochem Eng Asp*, vol. 570, pp. 172–181, Jun. 2019, doi: 10.1016/j.colsurfa.2019.03.024.

[30] K. Qi, W. A. Daoud, J. H. Xin, C. L. Mak, W. Tang, and W. P. Cheung, “Self-cleaning cotton,” *J Mater Chem*, vol. 16, no. 47, pp. 4567–4574, 2006, doi: 10.1039/b610861j.

[31] A. Peter, A. Mihaly-Cozmuta, C. Nicula, L. Mihaly-Cozmuta, A. Vulpoi, and L. Baia, “Fabric impregnated with TiO2 gel with self-cleaning property,” *Int J Appl Ceram Technol*, vol. 16, no. 2, pp. 666–681, Mar. 2019, doi: 10.1111/ijac.13075.

[32] M. Montazer and E. Pakdel, “Self-cleaning and color reduction in wool fabric by nano titanium dioxide,” *Journal of the Textile Institute*, vol. 102, no. 4, pp. 343–352, Apr. 2011, doi: 10.1080/00405001003771242.

[33] O. L. Galkina, V. V. Vinogradov, A. V. Vinogradov, and A. V. Agafonov, “Development of the low-temperature sol-gel synthesis of TiO2 to provide self-cleaning effect on the textile materials,” *Nanotechnol Russ*, vol. 7, no. 11–12, pp. 604–614, Dec. 2012, doi: 10.1134/S1995078012060031.

[34] S. Afzal, W. A. Daoud, and S. J. Langford, “Visible-light self-cleaning cotton by metalloporphyrin-sensitized photocatalysis,” in *Applied Surface Science*, Elsevier B.V., Jun. 2013, pp. 36–42. doi: 10.1016/j.apsusc.2013.01.141.

[35] E. Pakdel, W. A. Daoud, T. Afrin, L. Sun, and X. Wang, “Self-cleaning wool: effect of noble metals and silica on visible-light-induced functionalities of nano TiO2 colloid,” *Journal of the Textile Institute*, vol. 106, no. 12, pp. 1348–1361, Dec. 2015, doi: 10.1080/00405000.2014.995461.

[36] S. Tian *et al.*, “The Journal of The Textile Institute Facile preparation of multi-scale nanoarchitectures on cotton fabric with low surface energy for high performance self-cleaning) Facile preparation of multi-scale nanoarchitectures on cotton fabric with low surface energy for high performance self Facile preparation of multi-scale nanoarchitectures on cotton fabric with low surface energy for high performance self-cleaning,” vol. 111, no. 11, pp. 1603–1613, 2020, doi: 10.1080/00405000.2020.1713626.

[37] W. R. Hansen and K. Autumn, “Evidence for self-cleaning in gecko setae,” 2004. [Online]. Available: www.pnas.orgcgidoi10.1073pnas.0408304102

[38] R. Voo, M. Mariatti, and L. C. Sim, “Properties of epoxy nanocomposite thin films prepared by spin coating technique,” *Journal of Plastic Film and Sheeting*, vol. 27, no. 4, pp. 331–346, 2011, doi: 10.1177/8756087911419745.

[39] J. Teknologi, Y. Rilda, A. Alif, H. Aziz, S. Chandren, and H. Nur, “SELF-CLEANING TiO2-SiO2 CLUSTERS ON COTTON TEXTILE PREPARED BY DIP-SPIN COATING PROCESS,” 2016.

[40] N. Dissanayake, S. Abeysundara, and N. D. Wanasekara, “Investigating the Feasibility of Applying Spin Coating Method for Textiles,” *MERCon 2020 - 6th International Multidisciplinary Moratuwa Engineering Research Conference, Proceedings*, pp. 448–452, 2020, doi: 10.1109/MERCon50084.2020.9185265.

[41] C. Yao *et al.*, “Facile surface modification of textiles with photocatalytic carbon nitride nanosheets and the excellent performance for self-cleaning and degradation of gaseous formaldehyde,” *J Colloid Interface Sci*, vol. 533, pp. 144–153, Jan. 2019, doi: 10.1016/j.jcis.2018.08.058.

[42] S. Roy, H. C. Kim, L. Van Hai, and J. Kim, “Novel superhydrophobic cellulose coating and its multifunctional applications,” South Korea: SPIE-Intl Soc Optical Eng, Mar. 2019, pp. 1–5. doi: 10.1117/12.2513876.

[43] W. Li, H. Wang, and Z. Li, “Hierarchical structure microspheres of PCL block copolymers via electrospraying as coatings for fabric with mechanical durability and self-cleaning ability,” *Polym Adv Technol*, vol. 30, no. 9, pp. 2321–2330, Sep. 2019, doi: 10.1002/pat.4660.

[44] M. Krifa and & C. Prichard, “Nanotechnology in textile and apparel research-an overview of technologies and processes,” *The Journal of The Textile Institute*, vol. 111, pp. 1778–1793, 2020, doi: 10.1080/00405000.2020.1721696.

[45] N. M. Bedford and A. J. Steckl, “Photocatalytic self cleaning textile fibers by coaxial electrospinning,” *ACS Appl Mater Interfaces*, vol. 2, no. 8, pp. 2448–2455, Aug. 2010, doi: 10.1021/am1005089.

[46] I. Sas, R. E. Gorga, J. A. Joines, and K. A. Thoney, “Literature review on superhydrophobic self-cleaning surfaces produced by electrospinning,” *Journal of Polymer Science, Part B: Polymer Physics*, vol. 50, no. 12. pp. 824–845, Jun. 15, 2012. doi: 10.1002/polb.23070.

[47] F. Zareei Pour, H. Karimi, and V. Madadi Avargani, “Preparation of a superhydrophobic and superoleophilic polyester textile by chemical vapor deposition of dichlorodimethylsilane for Water–Oil separation,” *Polyhedron*, vol. 159, pp. 54–63, Feb. 2019, doi: 10.1016/j.poly.2018.11.040.

[48] P. Ragesh, V. Anand Ganesh, S. V. Nair, and A. S. Nair, “A review on ‘self-cleaning and multifunctional materials,’” *J Mater Chem A Mater*, vol. 2, no. 36, pp. 14773–14797, 2014, doi: 10.1039/c4ta02542c.

[49] Z. Zheng, N. Zhang, H. Wang, and X. Zhao, “Preparation of self-cleaning polyester fabrics by chemical vapor deposition of methyltrichlorosilane/ dimethyldichlorosilane,” *Fibres and Textiles in Eastern Europe*, vol. 25, no. 1, pp. 121–124, 2017, doi: 10.5604/12303666.1227892.

[50] L. Brockway and H. Taylor, “A statistical model for the wettability of surfaces with heterogeneous pore geometries,” *Mater Res Express*, vol. 3, no. 10, Oct. 2016, doi: 10.1088/2053-1591/3/10/105039.

[51] S. Li *et al.*, “Robust Flower-Like TiO2@Cotton Fabrics with Special Wettability for Effective Self-Cleaning and Versatile Oil/Water Separation,” *Adv Mater Interfaces*, vol. 2, no. 14, Sep. 2015, doi: 10.1002/admi.201500220.

[52] J. Y. Huang *et al.*, “Robust superhydrophobic TiO2@fabrics for UV shielding, self-cleaning and oil-water separation,” *J Mater Chem A Mater*, vol. 3, no. 6, pp. 2825–2832, Feb. 2015, doi: 10.1039/c4ta05332j.

[53] B. Tan, B. Gao, J. Guo, X. Guo, and M. Long, “A comparison of TiO2 coated self-cleaning cotton by the sols from peptizing and hydrothermal routes,” *Surf Coat Technol*, vol. 232, pp. 26–32, Oct. 2013, doi: 10.1016/j.surfcoat.2013.04.048.

[54] L. Wang *et al.*, “Superhydrophobic and ultraviolet-blocking cotton textiles,” *ACS Appl Mater Interfaces*, vol. 3, no. 4, pp. 1277–1281, 2011, doi: 10.1021/am200083z.

[55] S. Uğur, A. M. Sariişik, E. Çavuşlar, and M. Ertek, “Development of Self-Cleaning Denim Fabrics,” in *IOP Conference Series: Materials Science and Engineering*, Institute of Physics Publishing, Nov. 2017. doi: 10.1088/1757-899X/254/12/122012.

[56] T. Bahners, T. Textor, K. Opwis, and E. Schollmeyer, “Recent approaches to highly hydrophobic textile surfaces,” *J Adhes Sci Technol*, vol. 22, no. 3–4, pp. 285–309, 2008, doi: 10.1163/156856108X295437.

[57] S. Park, J. Kim, and C. H. Park, “Analysis of the wetting state of super-repellent fabrics with liquids of varying surface tension,” *RSC Adv*, vol. 6, no. 51, pp. 45884–45893, 2016, doi: 10.1039/c5ra27281e.

[58] Z. Komeily-Nia, M. Montazer, S. seint seint Aye, and B. Nasri-Nasrabadi, “A practical approach to load CuO/MnO2 core/shell nanostructures on textiles through in situ wet chemical synthesis,” *Colloids Surf A Physicochem Eng Asp*, vol. 583, Dec. 2019, doi: 10.1016/j.colsurfa.2019.123998.

[59] Z. Moridi Mahdieh, S. Shekarriz, F. Afshar Taromi, and M. Montazer, “A new method for in situ synthesis of Ag–TiO2 nanocomposite particles on polyester/cellulose fabric by photoreduction and self-cleaning properties,” *Cellulose*, vol. 25, no. 4, pp. 2355–2366, Apr. 2018, doi: 10.1007/s10570-018-1694-6.

[60] A. Panda, P. Varshney, S. S. Mohapatra, and A. Kumar, “Development of liquid repellent coating on cotton fabric by simple binary silanization with excellent self-cleaning and oil-water separation properties,” *Carbohydr Polym*, vol. 181, pp. 1052–1060, Feb. 2018, doi: 10.1016/j.carbpol.2017.11.044.

[61] X. Jiang, X. Tian, J. Gu, D. Huang, and Y. Yang, “Cotton fabric coated with nano TiO 2 -acrylate copolymer for photocatalytic self-cleaning by in-situ suspension polymerization,” *Appl Surf Sci*, vol. 257, no. 20, pp. 8451–8456, Aug. 2011, doi: 10.1016/j.apsusc.2011.04.128.

[62] T. Bahners, T. Textor, K. Opwis, and E. Schollmeyer, “Recent approaches to highly hydrophobic textile surfaces,” *J Adhes Sci Technol*, vol. 22, no. 3–4, pp. 285–309, Jun. 2008, doi: 10.1163/156856108X295437.

[63] L. Karimi, S. Zohoori, and A. Amini, “Multi-wall carbon nanotubes and nano titanium dioxide coated on cotton fabric for superior self-cleaning and UV blocking,” *Xinxing Tan Cailiao/New Carbon Materials*, vol. 29, no. 5, pp. 380–385, Oct. 2014, doi: 10.1016/S1872-5805(14)60144-X.

[64] F. A. P. Scacchetti, E. Pinto, and G. Soares, “A multifunctional cotton fabric using TiO2 and PCMs: Introducing thermal comfort and self-cleaning properties,” in *IOP Conference Series: Materials Science and Engineering*, Institute of Physics Publishing, Nov. 2017. doi: 10.1088/1757-899X/254/12/122011.

[65] J. Liu, X. Lin, and H. Liang, “Dyed fabrics modified via assembly with phytic acid/berberine for antibacterial, UV resistance, and self-cleaning applications,” *J Eng Fiber Fabr*, vol. 14, 2019, doi: 10.1177/1558925019888978.

[66] E. Pakdel, W. A. Daoud, and X. Wang, “Self-cleaning and superhydrophilic wool by TiO 2 /SiO 2 nanocomposite,” in *Applied Surface Science*, Elsevier B.V., Jun. 2013, pp. 397–402. doi: 10.1016/j.apsusc.2012.10.141.

[67] A. A. Hebeish, M. M. Abdelhady, and A. M. Youssef, “TiO2 nanowire and TiO2 nanowire doped Ag-PVP nanocomposite for antimicrobial and self-cleaning cotton textile,” *Carbohydr Polym*, vol. 91, no. 2, pp. 549–559, Jan. 2013, doi: 10.1016/j.carbpol.2012.08.068.

[68] K. Sundaresan, A. Sivakumar, C. Vigneswaran, and T. Ramachandran, “Influence of nano titanium dioxide finish, prepared by sol-gel technique, on the ultraviolet protection, antimicrobial, and self-cleaning characteristics of cotton fabrics,” *Journal of Industrial Textiles*, vol. 41, no. 3, pp. 259–277, 2012, doi: 10.1177/1528083711414962.

[69] N. Abidi, L. Cabrales, and E. Hequet, “Functionalization of a cotton fabric surface with titania nanosols: Applications for self-cleaning and UV-protection properties,” *ACS Appl Mater Interfaces*, vol. 1, no. 10, pp. 2141–2146, Oct. 2009, doi: 10.1021/am900315t.

[70] X. Wang, N. D. Georganas, and E. M. Petriu, “Fabric texture analysis using computer vision techniques,” *IEEE Trans Instrum Meas*, vol. 60, no. 1, pp. 44–56, 2011, doi: 10.1109/TIM.2010.2069850.

[71] K. Qi, J. H. Xin, W. A. Daoud, and C. Leung Mak, “Functionalizing Polyester Fiber with a Self-Cleaning Property Using Anatase TiO 2 and Low-Temperature Plasma Treatment.”

[72] I. Ahmad and C. W. Kan, “Visible-light-driven, dye-sensitized TiO 2 photo-catalyst for self-cleaning cotton fabrics,” *Coatings*, vol. 7, no. 11, Nov. 2017, doi: 10.3390/coatings7110192.

[73] A. Mishra and B. S. Butola, “Development of Cotton Fabrics with Durable UV Protective and Self-cleaning Property by Deposition of Low TiO2 Levels through Sol–gel Process,” *Photochem Photobiol*, vol. 94, no. 3, pp. 503–511, May 2018, doi: 10.1111/php.12888.

[74] M. Jin *et al.*, “Super-hydrophobic PDMS surface with ultra-low adhesive force,” *Macromol Rapid Commun*, vol. 26, no. 22, pp. 1805–1809, Nov. 2005, doi: 10.1002/marc.200500458.

[75] M. Yang, C. Jiang, W. Liu, L. Liang, and K. Pi, “A less harmful system of preparing robust fabrics for integrated self-cleaning, oil-water separation and water purification,” *Environmental Pollution*, vol. 255, Dec. 2019, doi: 10.1016/j.envpol.2019.113277.

[76] M. Liu, Y. Zheng, J. Zhai, and L. Jiang, “Bioinspired super-antiwetting interfaces with special liquid-solid adhesion,” *Acc Chem Res*, vol. 43, no. 3, pp. 368–377, Mar. 2010, doi: 10.1021/ar900205g.

[77] M. Ashraf, P. Champagne, A. Perwuelz, C. Campagne, and A. Leriche, “Photocatalytic solution discoloration and self-cleaning by polyester fabric functionalized with ZnO nanorods,” *Journal of Industrial Textiles*, vol. 44, no. 6, pp. 884–898, May 2015, doi: 10.1177/1528083713519662.

[78] J. Lim, “-,” 2014.

[79] G. Zhu, Y. Fang, L. Zhao, J. Wang, and W. Chen, “Prediction of structural parameters and air permeability of cotton woven fabric,” *Textile Research Journal*, vol. 88, no. 14, pp. 1650–1659, 2018, doi: 10.1177/0040517517705632.

[80] X. Feng and L. Jiang, “Design and creation of superwetting/antiwetting surfaces,” *Advanced Materials*, vol. 18, no. 23, pp. 3063–3078, Dec. 2006, doi: 10.1002/adma.200501961.

[81] R. Chen *et al.*, “A lotus effect-inspired flexible and breathable membrane with hierarchical electrospinning micro/nanofibers and ZnO nanowires,” *Mater Des*, vol. 162, pp. 246–248, Jan. 2019, doi: 10.1016/j.matdes.2018.11.041.

[82] M. H. Shim, J. Kim, and C. H. Park, “The effects of surface energy and roughness on the hydrophobicity of woven fabrics,” *Textile Research*

Journal, vol. 84, no. 12, pp. 1268–1278, 2014, doi: 10.1177/0040517513495945.

[83] S. Afzal, W. A. Daoud, and S. J. Langford, “Superhydrophobic and photocatalytic self-cleaning cotton,” *J Mater Chem A Mater*, vol. 2, no. 42, pp. 18005–18011, Nov. 2014, doi: 10.1039/c4ta02764g.

[84] J. Gao, X. Huang, H. Xue, L. Tang, and R. K. Y. Li, “Facile preparation of hybrid microspheres for super-hydrophobic coating and oil-water separation,” *Chemical Engineering Journal*, vol. 326, pp. 443–453, 2017, doi: 10.1016/j.cej.2017.05.175.

[85] T. Zhu, S. Li, J. Huang, M. Mihailiasa, and Y. Lai, “Rational design of multi-layered superhydrophobic coating on cotton fabrics for UV shielding, self-cleaning and oil-water separation,” *Mater Des*, vol. 134, pp. 342–351, Nov. 2017, doi: 10.1016/j.matdes.2017.08.071.

[86] S. S. Latthe, S. Liu, C. Terashima, K. Nakata, and A. Fujishima, “Transparent, adherent, and photocatalytic SiO 2 -TiO 2 coatings on polycarbonate for self-cleaning applications,” *Coatings*, vol. 4, no. 3, pp. 497–507, Sep. 2014, doi: 10.3390/coatings4030497.

[87] D. Khojasteh, M. Kazerooni, S. Salarian, and R. Kamali, “Droplet impact on superhydrophobic surfaces: A review of recent developments,” *Journal of Industrial and Engineering Chemistry*, vol. 42, pp. 1–14, 2016, doi: 10.1016/j.jiec.2016.07.027.

[88] L. Espinal, “POROSITY AND ITS MEASUREMENT Ã,” 2012.

[89] J. Lim, N. Powell, H. Lee, and S. Michielsen, “Geometric impact of void space in woven fabrics on oil resistance or repellency,” *J Mater Sci*, vol. 52, no. 13, pp. 8149–8158, Jul. 2017, doi: 10.1007/s10853-017-1022-9.

[90] J. Drelich and A. Marmur, “Physics and applications of superhydrophobic and superhydrophilic surfaces and coatings,” *Surf Innov*, vol. 2, no. 4, pp. 211–227, Dec. 2014, doi: 10.1680/si.13.00017.

[91] X. Chen, L. W. Taylor, and L. ju Tsai, “An overview on fabrication of three-dimensional woven textile preforms for composites,” *Textile Research Journal*, vol. 81, no. 9, pp. 932–944, 2011, doi: 10.1177/0040517510392471.

[92] J. Lim, N. Powell, H. Lee, and S. Michielsen, “Integration of yarn compression in modeling structural geometry of liquid resistant–repellent fabric surfaces and its impact on liquid behavior,” *J Mater Sci*, vol. 51, no. 15, pp. 7199–7210, Aug. 2016, doi: 10.1007/s10853-016-0001-x.

[93] M. Nagamadhu, P. Jeyaraj, and G. C. Mohan Kumar, “Influence of textile properties on dynamic mechanical behavior of epoxy composite reinforced with woven sisal fabrics,” *Sadhana - Academy Proceedings in Engineering Sciences*, vol. 45, no. 1, pp. 1–10, 2020, doi: 10.1007/s12046-019-1249-z.

[94] H. Li, N. Zhang, X. Fan, J. Gong, J. Zhang, and X. Zhao, “Investigation of effective factors of woven structure fabrics for acoustic absorption,” *Applied Acoustics*, vol. 161, p. 107081, 2020, doi: 10.1016/j.apacoust.2019.107081.

[95] W. Wang, T. Li, K. Liu, S. Wang, and H. Peng, “Effects of three fabric weave textures on the electrochemical and electrical properties of reduced graphene/textile flexible electrodes,” *RSC Adv*, vol. 10, no. 11, pp. 6249–6258, 2020, doi: 10.1039/c9ra08524f.

[96] K. M. Lee, H. Park, J. Kim, and D. M. Chun, “Fabrication of a superhydrophobic surface using a fused deposition modeling (FDM) 3D printer with poly lactic acid (PLA) filament and dip coating with silica nanoparticles,” *Appl Surf Sci*, vol. 467–468, pp. 979–991, Feb. 2019, doi: 10.1016/j.apsusc.2018.10.205.

[97] H. Jaouani, D. Matsouka, S. Vassiliadis, and K. S. Nikas, “Effect of weaving pattern and yarn density on the surface roughness of woven fabrics,” *Tekstil ve Muhendis*, vol. 26, no. 116, pp. 320–323, 2019, doi: 10.7216/1300759920192611601.

[98] B. Huan, H. Jiyong, Y. Xudong, J. Hongyan, T. Huating, and Y. Xiong, “Influence of woven fabric structural and material parameters on dielectric properties,” *AATCC Journal of Research*, vol. 6, pp. 50–53, 2019, doi: 10.14504/ajr.6.S1.11.

[99] A. Asayesh, F. Mirgoli, and A. Gholamhosseini, “An investigation into the effect of fabric structure on the compressional properties of woven fabrics,” *Journal of the Textile Institute*, vol. 109, no. 1, pp. 32–38, 2018, doi: 10.1080/00405000.2017.1320817.

[100] J. Lim and J. R. Kim, “Geometric structure modification in cellulose acetate nanofibers and its impact on liquid resistance/repellency,” *Cellulose*, vol. 27, no. 5, pp. 2521–2528, Mar. 2020, doi: 10.1007/s10570-019-02959-z.

[101] H. Shams, K. Basit, M. A. Khan, S. Saleem, and A. Mansoor, “3D Printing of Superamphiphobic Surfaces using Fused Deposition Modelling: Evolution and Challenges.”

[102] S. Li, J. Huang, Z. Chen, G. Chen, and Y. Lai, “A review on special wettability textiles: theoretical models, fabrication technologies and multifunctional applications,” *J Mater Chem A Mater*, vol. 5, no. 1, pp. 31–55, 2017, doi: 10.1039/c6ta07984a.

[103] S. Lee and C. H. Park, “Electric heated cotton fabrics with durable conductivity and self-cleaning properties,” *RSC Adv*, vol. 8, no. 54, pp. 31008–31018, 2018, doi: 10.1039/C8RA05530K.

[104] L. Li, Y. Bai, L. Li, S. Wang, and T. Zhang, “A Superhydrophobic Smart Coating for Flexible and Wearable Sensing Electronics,” *Advanced Materials*, vol. 29, no. 43, pp. 1–8, 2017, doi: 10.1002/adma.201702517.

[105] N. T. Padmanabhan and H. John, “Titanium dioxide based self-cleaning smart surfaces: A short review,” *J Environ Chem Eng*, vol. 8, no. 5, p. 104211, Oct. 2020, doi: 10.1016/j.jece.2020.104211.

[106] S. Roy, H. C. Kim, L. Van Hai, and J. Kim, “Novel superhydrophobic cellulose coating and its multifunctional applications,” no. March 2019, p. 25, 2019, doi: 10.1117/12.2513876.

[107] A. Tuteja *et al.*, “Designing Superoleophobic Surfaces.”

[108] D. Wu, L. Wang, X. Song, and Y. Tan, “Enhancing the visible-light-induced photocatalytic activity of the self-cleaning TiO2-coated cotton by loading Ag/AgCl nanoparticles,” *Thin Solid Films*, vol. 540, pp. 36–40, Jul. 2013, doi: 10.1016/j.tsf.2013.05.113.

[109] Y. C. Jung and B. Bhushan, “Wetting behavior of water and oil droplets in three-phase interfaces for hydrophobicity/philicity and oleophobicity/philicity,” *Langmuir*, vol. 25, no. 24, pp. 14165–14173, 2009, doi: 10.1021/la901906h.

[110] R. Blossey, “Self-cleaning surfaces — virtual realities,” pp. 301–306, 2003.

[111] Y. Zheng, X. Gao, and L. Jiang, “Directional adhesion of superhydrophobic butterfly wings,” *Soft Matter*, vol. 3, no. 2, pp. 178–182, 2007, doi: 10.1039/b612667g.

[112] Y. Chen, B. He, J. Lee, and N. A. Patankar, “Anisotropy in the wetting of rough surfaces,” *J Colloid Interface Sci*, vol. 281, no. 2, pp. 458–464, Jan. 2005, doi: 10.1016/j.jcis.2004.07.038.

[113] S. Kim, E. Cheung, and M. Sitti, “Wet self-cleaning of biologically inspired elastomer mushroom shaped microfibrillar adhesives,” *Langmuir*, vol. 25, no. 13, pp. 7196–7199, Jul. 2009, doi: 10.1021/la900732h.

[114] K. Koch, B. Bhushan, Y. C. Jung, and W. Barthlott, “Fabrication of artificial Lotus leaves and significance of hierarchical structure for superhydrophobicity and low adhesion,” *Soft Matter*, vol. 5, no. 7, pp. 1386–1393, 2009, doi: 10.1039/b818940d.

[115] S. Banerjee, D. D. Dionysiou, and S. C. Pillai, “Self-cleaning applications of TiO2 by photo-induced hydrophilicity and photocatalysis,” *Appl Catal B*, vol. 176–177, pp. 396–428, 2015, doi: 10.1016/j.apcatb.2015.03.058.

[116] A. Fernández *et al.*, “Hierarchical surfaces for enhanced self-cleaning applications,” *Journal of Micromechanics and Microengineering*, vol. 27, no. 4, Mar. 2017, doi: 10.1088/1361-6439/aa62bb.

[117] A. A. Atwah and M. A. Khan, “Influence of microscopic features on the self-cleaning ability of textile fabrics,” *Textile Research Journal*, 2022, doi: 10.1177/00405175211069881.

[118] R. T. Ogulata and S. Mavruz, “Investigation of porosity and air permeability values of plain knitted fabrics,” *Fibres and Textiles in Eastern Europe*, vol. 82, no. 5, pp. 71–75, 2010.

[119] A. A. Atwah, M. D. Almutairi, F. He, and M. A. Khan, “Influence of Printing Parameters on Self-Cleaning Properties of 3D Printed Polymeric Fabrics,” *Polymers (Basel)*, vol. 14, no. 15, p. 3128, 2022, doi: 10.3390/polym14153128.

[120] D. Jakšić and N. Jakšić, “Assessment of Porosity of Flat Textile Fabrics,” *Textile Research Journal*, vol. 77, no. 2, pp. 105–110, 2007, doi: 10.1177/0040517506065892.

[121] G. Zhang, M. A. Quetzeri-Santiago, C. A. Stone, L. Botto, and J. R. Castrejón-Pita, “Droplet impact dynamics on textiles,” *Soft Matter*, vol. 14, no. 40, pp. 8182–8190, 2018, doi: 10.1039/C8SM01082J.

[122] N. Cappetti, A. Naddeo, and G. Salerno, “Influence of control parameters on consumer FDM 3D printing,” *Advances in Transdisciplinary Engineering*, vol. 7, no. January, pp. 165–177, 2018, doi: 10.3233/978-1-61499-898-3-165.

[123] N. K. Myshkin, A. Y. Grigoriev, S. A. Chizhik, K. Y. Choi, and M. I. Petrokovets, “Surface roughness and texture analysis in microscale,”

Wear, vol. 254, no. 10, pp. 1001–1009, 2003, doi: 10.1016/S0043-1648(03)00306-5.

[124] M. S. Alsoufi, A. El-Sayed, and A. E. Elsayed, “How Surface Roughness Performance of Printed Parts Manufactured by Desktop FDM 3D Printer with PLA+ is Influenced by Measuring Direction Environmental sustainability and energy conservation during machining processes View project How Surface Roughness Per,” *American Journal of Mechanical Engineering*, vol. 5, no. 5, pp. 211–222, 2017, doi: 10.12691/ajme-5-5-4.

[125] H. Kalami and J. Urbanic, “Exploration of surface roughness measurement solutions for additive manufactured components built by multi-axis tool paths,” *Addit Manuf*, vol. 38, no. December 2020, p. 101822, 2021, doi: 10.1016/j.addma.2020.101822.

[126] H. Y. Erbil, “The debate on the dependence of apparent contact angles on drop contact area or three-phase contact line: A review,” *Surf Sci Rep*, vol. 69, no. 4, pp. 325–365, 2014, doi: 10.1016/j.surfrep.2014.09.001.

[127] J. Hartcher-O’Brien, J. Evers, and E. Tempelman, “Surface roughness of 3D printed materials: Comparing physical measurements and human perception,” *Mater Today Commun*, vol. 19, no. January, pp. 300–305, 2019, doi: 10.1016/j.mtcomm.2019.01.008.

[128] X. Yao, Y. Song, and L. Jiang, “Applications of bio-inspired special wettable surfaces,” *Advanced Materials*, vol. 23, no. 6, pp. 719–734, 2011, doi: 10.1002/adma.201002689.

[129] U. Modi and S. Prakash, “Wettability of 3D printed polylactic acid (PLA) parts,” *AIP Conf Proc*, vol. 2148, no. September 2017, 2019, doi: 10.1063/1.5123974.

[130] S. S. Chinchwade, S. M. Landage, and S. Bonsule, “Super-Hydrophobicity on Textiles – a Review,” *International Journal of Advances Research in Engineering and Applied Sciences*, vol. 3, no. 7, pp. 1–9, 2014.

[131] T. Kozior, T. Blachowicz, and A. Ehrmann, “Adhesion of three-dimensional printing on textile fabrics: Inspiration from and for other research areas,” *J Eng Fiber Fabr*, vol. 15, 2020, doi: 10.1177/1558925020910875.

[132] R. Summary, “Multiprocess 3D printing for increasing component functionality,” vol. 353, no. 6307, 2016, doi: 10.1126/science.aaf2093.

[133] M. Čuk, M. Bizjak, D. Muck, and T. N. Kočevar, “3D Printing and Functionalization of Textiles,” *International Symposium on Graphic Engineering and Design*, pp. 499–506, 2020, doi: 10.24867/GRID-2020-p56.

[134] H. Takahashi and J. Kim, “3D printed fabric: Techniques for design and 3D weaving programmable textiles,” in *UIST 2019 - Proceedings of the 32nd Annual ACM Symposium on User Interface Software and Technology*, Association for Computing Machinery, Inc, Oct. 2019, pp. 43–51. doi: 10.1145/3332165.3347896.

[135] X. Tang and X. Yan, “Dip-coating for fibrous materials: mechanism, methods and applications,” *J Solgel Sci Technol*, vol. 81, no. 2, pp. 378–404, 2017, doi: 10.1007/s10971-016-4197-7.

[136] F. F. F. Printing, A. Elkaseer, S. Schneider, and G. Scholz, “applied sciences Experiment-Based Process Modeling and Optimization for High-Quality and Resource-E ffi cient,” 2020.

[137] R. Wilhite and I. Wölfel, “3D Printing for veterinary anatomy : An overview,” no. September, pp. 609–620, 2019, doi: 10.1111/ahe.12502.

[138] D. B. Sitotaw, D. Ahrendt, and Y. Kyosev, “applied sciences Additive Manufacturing and Textiles — State-of-the-Art,” 2020.

[139] G. R. Pereira, F. Gasi, and S. R. Lourenço, “Review , Analysis , and Classification of 3D Printing Literature : Types of Research and Technology Benefits,” vol. 6495, no. 6, 2019.

[140] Y. Xiao and C. Kan, “Review on Development and Application of 3D-Printing,” 2022.

[141] J. D. Prince, “3D Printing : An Industrial Revolution 3D Printing : An Industrial Revolution,” vol. 4065, 2014, doi: 10.1080/15424065.2014.877247.

[142] L. Partsch, S. Vassiliadis, and P. Papageorgas, “3D PRINTED TEXTILE FABRICS STRUCTURES 3D PRINTED TEXTILE FABRICS STRUCTURES,” no. October, pp. 3–10, 2015.

[143] M. León-Calero, S. C. Reyburn Valés, Á. Marcos-Fernández, and J. Rodríguez-Hernandez, “3D printing of thermoplastic elastomers: Role of the chemical composition and printing parameters in the production of parts with controlled energy absorption and damping capacity,” *Polymers (Basel)*, vol. 13, no. 20, 2021, doi: 10.3390/polym13203551.

[144] S. Chakraborty and M. Chandra Biswas, “Fused Deposition Modeling 3D Printing Technology in Textile and Fashion Industry: Materials and Innovation.”

[145] T. C. Lee, R. Ramlan, N. Shahrubudin, T. C. Lee, and R. Ramlan, “ScienceDirect ScienceDirect ScienceDirect An Overview on 3D Printing Technology : Technological , Materials , and Technology : Applications Technological , Materials , An Overview on 3D Printing and Applications,” *Procedia Manuf*, vol. 35, pp. 1286–1296, 2019, doi: 10.1016/j.promfg.2019.06.089.

[146] M. Beecroft, “3D printing of weft knitted textile based structures by selective laser sintering of nylon powder,” in *IOP Conference Series: Materials Science and Engineering*, Institute of Physics Publishing, Jul. 2016. doi: 10.1088/1757-899X/137/1/012017.

[147] O. Access, “3D printing of textile-based structures by Fused Deposition Modelling (FDM) with different polymer materials 3D printing of textile-

based structures by Fused Deposition Modelling (FDM) with different polymer materials," 2014, doi: 10.1088/1757-899X/62/1/012018.

[148] T. Spahiu, E. Canaj, and E. Shehi, "3D printing for clothing production," *J Eng Fiber Fabr*, vol. 15, 2020, doi: 10.1177/1558925020948216.

[149] S. Kivioja, H. Suonsilta, and O. Fi, "Printed material and fabric," pp. 313–321, 2013.

[150] M. Javaid, A. Haleem, R. Pratap, R. Suman, and S. Rab, "Advanced Industrial and Engineering Polymer Research Role of additive manufacturing applications towards environmental sustainability," *Advanced Industrial and Engineering Polymer Research*, vol. 4, no. 4, pp. 312–322, 2021, doi: 10.1016/j.aiepr.2021.07.005.

[151] K. Chatterjee and T. K. Ghosh, "3D Printing of Textiles: Potential Roadmap to Printing with Fibers," *Advanced Materials*, vol. 32, no. 4. Wiley-VCH Verlag, Jan. 01, 2020. doi: 10.1002/adma.201902086.

[152] R. Jafari, C. Cloutier, A. Allahdini, and G. Momen, "Recent progress and challenges with 3D printing of patterned hydrophobic and superhydrophobic surfaces," *International Journal of Advanced Manufacturing Technology*, vol. 103, no. 1–4, pp. 1225–1238, Jul. 2019, doi: 10.1007/s00170-019-03630-4.

[153] B. Jackson, K. Fouladi, and B. Eslami, "Multi-Parameter Optimization of 3D Printing Condition for Enhanced Quality and Strength," *Polymers (Basel)*, vol. 14, no. 8, 2022, doi: 10.3390/polym14081586.

[154] T. Kamegawa, Y. Shimizu, and H. Yamashita, "Superhydrophobic Surfaces with Photocatalytic Self- Cleaning Properties by Nanocomposite Coating of TiO 2 and Polytetrafl uoroethylene", doi: 10.1002/adma.201201037.

[155] R. Kuhn, "THE 3D PRINTING'S PANORAMA IN FASHION DESIGN".

[156] E. Pei, J. Shen, and J. Watling, “Direct 3D printing of polymers onto textiles: Experimental studies and applications,” *Rapid Prototyp J*, vol. 21, no. 5, pp. 556–571, Aug. 2015, doi: 10.1108/RPJ-09-2014-0126.

[157] R. Hashemi, C. Campagne, and V. Nierstrasz, “Applied Surface Science Investigation of the adhesion properties of direct 3D printing of polymers and nanocomposites on textiles : Effect of FDM printing process parameters,” *Appl Surf Sci*, vol. 403, pp. 551–563, 2017, doi: 10.1016/j.apsusc.2017.01.112.

[158] X. Fang *et al.*, “An investigation on effects of process parameters in fused-coating based metal additive manufacturing,” *J Manuf Process*, vol. 28, pp. 383–389, 2017, doi: 10.1016/j.jmapro.2017.01.008.

[159] A. J. Sheoran and H. Kumar, “Materials Today : Proceedings Fused Deposition modeling process parameters optimization and effect on mechanical properties and part quality : Review and reflection on present research,” *Mater Today Proc*, vol. 21, pp. 1659–1672, 2020, doi: 10.1016/j.matpr.2019.11.296.

[160] J. M. Barrios and P. E. Romero, “Improvement of surface roughness and hydrophobicity in PETG parts manufactured via fused deposition modeling (FDM): An application in 3D printed self-cleaning parts,” *Materials*, vol. 12, no. 15, Aug. 2019, doi: 10.3390/ma12152499.

[161] L. Sabantina, F. Kinzel, A. Ehrmann, and K. Finsterbusch, “Combining 3D printed forms with textile structures - Mechanical and geometrical properties of multi-material systems,” in *IOP Conference Series: Materials Science and Engineering*, Institute of Physics Publishing, Jul. 2015. doi: 10.1088/1757-899X/87/1/012005.

[162] M. Akgun, “Effect of yarn filament fineness on the surface roughness of polyester woven fabrics,” *J Eng Fiber Fabr*, vol. 10, no. 2, pp. 121–128, 2015, doi: 10.1177/155892501501000214.

[163] F. He, V. K. Thakur, and M. Khan, “Evolution and new horizons in modeling crack mechanics of 3D printing polymeric structures,” *Mater Today Chem*, vol. 20, 2021, doi: 10.1016/j.mtchem.2020.100393.

[164] I. Buj-Corral, A. Domínguez-Fernández, and R. Durán-Llucià, “Influence of print orientation on surface roughness in fused deposition modeling (FDM) processes,” *Materials*, vol. 12, no. 23, 2019, doi: 10.3390/ma122333834.

[165] P. Mercedes, G. Medina-s, and D. Carou, “Surface Quality Enhancement of Fused Deposition Modeling (FDM) Printed Samples Based on the Selection of Critical Printing Parameters”, doi: 10.3390/ma11081382.

[166] M. Chaudhari, B. F. Jogi, and R. S. Pawade, “Comparative Study of Part Characteristics Built Using Additive Manufacturing (FDM),” *Procedia Manuf*, vol. 20, no. 2017, pp. 73–78, 2018, doi: 10.1016/j.promfg.2018.02.010.

[167] M. Asadi-eydivand, M. Solati-hashjin, and A. Farzad, “Robotics and Computer-Integrated Manufacturing Effect of technical parameters on porous structure and strength of 3D printed calcium sulfate prototypes,” *Robotics and Computer Integrated Manufacturing*, vol. 37, pp. 57–67, 2016, doi: 10.1016/j.rcim.2015.06.005.

[168] C. Do-Seung, K.-B. Kim, and J.-S. Jang, “A Study on 3D Printer Design for Clothing Printing: Focusing on Knitted Wearable Clothing Output,” *International Journal of Advanced Smart Convergence*, vol. 9, no. 1, pp. 82–89, 2020, doi: 10.7236/IJASC.2020.9.1.82.

[169] M. Korger, J. Bergschneider, M. Lutz, B. Mahltig, K. Finsterbusch, and M. Rabe, “Possible applications of 3D printing technology on textile substrates,” in *IOP Conference Series: Materials Science and Engineering*, Institute of Physics Publishing, Aug. 2016. doi: 10.1088/1757-899X/141/1/012011.

[170] J. Hartcher-O'Brien, J. Evers, and E. Tempelman, "Surface roughness of 3D printed materials: Comparing physical measurements and human perception," *Mater Today Commun*, vol. 19, no. January, pp. 300–305, 2019, doi: 10.1016/j.mtcomm.2019.01.008.

[171] Y. Li, Q. Zhu, and K. W. Yeung, "Influence of Thickness and Porosity on Coupled Heat and Liquid Moisture Transfer in Porous Textiles," *Textile Research Journal*, vol. 72, no. 5, pp. 435–446, 2002, doi: 10.1177/004051750207200511.

[172] I. Buj-Corral, A. Bagheri, and M. Sivatte-Adroer, "Effect of printing parameters on dimensional error, surface roughness and porosity of FFF printed parts with grid structure," *Polymers (Basel)*, vol. 13, no. 8, 2021, doi: 10.3390/polym13081213.

[173] C. Arnold, D. Monsees, J. Hey, and R. Schweyen, "Surface Quality of 3D-Printed Models as a Function of Various Printing Parameters," pp. 1–15, 2019.

[174] M. Korger, J. Bergschneider, M. Lutz, B. Mahltig, K. Finsterbusch, and M. Rabe, "Possible applications of 3D printing technology on textile substrates," *IOP Conf Ser Mater Sci Eng*, vol. 141, no. 1, 2016, doi: 10.1088/1757-899X/141/1/012011.

[175] J. Hartcher-O'Brien, J. Evers, and E. Tempelman, "Surface roughness of 3D printed materials: Comparing physical measurements and human perception," *Mater Today Commun*, vol. 19, pp. 300–305, Jun. 2019, doi: 10.1016/j.mtcomm.2019.01.008.

APPENDICES

Appendix A: MATLAB code

The optimisation codes

```
i = 1;
for X1 = 45:1:90
   for X2=0:0.01:0.5
      for X3= 0:0.02:1
         % TPU Wettability
         wettability = 100.51 + 0.17*X1+ 137.22*X2 + 3.306*X3;
         if wettability >= 150
         matrix(i,:) = [X1 X2 X3 wettability];
         roughness = (-0.23)+ 0.001*X1+1.20*X2+0.62*X3;
         porosity = 48.12+0.03*X1+44.03*X2+8.19*X3;
         matrix2(i,:) = [X1 X2 X3 roughness];
         matrix3(i,:) = [X1 X2 X3 porosity];
         i = i+1;
                  end
      end
   end
end
a = matrix(:,1);
b = matrix(:,2);
c = matrix(:,3);
d = matrix(:,4);
scatter3(a,b,c,40,d,'filled')
xlabel('Oreintation')
ylabel('Layer height')
zlabel('Extruder width')
cb=colorbar;
cb.Label.String = 'Wettability';

figure

a2 = matrix2(:,1);
b2 = matrix2(:,2);
c2 = matrix2(:,3);
d2 = matrix2(:,4);
scatter3(a2,b2,c2,40,d2,'filled')
xlabel('Oreintation')
ylabel('Layer height')
zlabel('Extruder width')
cb=colorbar;
cb.Label.String = 'Roughness';

figure
a3 = matrix3(:,1);
b3 = matrix3(:,2);
c3 = matrix3(:,3);
d3 = matrix3(:,4);
scatter3(a3,b3,c3,40,d3,'filled')
xlabel('Oreintation')
```

```
ylabel('Layer height')
zlabel('Extruder width')
cb=colorbar;
cb.Label.String = 'Porosity';
```

Porosity code

```
I = imread('TPE(White).jpg');
I = rgb2gray(I);
bw = imbinarize(I);
white = sum(bw(:)== 1);
b = size(bw);
imshow(bw);
totalsize = (b(1) * b(2));
porositynumber = white/totalsize * 100
```

The regression code

```
x = Book1(:,1:4);
poro = Book1(:,5);
rou = Book1(:,6);


bporo = regress(poro,x);
brou = regress(rou,x);

%%
plot(Book1(:,6),Book1(:,7),'o');
xlabel('Roughness ');
ylabel('wettabilty ');
```